

Abnormal conduction in the diseased heart

Enhanced fibrosis due to reduced gap junction and sodium channel expression

Abnormale geleiding in het zieke hart - Toegenomen fibrose ten gevolge van een afgenomen expressie van gap junction- en natriumkanalen

(met een samenvatting in het Nederlands)

Proefschrift

ter verkrijging van de graad van doctor aan de Universiteit Utrecht op gezag van de rector magnificus, prof.dr. G.J. van der Zwaan, ingevolge het besluit van het college voor promoties in het openbaar te verdedigen op dinsdag 1 november 2011 des middags te 2.30 uur

door

Johannes Arnoldus Jansen

geboren op 11 januari 1982 te Tiel

Promotoren: prof.dr.ir. J.M.T. de Bakker
 prof.dr. M.A. Vos

Co-promotoren: dr. H.V.M. van Rijen
 dr. A.A.B. van Veen

The work in this thesis was supported by the Netherlands Heart Foundation (NHF grant number 2005B170).

Abnormal conduction in the diseased heart

Enhanced fibrosis due to reduced gap junction and sodium channel expression

Abnormale geleiding in het zieke hart - Toegenomen fibrose ten gevolge van een afgenomen expressie van gap junction- en natriumkanalen

(met een samenvatting in het Nederlands)

Proefschrift

ter verkrijging van de graad van doctor aan de Universiteit Utrecht op gezag van de rector magnificus, prof.dr. G.J. van der Zwaan, ingevolge het besluit van het college voor promoties in het openbaar te verdedigen op dinsdag 1 november 2011 des middags te 2.30 uur

door

Johannes Arnoldus Jansen

geboren op 11 januari 1982 te Tiel

Part of the research described in this thesis was supported by a grant of the Dutch Heart Foundation (DHF-2005B170). Financial support by the Dutch Heart Foundation for the publication of this thesis is gratefully acknowledged. Financial support by the Heart Lung Foundation Utrecht for the publication of this thesis is gratefully acknowledged.

ISBN: 978-90-8891-332-7

Table of Contents

Preface	7
1. Cardiac connexins and impulse conduction	19
2. Lysosome mediated Kir2.1 breakdown directly influences inward rectifier current density	37
3. Reduced Cx43 expression triggers increased fibrosis due to enhanced fibroblast activity	49
4. Progressive AV-block in a mouse-model of Lev / Lenègre disease	71
5. Reduced heterogeneous expression of Cx43 combined with decreased Nav1.5 expression account for arrhythmia vulnerability in conditional Cx43 knockout mice	87
6. General discussion	105
7. Summary	121
8. Nederlandse samenvatting	125
9. Dankwoord	129
10. Curriculum Vitae	137

Preface

John Jansen

Normally, every heart beat starts in the sinoatrial (SA) node, which initiates depolarization and subsequent contraction of the atria and carries activation towards the atrioventricular (AV) node¹. Here the impulse propagation is delayed, after which it travels through the His-bundle and both bundle branches towards the Purkinje fibers^{2,3}. Via these Purkinje fibers the ventricular myocardium is activated, followed by ventricular contraction, which leads to pumping of blood into the aorta and pulmonary arteries.

The trip of the electrical impulse can be followed in the electrocardiogram (ECG, Figure 1A). The P-wave represents electrical activation of the atria, the QRS-complex the activation of the ventricles. The iso-electric part between P-wave and QRS-complex (PQ-segment) coincides with delay in the AV node and activation of the bundle of His and the bundle branches. Finally, a T-wave is measured, representing the repolarization of the ventricles⁴.

The electrical activity, reflected by the ECG, is the resultant of consecutive depolarization and repolarization of individual ventricular cardiomyocytes, called action potentials. Every action potential is generated by a sophisticated interplay of many ion channels, mainly sodium, potassium and calcium channels. During rest, the inside of the cardiomyocyte is negatively charged compared to the outside (resting membrane potential, $\pm -80\text{mV}$), which keeps the inward sodium channel (Nav1.5) in a closed state. The axial current of activated cells slightly depolarizes neighboring cardiomyocytes, until the activation threshold for sodium channels is reached. Then, a positive feedback loop of activated sodium channels on other sodium channels results in a fast inward sodium current (I_{Na}), responsible for the upstroke of the action potential (phase 0). Afterwards, these Nav1.5 channels are inactivated for the duration of the action potential, determining the refractory period^{5,6}.

The fast upstroke of the human action potential is followed by a brief repolarization (phase 1), due to efflux of potassium ions, caused by the transient outward current (I_{TO}). Concurrently, calcium ions enter the cell through voltage-gated calcium channels, mainly L-type calcium channels. These calcium ions are key players in the excitation-contraction coupling, resulting in mechanical activity of the cell. This influx of positively charged calcium is counterbalanced by the efflux of positively charged potassium ions, explaining the plateau phase of the action potential (phase 2). The closure of the calcium channels initiates the repolarization phase 3. The outward potassium current during phase 2 and 3 is caused by I_{TO} , the inward rectifier current (I_{K1}) and the delayed rectifier current (I_{K}), which is divided in a slow (I_{Ks}) and a fast (I_{Kr}) component^{5,7}. The inward rectifier potassium current (I_{K1}) is particularly involved in the final repolarization at the end of phase 3, which brings the membrane potential back to $\pm -80\text{mV}$. In addition, I_{K1} is the major determinant of the resting membrane potential during phase 4^{8,9}.

Expression of the different ion channels varies among the mammal-species, explaining the significant differences in the shape of the action potential. Figure 1B shows a short murine

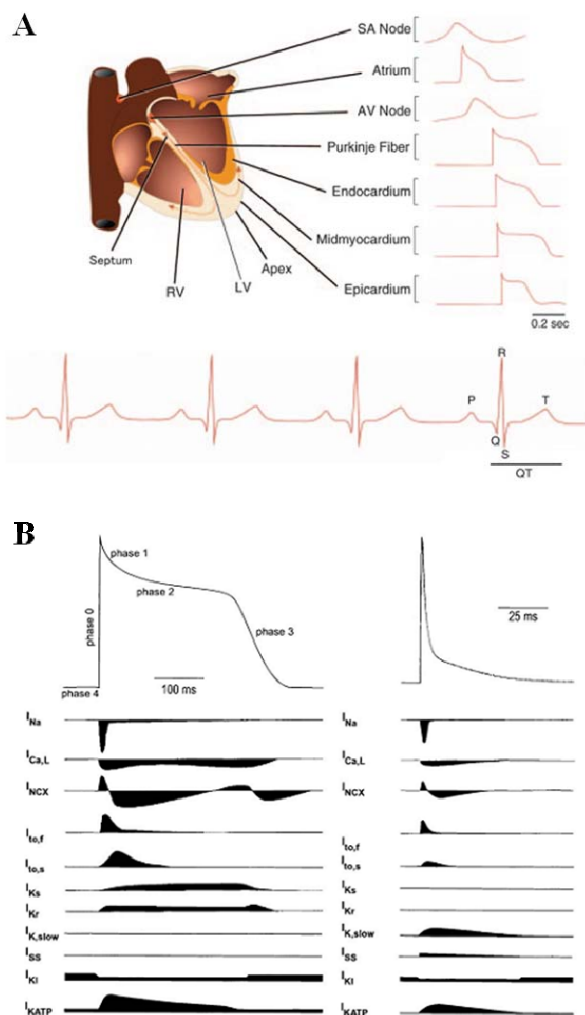


Figure 1 – Electrical activation of the heart (redrawn from ⁷ and ¹¹). Panel A shows a schematic of the human heart, with the region-specific action potentials and the resulting ECG. Panel B shows a human and murine ventricular action potential, respectively, with the active currents during the different phases of the action potential.

action potential that lacks a plateau phase, in contrast to the human action potential ¹⁰⁻¹². Ion channels are also not equally distributed in the heart. For example, Nav1.5 expression is high in ventricular myocardium, especially in Purkinje fibers, but low in the SA- and AV-node. Furthermore, several ion channels have different expression levels from endo- to

epicard, from base to apex and from the right to the left ventricle. As a result, endocardial action potentials are longer compared to epicardial action potentials, left ventricular action potentials are longer than those in the right ventricle and action potential duration increases from base to apex¹³⁻¹⁶.

Many defects in ion channels, so-called channelopathies, have been described, which are frequently caused by mutations in the genes, encoding for the channels. Loss of function mutations in the gene *Scn5a*, encoding for Nav1.5 channels, have been found in patients with Brugada syndrome, sick sinus syndrome and Lev / Lenègre disease. Loss of function mutations result in less sodium current and impaired conduction of the electrical impulse. Also gain of function mutations in *Scn5a* have been described, resulting in a persistent sodium current, increasing action potential duration, as found in patients with long-QT3 (LQT₃) syndrome¹⁷⁻²⁰.

Another channelopathy is Andersen-Tawil syndrome, which is characterized by a high mortality due to ventricular arrhythmias. This disease is caused by mutations in the *KCNJ2*-gene, encoding for Kir2.1-channels, which are the main contributors to the I_{K1} current^{21, 22}. A downregulation of Kir2.1 channels is a predominant finding in patients suffering from heart failure, partly responsible for the impaired conduction in these patients^{23, 24}.

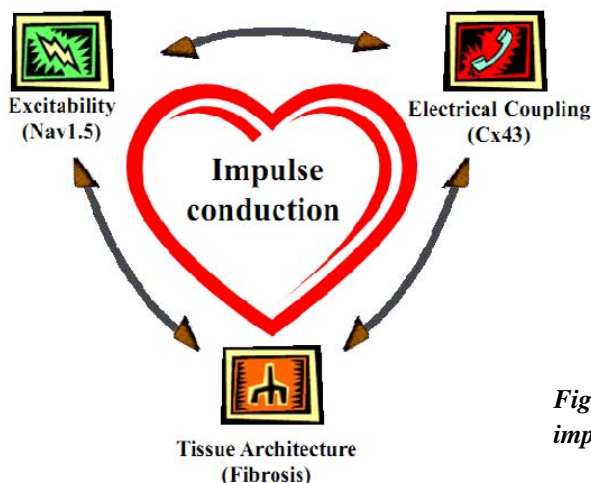


Figure 2 – Determinants of impulse conduction

The velocity with which the action potential is conducted from cell to cell depends on the excitability, cell-to-cell coupling and tissue characteristics, as shown in figure 2. The first factor as mentioned is mainly determined by Nav1.5 channels, but also Kir2.1 channels play an important role. The second determinant of impulse conduction is cell-to-cell coupling, which is dependent on gap junctions. These communicating junctions are formed by connexin proteins, in the ventricular myocardium mainly connexin43 (Cx43). Chapter 1

gives an extensive overview of the different cardiac connexins, and their expressions patterns in the healthy and diseased heart. A decreased expression of Nav1.5 and/or Cx43, as found in a variety of cardiac disorders, can decrease impulse conduction velocity, increasing the risk for lethal ventricular arrhythmias^{25, 26}. Those downregulations are frequently accompanied by a more heterogeneous expression of those proteins, which is often associated with an increased dispersion of conduction and / or repolarization²⁷⁻²⁹. Furthermore, lateralization of Cx43 plaques is often observed³⁰.

The final conduction-determinant is the tissue architecture, mainly determined by the amount of collagen. In the healthy heart, cardiomyocytes are imbedded in thin fibers of collagen, providing essential strength during contraction and relaxation. However, excessive deposition of collagen, which is called fibrosis, can disrupt intracellular communication, thereby slowing impulse conduction and increasing the risk for cardiac arrhythmias^{31, 32}. This risk is also dependent on the architecture of the fibrotic strands: patchy fibrosis with long strands of dense collagen significantly affects conduction, whereas diffuse fibrosis only has a marginal impact. Besides, transverse conduction is more severely reduced compared to longitudinal conduction³³.

Besides slowed conduction, an increased dispersion of conduction, with parts of local slow conduction, can increase the risk for arrhythmias. Those areas of slow conduction are more vulnerable to functional block during premature activation, which can initiate a reentry-based tachycardia. Particularly a more heterogeneous expression or a local depletion of Cx43 proteins, together with patchy fibrosis, is assumed to promote a more dispersed conduction^{29, 33}.

Although cardiac excitability, cell-to-cell coupling and tissue architecture are considered as individual parameters, their remodeling occurs in concert in many cardiac disorders. Patients with hypertrophic and ischemic cardiomyopathy have both decreased inward sodium current and Cx43-expression, and increased collagen levels³⁴⁻³⁷. In the process towards heart failure, remodeling increases and impulse conduction gets progressively impaired, increasing the risk for triggered activity and reentry-based ventricular tachycardias. This may account, at least in part, for the high incidence of sudden cardiac death³⁸. In patients with arrhythmogenic right ventricular cardiomyopathy (ARVC), decreased Cx43 levels are found, together with increased fibrosis^{39, 40}. Lev / Lenègre disease, recently related to Scn5a-mutations, was originally characterized by fibrosis and degeneration of the conduction system^{41, 42}. Increased fibrosis in concert with decreased Cx43 and Nav1.5 are also observed in the physiological process of aging⁴³⁻⁴⁵.

Several studies on animal models have shown that a moderate alteration in one of the conduction parameters did not have a significant effect on impulse conduction, and did not increase arrhythmia vulnerability: mice with a 50% reduction in Cx43 expression, a 50% reduction in Nav1.5, or a 5 times increase in fibrosis showed near normal conduction^{43, 46}. This resistance to moderate changes in single conduction parameters has been coined

‘conduction reserve’⁴⁷. Combining a decrease in Cx43 and Nav1.5 or a decrease in Nav1.5 with an increase in fibrosis had slightly more impact on impulse conduction, but arrhythmias were still absent^{43, 48}. Just a further decreased Cx43 expression to 5% did result in high arrhythmia susceptibility due to severely disturbed conduction⁴⁶.

Arrhythmias were also provoked in senescent mice, in which both a decreased expression of Nav1.5 and Cx43 and an increase in fibrosis were found. In these mice, arrhythmia susceptibility was mainly associated with right ventricular fibrosis⁴⁴. Another study shows that inhibition of the renin-angiotensin-aldosterone system (RAAS) in aged mice reduced fibrosis, and subsequently the vulnerability for arrhythmias⁴⁵. Others have shown that in cardiomyopathic hamsters and mice with pressure overload, RAAS-inhibition not only protects against fibrosis, but also prevents Cx43 remodeling^{49, 50}. These studies show that (1) fibrosis is a key factor in arrhythmogenesis and (2) increased levels of fibrosis are generally accompanied by reduced Cx43 expression. This last point is further strengthened by the finding that aged mice with a 50% reduction in Nav1.5 expression have both decreased levels of Cx43 and increased amounts of collagen⁴³. From these results, we postulated the following general hypothesis:

‘Abnormal Nav1.5 expression leads to abnormal Cx43 expression, which in turn enhances the formation of fibrosis. This ultimately forms the arrhythmogenic substrate.’

This hypothesis directly leads to the first 2 research questions of this thesis:

1. Does reduced Cx43 expression lead to enhanced fibrosis and arrhythmias?
2. Does reduced Nav1.5 expression lead to reduced Cx43 expression and enhanced fibrosis?

These aims are illustrated in Figure 3. However, when Cx43 levels are down to ~5%, the hearts become arrhythmogenic in the absence of fibrosis and without severe overall conduction slowing. Arrhythmogeneity may therefore be due to local heterogeneities in Cx43 expression possibly combined with changes in sodium channel expression as observed in ARVC models. This raised the third research question:

3. Are decreased Cx43 levels arrhythmogenic due to a heterogeneous reduction of Cx43, combined with decreased Nav1.5 levels?

Finally, we focused on one of the mechanisms that could be responsible for a decreased expression of gap junction or ion channels in many cardiac disorders i.e. modified degradation of the proteins via the lysosomal or proteasomal pathway. Since the exact degradation pathway for many ion channels is unknown, we examined the breakdown of one of the ion channels that determines excitability of cardiomyocytes, Kir2.1. This brings up the last research question:

4. Is the lysosomal degradation pathway involved in the breakdown of Kir2.1?

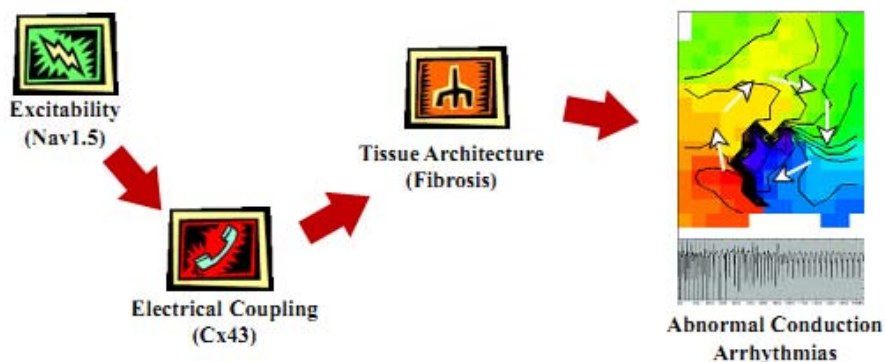


Figure 3 – General hypothesis

This thesis starts with an extensive overview of connexin expression in the heart. In this first chapter, the different cardiac connexins, and their expression patterns in the healthy and diseased heart, are reviewed.

In chapter 2, we used Kir2.1-overexpressing cells to investigate whether the lysosomal degradation pathway was involved in the breakdown of Kir2.1 (aim 4). This was tested by incubation with several lysosomal degradation inhibitors, and measuring Kir2.1 protein levels and I_{K1} currents.

In chapter 3 and 4, we focused on the general hypothesis of this thesis by challenging hearts in the background of an affected conduction parameter. We analyzed the arrhythmogenic phenotype of the mice, and focused on the influence on other conduction determinants. In chapter 3, we used mice with a 50% reduction in Cx43 expression (Cx43^{Cre-ER(T)/fl} mice) compared to their control, Cx43^{fl/fl} mice⁴⁶. We hypothesized that challenging these mice would result in enhanced fibrosis and high arrhythmia vulnerability (aim 1). This was tested by applying both physiological (aging) and pathological (pressure overload by transverse aortic constriction, TAC) stress to these animals. The process of collagen deposition was further analyzed in TAC-operated mice.

In chapter 4, we used Scn5a^{1798insD/+} mice, carrying the mouse equivalent of the human 1795insD mutation⁵¹. This mutation has been linked to long-QT3 (LQT₃), Brugada syndrome and progressive conduction disease^{17, 52}. Since aortic stenosis is frequently observed in Lev / Lenègre disease, we hypothesized that TAC-operation in these mice would mimic aortic stenosis in Scn5a^{1798insD/+} mice, resulting in a Lev / Lenègre phenotype⁴¹. Since patients with Lev / Lenègre disease have increased levels of fibrosis in the conduction system, we hypothesized that these mice would have enhanced collagen deposition, accompanied by decreased Cx43 levels (aim 2).

When Cx43 expression levels are further reduced to <5%, conduction is severely impaired, with high arrhythmia vulnerability ⁴⁶. We hypothesized that the arrhythmogenic vulnerability is determined by the degree of heterogeneous downregulation of Cx43, together with a decreased Nav1.5 expression (aim 3). For this purpose, we further analyzed these mice by comparing arrhythmogenic to non-arrhythmogenic animals in chapter 5.

Finally, chapter 6 summarizes and discusses the results of preceding chapters.

References

1. Irisawa H, Brown HF, Giles W. Cardiac pacemaking in the sinoatrial node. *Physiol Rev.* 1993;73:197-227
2. Meijler FL, Janse MJ. Morphology and electrophysiology of the mammalian atrioventricular node. *Physiol Rev.* 1988;68:608-647
3. Billette J, Nattel S. Dynamic behavior of the atrioventricular node: A functional model of interaction between recovery, facilitation, and fatigue. *J Cardiovasc Electrophysiol.* 1994;5:90-102
4. Einthoven W. Ueber die form des menschlichen electrocardiogramms. *Arch Ges Physiol.* 1895;60:101-123
5. Kleber AG, Rudy Y. Basic mechanisms of cardiac impulse propagation and associated arrhythmias. *Physiol Rev.* 2004;84:431-488
6. Hodgkin AL, Huxley AF. A quantitative description of membrane current and its application to conduction and excitation in nerve. *J Physiol.* 1952;117:500-544
7. Nerbonne JM, Kass RS. Molecular physiology of cardiac repolarization. *Physiol Rev.* 2005;85:1205-1253
8. Dhamoon AS, Jalife J. The inward rectifier current (ik1) controls cardiac excitability and is involved in arrhythmogenesis. *Heart Rhythm.* 2005;2:316-324
9. de Boer TP, Houtman MJ, Compier M, van der Heyden MA. The mammalian k(ir)2.X inward rectifier ion channel family: Expression pattern and pathophysiology. *Acta Physiol (Oxf).* 2010;199:243-256
10. Nerbonne JM, Nichols CG, Schwarz TL, Escande D. Genetic manipulation of cardiac k(+) channel function in mice: What have we learned, and where do we go from here? *Circ Res.* 2001;89:944-956
11. London B, Guo W, Pan X, Lee JS, Shusterman V, Rocco CJ, Logothetis DA, Nerbonne JM, Hill JA. Targeted replacement of kv1.5 in the mouse leads to loss of the 4-aminopyridine-sensitive component of i(k,slow) and resistance to drug-induced qt prolongation. *Circ Res.* 2001;88:940-946
12. Sabir IN, Killeen MJ, Grace AA, Huang CL. Ventricular arrhythmogenesis: Insights from murine models. *Prog Biophys Mol Biol.* 2008;98:208-218
13. Nabauer M. Electrical heterogeneity in the ventricular wall--and the m cell. *Cardiovasc Res.* 1998;40:248-250
14. Antzelevitch C. Electrical heterogeneity, cardiac arrhythmias, and the sodium channel. *Circ Res.* 2000;87:964-965
15. Szentadrassy N, Banyasz T, Biro T, Szabo G, Toth BI, Magyar J, Lazar J, Varro A, Kovacs L, Nanasi PP. Apico-basal inhomogeneity in distribution of ion channels in canine and human ventricular myocardium. *Cardiovasc Res.* 2005;65:851-860
16. Volders PG, Sipido KR, Carmeliet E, Spatjens RL, Wellens HJ, Vos MA. Repolarizing k+ currents ito1 and iks are larger in right than left canine ventricular midmyocardium. *Circulation.* 1999;99:206-210
17. Bezzina C, Veldkamp MW, van Den Berg MP, Postma AV, Rook MB, Viersma JW, van Langen IM, Tan-Sindhunata G, Bink-Boelkens MT, van Der Hout AH, Mannens MM, Wilde AA. A single na(+) channel mutation causing both long-qt and brugada syndromes. *Circ Res.* 1999;85:1206-1213
18. Schott JJ, Alshinawi C, Kyndt F, Probst V, Hoorntje TM, Hulsbeek M, Wilde AA, Escande D, Mannens MM, Le Marec H. Cardiac conduction defects associate with mutations in scn5a. *Nat Genet.* 1999;23:20-21
19. Kyndt F, Probst V, Potet F, Demolombe S, Chevallier JC, Baro I, Moisan JP, Boisseau P, Schott JJ, Escande D, Le Marec H. Novel scn5a mutation leading either to isolated cardiac conduction defect or brugada syndrome in a large french family. *Circulation.* 2001;104:3081-3086
20. Benson DW, Wang DW, Dymont M, Knilans TK, Fish FA, Strieper MJ, Rhodes TH, George AL, Jr. Congenital sick sinus syndrome caused by recessive mutations in the cardiac sodium channel gene (scn5a). *J Clin Invest.* 2003;112:1019-1028
21. Plaster NM, Tawil R, Tristani-Firouzi M, Canun S, Bendahhou S, Tsunoda A, Donaldson MR, Iannaccone ST, Brunt E, Barohn R, Clark J, Deymeer F, George AL, Jr., Fish FA, Hahn A, Nitu A,

- Ozdemir C, Serdaroglu P, Subramony SH, Wolfe G, Fu YH, Ptacek LJ. Mutations in kir2.1 cause the developmental and episodic electrical phenotypes of andersen's syndrome. *Cell*. 2001;105:511-519
22. Jongsma HJ, Wilders R. Channelopathies: Kir2.1 mutations jeopardize many cell functions. *Curr Biol*. 2001;11:R747-750
23. Nattel S, Maguy A, Le Bouter S, Yeh YH. Arrhythmogenic ion-channel remodeling in the heart: Heart failure, myocardial infarction, and atrial fibrillation. *Physiol Rev*. 2007;87:425-456
24. Sekar RB, Kizana E, Cho HC, Molitoris JM, Hesketh GG, Eaton BP, Marban E, Tung L. Ik1 heterogeneity affects genesis and stability of spiral waves in cardiac myocyte monolayers. *Circ Res*. 2009;104:355-364
25. Borlak J, Thum T. Hallmarks of ion channel gene expression in end-stage heart failure. *Faseb J*. 2003;17:1592-1608
26. Dhein S. Cardiac ischemia and uncoupling: Gap junctions in ischemia and infarction. *Adv Cardiol*. 2006;42:198-212
27. Polontchouk L, Haefliger JA, Ebel B, Schaefer T, Stuhlmann D, Mehlhorn U, Kuhn-Regnier F, De Vivie ER, Dhein S. Effects of chronic atrial fibrillation on gap junction distribution in human and rat atria. *J Am Coll Cardiol*. 2001;38:883-891
28. Wiegierinck RF, van Veen TA, Belterman CN, Schumacher CA, Noorman M, de Bakker JM, Coronel R. Transmural dispersion of refractoriness and conduction velocity is associated with heterogeneously reduced connexin43 in a rabbit model of heart failure. *Heart Rhythm*. 2008;5:1178-1185
29. Boulaksil M, Winkels SK, Engelen MA, Stein M, van Veen TA, Jansen JA, Linnenbank AC, Bierhuizen MF, Groenewegen WA, van Oosterhout MF, Kirkels JH, de Jonge N, Varro A, Vos MA, de Bakker JM, van Rijen HV. Heterogeneous connexin43 distribution in heart failure is associated with dispersed conduction and enhanced susceptibility to ventricular arrhythmias. *Eur J Heart Fail*. 2010;12:913-921
30. Kitamura H, Ohnishi Y, Yoshida A, Okajima K, Azumi H, Ishida A, Galeano EJ, Kubo S, Hayashi Y, Itoh H, Yokoyama M. Heterogeneous loss of connexin43 protein in nonischemic dilated cardiomyopathy with ventricular tachycardia. *J Cardiovasc Electrophysiol*. 2002;13:865-870
31. La Vecchia L, Ometto R, Bedogni F, Finocchi G, Mosele GM, Bozzola L, Bevilacqua P, Vincenzi M. Ventricular late potentials, interstitial fibrosis, and right ventricular function in patients with ventricular tachycardia and normal left ventricular function. *Am J Cardiol*. 1998;81:790-792
32. Swynghedauw B. Molecular mechanisms of myocardial remodeling. *Physiol Rev*. 1999;79:215-262
33. Kawara T, Derksen R, de Groot JR, Coronel R, Tasseron S, Linnenbank AC, Hauer RN, Kirkels H, Janse MJ, de Bakker JM. Activation delay after premature stimulation in chronically diseased human myocardium relates to the architecture of interstitial fibrosis. *Circulation*. 2001;104:3069-3075
34. Winterton SJ, Turner MA, O'Gorman DJ, Flores NA, Sheridan DJ. Hypertrophy causes delayed conduction in human and guinea pig myocardium: Accentuation during ischaemic perfusion. *Cardiovasc Res*. 1994;28:47-54
35. Peters NS. New insights into myocardial arrhythmogenesis: Distribution of gap-junctional coupling in normal, ischaemic and hypertrophied human hearts. *Clin Sci (Lond)*. 1996;90:447-452
36. McIntyre H, Fry CH. Abnormal action potential conduction in isolated human hypertrophied left ventricular myocardium. *J Cardiovasc Electrophysiol*. 1997;8:887-894
37. Kostin S, Rieger M, Dammer S, Hein S, Richter M, Klovekorn WP, Bauer EP, Schaper J. Gap junction remodeling and altered connexin43 expression in the failing human heart. *Mol Cell Biochem*. 2003;242:135-144
38. Levy D, Anderson KM, Savage DD, Balkus SA, Kannel WB, Castelli WP. Risk of ventricular arrhythmias in left ventricular hypertrophy: The framingham heart study. *Am J Cardiol*. 1987;60:560-565
39. Saffitz JE. Arrhythmogenic cardiomyopathy and abnormalities of cell-to-cell coupling. *Heart Rhythm*. 2009;6:S62-65
40. Oxford EM, Everitt M, Coombs W, Fox PR, Kraus M, Gelzer AR, Saffitz J, Taffet SM, Moise NS, Delmar M. Molecular composition of the intercalated disc in a spontaneous canine animal model of arrhythmogenic right ventricular dysplasia/cardiomyopathy. *Heart Rhythm*. 2007;4:1196-1205

41. Lenegre J, Moreau P, Iris L. [2 cases of complete auriculo-ventricular block due to primary sarcoma of the heart.]. *Arch Mal Coeur Vaiss.* 1964;56:361-387
42. Lev M. Anatomic basis for atrioventricular block. *Am J Med.* 1964;37:742-748
43. van Veen TA, Stein M, Royer A, Le Quang K, Charpentier F, Colledge WH, Huang CL, Wilders R, Grace AA, Escande D, de Bakker JM, van Rijen HV. Impaired impulse propagation in scn5a-knockout mice: Combined contribution of excitability, connexin expression, and tissue architecture in relation to aging. *Circulation.* 2005;112:1927-1935
44. Stein M, Noorman M, van Veen TA, Herold E, Engelen MA, Boulaksil M, Antoons G, Jansen JA, van Oosterhout MF, Hauer RN, de Bakker JM, van Rijen HV. Dominant arrhythmia vulnerability of the right ventricle in senescent mice. *Heart Rhythm.* 2008;5:438-448
45. Stein M, Boulaksil M, Jansen JA, Herold E, Noorman M, Joles JA, van Veen TA, Houtman MJ, Engelen MA, Hauer RN, de Bakker JM, van Rijen HV. Reduction of fibrosis-related arrhythmias by chronic renin-angiotensin-aldosterone system inhibitors in an aged mouse model. *Am J Physiol Heart Circ Physiol.* 2010;299:H310-321
46. van Rijen HV, Eckardt D, Degen J, Theis M, Ott T, Willecke K, Jongsma HJ, Opthof T, de Bakker JM. Slow conduction and enhanced anisotropy increase the propensity for ventricular tachyarrhythmias in adult mice with induced deletion of connexin43. *Circulation.* 2004;109:1048-1055
47. van Rijen HV, de Bakker JM, van Veen TA. Hypoxia, electrical uncoupling, and conduction slowing: Role of conduction reserve. *Cardiovasc Res.* 2005;66:9-11
48. Stein M, van Veen TA, Remme CA, Boulaksil M, Noorman M, van Stuijvenberg L, van der Nagel R, Bezzina CR, Hauer RN, de Bakker JM, van Rijen HV. Combined reduction of intercellular coupling and membrane excitability differentially affects transverse and longitudinal cardiac conduction. *Cardiovasc Res.* 2009;83:52-60
49. De Mello WC, Specht P. Chronic blockade of angiotensin ii at1-receptors increased cell-to-cell communication, reduced fibrosis and improved impulse propagation in the failing heart. *J Renin Angiotensin Aldosterone Syst.* 2006;7:201-205
50. Qu J, Volpicelli FM, Garcia LI, Sandeep N, Zhang J, Marquez-Rosado L, Lampe PD, Fishman GI. Gap junction remodeling and spironolactone-dependent reverse remodeling in the hypertrophied heart. *Circ Res.* 2009;104:365-371
51. Remme CA, Verkerk AO, Nuyens D, van Ginneken AC, van Brunschot S, Belterman CN, Wilders R, van Roon MA, Tan HL, Wilde AA, Carmeliet P, de Bakker JM, Veldkamp MW, Bezzina CR. Overlap syndrome of cardiac sodium channel disease in mice carrying the equivalent mutation of human scn5a-1795insd. *Circulation.* 2006;114:2584-2594
52. Postema PG, Van den Berg M, Van Tintelen JP, Van den Heuvel F, Grundeken M, Hofman N, Van der Roest WP, Nannenber EA, Krapels IP, Bezzina CR, Wilde A. Founder mutations in the netherlands: Scn5a 1795insd, the first described arrhythmia overlap syndrome and one of the largest and best characterised families worldwide. *Neth Heart J.* 2009;17:422-428

Chapter 1 – Cardiac Connexins and Impulse Propagation

John A. Jansen, Toon A.B. van Veen, Jacques M.T. de Bakker and Harold V.M. van Rijen

J Mol Cell Cardiol 2010;48:76-82

Cardiac Connexins and Impulse Propagation

John A. Jansen¹; Toon A.B. van Veen¹; Jacques M.T. de Bakker^{1,2,3}; Harold V.M. van Rijen¹

1. Department of Medical Physiology, Division Heart and Lungs, University Medical Center Utrecht, The Netherlands
2. Heart Failure Research Center, Academic Medical Center, Amsterdam, The Netherlands
3. Interuniversity Cardiology Institute of the Netherlands, Utrecht, The Netherlands

Abstract

Gap junctions form the intercellular pathway for cell-to-cell transmission of the cardiac impulse from its site of origin, the sinoatrial node, along the atria, the atrioventricular conduction system to the ventricular myocardium. The component parts of gap junctions are proteins called connexins (Cx), of which 3 main isoforms are found in the conductive and working myocardial cells: Cx40, Cx43, and Cx45. These isoforms are regionally expressed in the heart, which suggests a specific role or function of a specific connexin in a certain part of the heart. Using genetically modified mice, the function of these connexins in the different parts of the heart have been assessed in the past years. This review will follow the cardiac impulse on its path through the heart and recapitulate the role of the different connexins in the different cardiac compartments.

Introduction

Every normal heart beat is initiated in the sinoatrial node, conducted along the atria, delayed at the AV-node, after which the ventricular myocardium is activated via the specialized conduction system. After activation, the impulse is conducted from myocyte to myocyte along the entire myocardium.

The process of impulse conduction is governed by three factors: 1. Excitability of single cardiomyocytes, 2. Electrical coupling between myocytes, and 3. Network properties of cardiac tissue¹. Excitability of single myocytes is determined by the amount of sodium current, which not only generates the depolarizing current for local cellular activation, but also for activation of adjacent cells by passing depolarizing current through gap junctions. Impulse propagation is dependent on multiple factors, in which the interaction between inward currents, such as I_{Na} and I_{Ca} , electrical coupling, cell size, resting potential and input impedance are involved²⁻⁵. This review will focus on the role of gap junctions in impulse conduction in the heart under physiological and pathophysiological conditions.

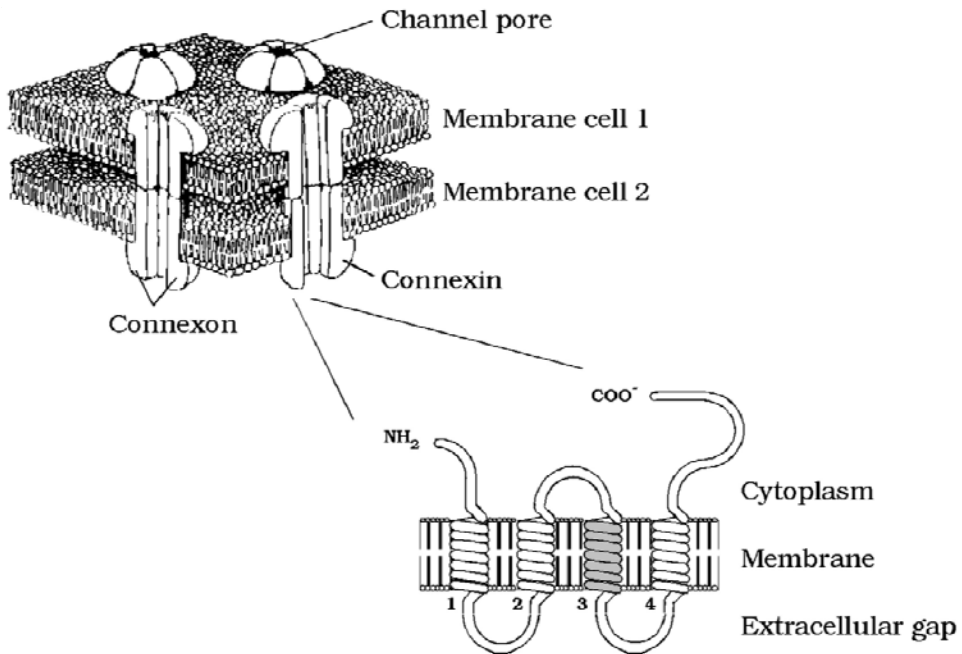


Figure 1- Artists impression of a gap junction plaque. Every gap junction channel is composed of 2 connexons, each of which is composed of 6 connexins. Adapted from⁸.

Cardiac Gap Junctions

Gap junctions were named after their appearance in transmission electron microscopy. At the interface of 2 adjacent cells, the two membranes are separated by an electron-dense structure with a characteristic gap of 2-3 nm.

Each gap junction channel is composed of 2 hemichannels, also called connexons, one provided by each cell. Two connexons of adjoining cells pair to form a functional channel, which connects the cytoplasm of both cells (figure 1, upper panel). Connexons are hexamers of proteins called connexins. At present, more than 20 connexin genes have been identified in mouse and human^{6,7}. They are named after their theoretical molecular mass. The molecular structure of the connexins is very similar among all members. They all have 4 membrane spanning domains, 2 extracellular loops and the amino- and carboxy-terminus, which are located at the cytoplasmic side (figure 1, lower panel). Although very similar in structure, the biophysical properties of the channels formed by different connexin family members is very different^{8,9}.

In the heart, 3 main isoforms are found in the conductive and working myocardial cells: Cx40, Cx43, and Cx45. Figure 2 shows the regional expression of these Cxs in the mouse heart. Cx40 is mainly expressed in the atrial myocytes, in the AV-node, His-bundle and the ventricular conduction system¹⁰⁻¹⁵. Cx43 is by far the most abundant, and is expressed between atrial and ventricular myocytes and distal parts of the conduction system^{12, 15-23}. The expression of Cx45 is mainly localized in the sinoatrial node (SAN), the atrioventricular node (AVN), His-bundle and bundle branches^{15, 24-27}. Low levels of Cx45 were also detected in atrial and ventricular myocytes^{28, 29}, although other studies, using different antibodies, were not able to confirm these findings²⁴.

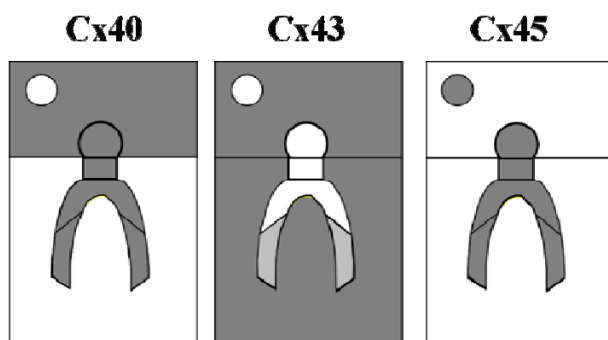


Figure 2: Chamber specific expression of Cx40, Cx43, and Cx45 in the mouse heart (redrawn after³⁴).

In mice, a fourth connexin is found, i.e. Cx30.2 which is expressed in the SAN, AVN and His-bundle³⁰. Since the human orthologue of Cx30.2, Cx31.9, was detected in the human heart, Cx30.2 may represent a mouse specialization³¹.

Gap junctions between ventricular myocytes are expressed in a polarized way. Gap junctions are mainly localized at intercalated disks, and have relatively low density at lateral sides^{22, 23, 32-35}. The intercalated disk region itself is a highly three-dimensional structure, in which gap junctions connect adjacent cells both in the plicate (regions perpendicular to the long axis of the cells) and interplicate regions (those more or less parallel to the long axis of the cells). Several studies suggest that gap junctions are more abundant in the interplicate regions than in the plicate regions^{32, 35-41}. It seems that the gap junctions in the interplicate regions are also involved in transverse conduction.

The role of the individual cardiac connexins has been extensively studied in genetically modified mouse models, in which one or more connexins were partly or fully absent. However, because most cardiac connexins are expressed in multiple celltypes in the heart, we will follow the cardiac impulse on its path through the heart and recapitulate the role of the different connexins in the different cardiac compartments.

Connexin function in the Sinoatrial node

In the SAN, gap junctions are responsible for two main functions: 1) Maintaining regular beating frequency and 2) transferring the impulse to the atrial myocardium in the face of the hyperpolarizing atrial load⁴². Only little coupling is needed for synchronization of both frequency and waveform of individual SAN cells, thereby averaging out the small differences in intrinsic frequency and action potential shape⁴³. The issue of transfer of the electrical impulse to the atrial myocardium is not fully resolved yet. Early model studies have shown that a gradual increase in electrical coupling would be prerequisite for successful conduction of the generated impulse from SAN to the atrial myocardium^{44, 45}. Immunohistochemical studies have shown that in the center of the SAN, Cx45 is the predominant gap junction protein, although Cx40 was also found, while in the peripheral parts, Cx40 and/or Cx43 are expressed^{10, 25, 26, 46}, but some controversy exists. For an extensive review see Boyett et al⁴⁷. No clear gradient was found, but interestingly, interdigitation of strands of Cx43 expressing atrial myocytes and SAN cells were found, which may serve as transitional zone^{26, 48}. Jongsma hypothesized that heterotypic gap junctions formed of one Cx43-connexon and one Cx45-connexon, which have been shown to exhibit rectifying properties⁴⁹, may close when current flows from the atria to the SAN, while facilitating current flow from SAN to atrium⁴². In this way, the specific expression of Cxs may support SAN function.

Studies using mice knockout for Cx43 or Cx45 did not reveal significant sinus node abnormalities. Cx40^{-/-} mice displayed leading pacemaker activity as breakthrough activation at the base of the sulcus terminalis, RA free wall, and right superior vena cava, rather than at the sinoatrial node as found in wildtype mice. In Cx40^{-/-} mice, heart rate was mostly normal⁵⁰⁻⁵⁵, although some slowing was observed^{56, 57}. Haploinsufficiency for Cx45 alone or combined with Cx40 deficiency had no effect on heart rate⁵⁸. Similarly, the

absence of Cx30.2 alone, or combined with Cx40 deficiency resulted in normal sinus node function⁵⁹. Finally, haploinsufficiency for or full deletion of Cx43 did not alter sinus node function⁶⁰⁻⁶⁴.

Overall, the sinoatrial node function seems fairly robust, even when apparently essential connexins are expressed in reduced amounts. This fits well with the fact that only little amount of coupling is needed for synchronization within the sinus node⁴³. Moreover, the current-to-load mismatch between the sinus node and the atrium would presumably benefit from reduced levels of intercellular coupling⁶⁵.

Atrial Connexins

In the atria, three types of connexins are expressed, i.e. Cx40, Cx43, and Cx45. The expression level of Cx45, however is very low²⁹. In human atria Cx43 expression was found to be similar between human LA and RA, but Cx40 levels were higher in RA compared to LA²⁹. In goats however, Cx40 content was lower in RA, compared to LA, while Cx43 levels were similar between both chambers⁶⁶.

Functional measurements were performed on mice which were deficient for Cx43 or Cx40. These measurements involved ECG measurements and epicardial conduction velocity measurements. Total atrial activation times are reflected in the P-wave of the ECG, but are not only determined by atrial impulse conduction velocity, but also by the pattern of impulse spread and atrial size.

Mouse models haploinsufficient for Cx43 or conditional knockouts for Cx43 showed no significant changes in P-wave duration^{61, 64, 67} or atrial conduction velocity⁶¹. These studies indicated that Cx43 is not the dominant connexin for atrial conduction in the presence of Cx40.

To unravel the role of Cx40 in atrial conduction, many studies have been performed on Cx40 KO mice. As a general finding, haploinsufficient Cx40 KO mice were indistinguishable from wildtype mice^{50, 51, 55, 57}.

ECG recordings on homozygous Cx40 KO mice exhibited prolonged P-wave duration^{50-52, 55, 57}, which is compatible with the detected reduced right-atrial conduction velocity^{52, 55}. However, prolongation of the P-wave was not a common finding, as in other studies such a P-wave prolongation was not found^{53, 54, 56}. Moreover, Cx40 KO mice were more vulnerable to supraventricular arrhythmias^{55, 57}.

Some studies have shown that absence of Cx40 during development may result in cardiac abnormalities and malformations, such as cardiac hypertrophy in conjunction with common atrioventricular junction or a ventricular septal defect⁶⁸. This developmental aspect may not be recognized in other studies and can therefore be partly be responsible for the

observed conduction abnormalities. Alternatively, the different genetic background may be an important modulator in the developmental abnormalities in Cx40KO mice, which determines the presence or absence of malformations.

An unexpected finding is the relationship between atrial impulse conduction and the ratio of Cx40 and Cx43 expression. Kanagaratnam and coworkers showed that right atrial conduction velocity in humans was *inversely* related to the ratio $Cx40/(Cx40+Cx43)$, but linearly related to $Cx43/(Cx40+Cx43)$ ⁶⁹. Interestingly, conduction velocity was not related to Cx43 levels or total Cx (Cx40+Cx43) levels. These findings were confirmed by Beauchamp et al in cultured strands of atrial myocytes derived from mice with genetic deficiency for Cx40 or Cx43⁷⁰. Relative abundance of Cx40 decreased conduction velocity, while dominance of Cx43 increased conduction velocity.

Studies in exogenous expression systems have shown that gap junctions composed of Cx40 hemichannels and Cx43 hemichannels (homomeric/heterotypic) are not compatible⁷¹⁻⁷³ or form gap junctions with much lower total conductance⁷⁴. In atrial myocytes, where Cx40 and Cx43 are coexpressed in the same gap junctions^{69,75}, heteromeric/heterotypic channels may theoretically be formed. The presence of both Cx40 and Cx43 in the same hemichannel channels was confirmed^{76,77}, but it is not clear whether such channels are truly functional. Some studies suggested the functional presence of heteromeric/heterotypic Cx40/Cx43 channels⁷⁸, while others showed that these channels are presumably functionally insignificant⁷⁷. Taken altogether, the coexpression of Cx40 and Cx43 is associated with reduced intercellular conductance, which may explain the findings by Kanagaratnam and Beauchamp.

In the previously mentioned studies, haploinsufficiency for Cx40 was not associated with increased conduction velocity, which may be due to specific expression patterns in adult mouse myocytes⁷⁰.

The most common arrhythmia in humans is atrial fibrillation⁷⁹. A common finding in animal models and human atrial fibrillation is abnormal expression and distribution of atrial Cx40. The literature on this subject is vast and several reviews have focused on this issue⁸⁰⁻⁸³. Such abnormal expression levels and patterns of Cx40 may lead to inhomogeneous electrical coupling resulting in dispersed conduction, which forms the substrate for atrial arrhythmias.

Connexins and atrioventricular conduction

In the atrioventricular conduction system of mice, 3 types of connexins have been described, Cx40, Cx30.2, and Cx45^{10, 30, 51, 59, 84-86}. Cx31.9, the human orthologue for Cx30.2 is presumably not expressed in the human AV-node³¹, and Cx30.2 may therefore reflect a mouse specialization.

The absence of Cx40 was consistently associated with abnormal AV-conduction, i.e., prolonged PQ intervals and QRS duration^{50-52, 54-59}. The prolongation of the PQ interval was mainly located in the his-ventricle (HV) interval⁵⁹, but some reported a prolonged atrial-his (AH) interval as well^{54, 56}.

A typical finding was the delayed activation of the ventricles as detected by QRS widening and fractionation⁵⁰⁻⁵⁹. Verheule *et al.* elegantly showed that this prolonged QRS duration was only present during anterograde activation of the ventricles, but not during ventricular pacing at the apex⁵⁵. Conduction velocity in the ventricles of Cx40 KO mice was normal^{53, 55}, and the QRS-widening was attributed to abnormal conduction in the bundle branches of Cx40 KO mice. In the right bundle branch (RBB) slow conduction⁵³ or conduction block⁸⁷ was reported. In the left bundle branch, conduction was slowed by 33%⁸⁷.

The relative role of Cx45 in atrioventricular conduction was investigated in mice haploinsufficient for Cx45 in the presence or absence of Cx40⁵⁸. Haploinsufficiency for Cx45 alone did not affect atrioventricular conduction, as PQ and QRS duration was similar to control⁵⁸. Full deletion of Cx45 was not studied, because homozygous deficiency for Cx45 is lethal due to defective vascular development^{88, 89}. Interestingly, in the absence of Cx40, which by itself prolongs PQ and QRS duration, additional haploinsufficiency of Cx45 further delays atrioventricular conduction and ventricular activation⁵⁸.

The last atrioventricular connexin, Cx30.2 has an intriguing role. Cx30.2 is expressed in the atrioventricular node and His-bundle³⁰. Mice, knockout for Cx30.2 exhibited a decreased PQ duration, indicating *increased* atrioventricular conduction⁹⁰. This decrease in AV delay was attributable to decreased AH, but not HV intervals, indicating increased supraHisian conductivity⁹⁰. Mice double deficient for Cx40 and Cx30.2 showed normal AH and HV intervals. Schrickel *et al.* concluded that in the atrioventricular conduction system, Cx45 is sufficient for impulse propagation in the AV node, where Cx40 and Cx30.2 act as counterparts which increase or decrease conduction velocity, respectively⁵⁹.

Ventricular Connexins

In the ventricular myocardium, Cx43 is the main connexin. Cx43 KO mice died perinatally, due to a cardiac malformation of the pulmonary outflow tract⁹¹⁻⁹³. Cx43 haploinsufficient and conditional knockout mice have been generated and analyzed.

A 50% reduction in Cx43 expression (Cx43^{+/-} mice) was found to result in an increased activation delay of the ventricles and reduced conduction velocity^{60, 61, 94, 95}. In other studies, however, a similar 50% reduction of Cx43 expression, did not alter conduction velocity in the mouse heart^{62, 96}.

Because the perinatal death of Cx43^{-/-} mice prevented analysis of conduction in those hearts, conduction was determined in strands of ventricular myocytes from germline Cx43^{-/-} mice. In strands of Cx43^{+/-} myocytes, Cx43 protein expression was reduced by 43%, but conduction velocity was unchanged⁹⁷. The same group showed that in strands of Cx43^{-/-} ventricular myocytes, Cx43 expression was absent and conduction velocity was reduced by 96%⁹⁸. This very slow conductance was dependent on the presence of low levels Cx45.

To obtain a mouse model with more than 50% Cx43 protein reduction without perinatal lethality, several conditional Cx43 knockout mouse models, based on the Cre/LoxP system were generated. In one study, expression of the Cre enzyme was driven by the α -myosin heavy chain (aMHC) or myosin light chain 2v (MLC2v) promoter⁶³. The mice developed normally, but died suddenly within 2 months after birth. A selective bred, selecting for progressively older aMHC-Cre/Cx43^{fl/fl} mice resulted in mice with a more gradual loss of Cx43 and prolonged lifespan (up to 300 days)⁶⁷. In another model, one coding region of the Cx43 gene was replaced by Cre-ER(T), a fusion construct of the Cre recombinase and a specifically mutated version of the ligand binding domain of the human estrogen receptor⁹⁹. The second Cx43 region was floxed and deletion was induced by injection of 4-hydroxytamoxifen (4-OHT; Cx43^{Cre-ER(T)/fl} model)⁶⁴. This resulted in sudden death of all induced Cx43^{Cre-ER(T)/fl} mice within 1 month after the induced deletion⁶⁴.

The general outcome of the studies on the conditional Cx43 KO models is that ventricular conduction slowing and ventricular arrhythmias become prominent only when Cx43 levels drop to levels below 20% of control^{63, 67, 96}. At these low levels, Cx43 expression was found to be heterogeneous^{63, 67, 96}. Telemetric recordings revealed lethal ventricular tachyarrhythmias^{63, 64}. Epicardial mapping showed that conduction slowing was more prominent transverse to myocardial fiber direction (CV_{trans}) than in the longitudinal direction (CV_{long})^{63, 96} and that the right ventricle is more sensitive to Cx43 changes than the left⁹⁶. Arrhythmias were induced during epicardial mapping, which originated from the RV, showing stable anisotropic reentry and fibrillatory conduction on the LV⁹⁶.

The intriguing outcome of the Cx43 conditional KO studies was that even at very low levels of Cx43, conduction was maintained at ~50% of normal velocity. These observations compare well to studies performed *in silico* which showed that the relationship between junctional conductance and conduction velocity was non linear, and very substantial reductions were required for conduction slowing^{100, 101}. During uncoupling, conduction slowing was paralleled by two other changes: 1. increasing safety factor and 2. increased action potential upstroke velocity (V_{max}). 1. Safety Factor (SF) describes the relationship between activated cells acting as current source and current sinks, which are the cells that receive the current for activation. For a detailed explanation please refer to reference 1. If the amount of source current exactly matches the required sink current, SF equals 1. A SF >1 means that more current is generated during excitation than needed for exciting the sink cells. If SF <1 conduction block occurs. Computer modeling and *in vitro* studies showed that mild uncoupling increases SF, and can sustain very slow conduction successfully;

however, a high level of uncoupling reduces SF and results in conduction block^{2, 102}. 2. The second *in silico* finding during uncoupling was an increased Vmax¹⁰⁰. This was also reported during experiments *in vivo*¹⁰³ and *in vitro*^{97, 98}. These combined findings fit well in the concept of ‘discontinuous conduction’ in the heart. This concept is explained well by Spach: ‘At the microscopic level, there are recurrent discontinuities of intercellular resistance, which in turn alter the membrane ionic currents by means of electrical loading’¹⁰⁴. In cardiac preparations, Vmax was dependent on the direction of conduction and was, apparently paradoxical, larger during slow conduction in the high resistive direction perpendicular to myocyte orientation. Vmax was lower parallel the long and low resistive axis of the myocytes⁴. In conclusion, partial or substantial uncoupling may lead to slowed conduction with higher safety, but may be partly counteracted by concomitant increase of Vmax.

Virtually any type of ventricular remodeling, due to cardiac overload is characterized by changes in the expression and distribution of Cx43. The first reports on gap junction remodeling in human cardiac disease involved lateralized and reduced Cx43 expression with fiber disarray in the infarct border zone^{40, 41, 105}. In hypertrophic cardiomyopathy, early compensated hypertrophic remodeling resulting from aortic stenosis was correlated with a strong increase in Cx43 expression with extensive lateral staining¹⁰⁶. Interestingly, Cx43 expression was reduced and heterogeneously distributed without lateralization in more progressive decompensated stages of this disease¹⁰⁶. Other studies have shown that in humans, hypertrophic cardiomyopathy (HCM) can be related to downregulation of Cx43 without lateralization⁴⁰ or to lateralization without changes in Cx43 levels³⁵. Dilated cardiomyopathies in humans are reported to be linked to reduced Cx43 expression, mostly with a lateralized expression pattern¹⁰⁷⁻¹¹⁰. In patients with DCM, those with VT showed a heterogeneously reduced expression of Cx43 compared to those without VT¹⁰⁷. In the case of ischemic cardiomyopathy, the infarct border zone, the myocardial zone located directly next to the infarct scar, is most subject to remodeling.

Concluding remarks

Gap junctions, formed of various connexins form the intercellular pathway for transmission of the cardiac impulse from the sinoatrial node to the ventricular myocardium. The chamber specific expression and function of connexin isoforms is also reflected by the pathophysiological changes. Abnormal Cx40 expression is associated with atrial fibrillation, while abnormal Cx43 expression in the ventricle is associated with ventricular arrhythmias.

However, changes in gap junction expression alone are presumably not sufficient for conduction slowing and enhanced arrhythmogeneity. The observed reduction in, e.g., Cx43 expression in patients with ventricular remodeling ranges between 30-50%^{36, 106, 109-112}. Mouse experiments have shown that such changes do not necessarily lead to reduced

conduction velocities^{62, 96}. With regard to connexins, there is a large ‘conduction reserve’¹¹³⁻¹¹⁵, the myocardium is able to maintain near normal conduction velocities, even when electrical coupling is substantially reduced. Interestingly, this conduction reserve also applies to other determinants of impulse conduction. Besides changes in connexin expression, ventricular remodeling is also characterized by reduced excitability (impaired sodium channel expression and function)¹¹⁶⁻¹¹⁸, and increased intercellular collagen deposition (fibrosis)¹¹⁹⁻¹²¹. Experiments in mice have shown that such clinically relevant, isolated reductions in sodium channel expression or increased fibrosis only have minor effect on impulse conduction, while their combination severely slowed conduction¹²². Recently, we have shown that a 50% reduction in Cx43 expression is very arrhythmogenic when combined with increased fibrosis¹²³, but not in combination with decreased sodium channel function¹²⁴. Therefore, to explain abnormal conduction and arrhythmogenesis in cardiac disease, the description of aberrant connexin expression alone is presumably not sufficient. Conversely, if other factors, combined with reduced coupling are needed, restoring one may be sufficient to normalize conduction and reduce arrhythmogeneity. As such, strategies aiming for improved gap junctional coupling may be anti-arrhythmogenic. An example of such strategy is the use of anti arrhythmogenic peptides (AAP10, ZP123, Rotigaptide) which were shown to reduce atrial fibrillation^{125, 126}, and ventricular tachycardia during myocardial ischemia in dogs¹²⁷, although their beneficial effect in explanted human failing hearts was not straightforward¹²⁸. These peptides presumably act by modulating Cx43 phosphorylation¹²⁹⁻¹³¹. Cx43 is a phosphoprotein, and the level of phosphorylation is implicated in the regulation of electrical coupling⁹. Under normal conditions in the heart, Cx43 is phosphorylated¹³², but becomes dephosphorylated leading to uncoupling under pathological conditions, such as ischemia¹³³ and heart failure¹³⁴. Direct suppression of Cx43 dephosphorylation resulted in improved coupling¹³⁴.

Finally, post-transcriptional mechanisms, such as the microRNA miR-1, were shown to regulate Cx43 expression and arrhythmogenesis in health and disease¹³⁵ and may therefore also be a potential antiarrhythmic target.

Acknowledgements

This work was financially supported by the Netherlands Heart Foundation (Grant number 2005B170).

References

1. Kleber AG, Rudy Y. Basic mechanisms of cardiac impulse propagation and associated arrhythmias. *Physiol Rev.* 2004;84:431-488
2. Shaw RM, Rudy Y. Ionic mechanisms of propagation in cardiac tissue: Roles of the sodium and l-type calcium currents during reduced excitability and decreased gap junction coupling. *Circulation Research.* 1997;81:727-741
3. Spach MS, Heidlage JF, Dolber PC, Barr RC. Electrophysiological effects of remodeling cardiac gap junctions and cell size. Experimental and model studies of normal cardiac growth. *Circulation Research.* 2000;86:302-311
4. Spach MS, Miller WT, III, Geselowitz DB, Barr RC, Kootsey JM, Johnson EA. The discontinuous nature of propagation in normal canine cardiac muscle: Evidence for recurrent discontinuities of intracellular resistance that affect the membrane currents. *Circ Res.* 1981;48:39-54
5. Shaw RM, Rudy Y. Electrophysiologic effects of acute myocardial ischemia: A theoretical study of altered cell excitability and action potential duration. *Cardiovasc Res.* 1997;35:256-272
6. Willecke K, Eiberger J, Degen J, Eckardt D, Romualdi A, Guldenagel M, Deutsch U, Sohl G. Structural and functional diversity of connexin genes in the mouse and human genome. *Biol Chem.* 2002;383:725-737
7. Duffy HS, Fort AG, Spray DC. Cardiac connexins: Genes to nexus. *Adv Cardiol.* 2006;42:1-17
8. van Veen AA, van Rijen HV, Ophof T. Cardiac gap junction channels: Modulation of expression and channel properties. *Cardiovasc Res.* 2001;51:217-229.
9. Saez JC, Berthoud VM, Branes MC, Martinez AD, Beyer EC. Plasma membrane channels formed by connexins: Their regulation and functions. *Physiol Rev.* 2003;83:1359-1400
10. Davis LM, Rodefeld ME, Green K, Beyer EC, Saffitz JE. Gap junction protein phenotypes of the human heart and conduction system. *J Cardiovasc Electrophysiol.* 1995;6:813-822
11. Gros D, Jarry-Guichard T, Ten Velde I, De Mazière AMGL, Van Kempen MJA, Davoust J, Briand JP, Moorman AFM, Jongsma HJ. Restricted distribution of connexin40, a gap junctional protein, in mammalian heart. *Circulation Research.* 1994;74:839-851
12. Delorme B, Dahl E, Jarry-Guichard T, Briand JP, Willecke K, Gros D, Theveniau-Ruissy M. Expression pattern of connexin gene products at the early developmental stages of the mouse cardiovascular system. *Circ Res.* 1997;81:423-437.
13. Delorme B, Dahl E, Jarry-Guichard T, Marics I, Briand JP, Willecke K, Gros D, Theveniau-Ruissy M. Developmental regulation of connexin 40 gene expression in mouse heart correlates with the differentiation of the conduction system. *Dev Dyn.* 1995;204:358-371
14. Miquerol L, Meysen S, Mangoni M, Bois P, Van Rijen HVM, Abran P, Jongsma HJ, Nargeot J, Gros D. Architectural and functional asymmetry of the his-purkinje system of the murine heart. *Cardiovasc Res.* 2004;63:77-86
15. Van Veen AAB, Van Rijen HVM, van Kempen MJA, Miquerol L, Ophof T, Gros D, Vos MA, Jongsma HJ, de Bakker JMT. Discontinuous conduction in mouse bundle branches is caused by bundle architecture. *Circulation.* 2005;112:2235-2244
16. Manjunath CK, Page E. Cell biology and protein composition of cardiac gap junctions. *American Journal of Physiology.* 1985;248:H783-H791
17. Beyer EC, Paul DL, Goodenough DA. Connexin43: A protein from rat heart homologous to a gap junction protein from liver. *Journal of Cell Biology.* 1987;105:2621-2629
18. Beyer EC, Kistler J, Paul DL, Goodenough DA. Antisera directed against connexin43 peptides react with a 43-kd protein localized to gap junctions in myocardium and other tissues. *Journal of Cell Biology.* 1989;108:595-605
19. Yancey SB, John SA, Lal R, Austin BJ, Revel JP. The 43-kd polypeptide of heart gap junctions: Immunolocalization (i), topology (ii), and functional domains (iii). *Journal of Cell Biology.* 1989;108:2241-2254
20. Kanter HL, Saffitz JE, Beyer EC. Cardiac myocytes express multiple gap junction proteins. *Circulation Research.* 1992;70:438-444

21. Gourdie RG, Green CR, Severs NJ. Gap junction distribution in adult mammalian myocardium revealed by an anti-peptide antibody and laser scanning confocal microscopy. *J Cell Sci.* 1991;99 (Pt 1):41-55
22. Van Kempen MJA, Fromaget C, Gros D, Moonman AFM, Lamers WH. Spatial distribution of connexin43, the major cardiac gap junction protein, in the developing and adult rat heart. *Circ Res.* 1991;68:1638-1651
23. Fromaget C, El Auomari A, Gros D. Distribution pattern of connexin43, a gap junctional protein, during the differentiation of mouse heart myocytes. *Differentiation.* 1992;51:9-20
24. Coppen SR, Dupont E, Rothery S, Severs NJ. Connexin45 expression is preferentially associated with the ventricular conduction system in mouse and rat heart. *Circ Res.* 1998;82:232-243
25. Coppen SR, Kodama I, Boyett MR, Dobrzynski H, Takagishi Y, Honjo H, Yeh HI, Severs NJ. Connexin45, a major connexin of the rabbit sinoatrial node, is co-expressed with connexin43 in a restricted zone at the nodal-crista terminalis border. *J Histochem Cytochem.* 1999;47:907-918
26. Verheijck EE, van Kempen MJ, Veereschild M, Lurvink J, Jongsma HJ, Bouman LN. Electrophysiological features of the mouse sinoatrial node in relation to connexin distribution. *Cardiovasc Res.* 2001;52:40-50
27. Honjo H, Boyett MR, Coppen SR, Takagishi Y, Opthof T, Severs NJ, Kodama I. Heterogeneous expression of connexins in rabbit sinoatrial node cells: Correlation between connexin isotype and cell size. *Cardiovasc Res.* 2002;53:89-96.
28. Kanter HL, Laing JG, Beyer EC, Green KG, Saffitz JE. Multiple connexins colocalize in canine ventricular myocyte gap junctions. *Circ Res.* 1993;73:344-350
29. Vozzi C, Dupont E, Coppen SR, Yeh HI, Severs NJ. Chamber-related differences in connexin expression in the human heart. *J Mol Cell Cardiol.* 1999;31:991-1003
30. Kreuzberg MM, Sohl G, Kim JS, Verselis VK, Willecke K, Bukauskas FF. Functional properties of mouse connexin30.2 expressed in the conduction system of the heart. *Circ Res.* 2005;96:1169-1177
31. Kreuzberg MM, Liebermann M, Segschneider S, Dobrowolski R, Dobrzynski H, Kaba R, Rowlinson G, Dupont E, Severs NJ, Willecke K. Human connexin31.9, unlike its orthologous protein connexin30.2 in the mouse, is not detectable in the human cardiac conduction system. *J Mol Cell Cardiol.* 2009;46:553-559
32. Hoyt RH, Cohen ML, Saffitz JE. Distribution and three-dimensional structure of intercellular junctions in canine myocardium. *Circ Res.* 1989;64:563-574
33. Severs NJ. Gap junction shape and orientation at the cardiac intercalated disk. *Circ Res.* 1989;65:1458-1462
34. Luque EA, Veenstra RD, Beyer EC, Lemanski LF. Localization and distribution of gap junctions in normal and cardiomyopathic hamster heart. *Journal of Morphology.* 1994;222:203-213
35. Sepp R, Severs NJ, Gourdie RG. Altered patterns of intercellular junction distribution in human patients with hypertrophic cardiomyopathy. *Heart.* 1996;76:412-417
36. Kaprielian RR, Gunning M, Dupont E, Sheppard MN, Rothery SM, Underwood R, Pennell DJ, Fox K, Pepper J, Poole-Wilson PA, Severs NJ. Downregulation of immunodetectable connexin43 and decreased gap junction size in the pathogenesis of chronic hibernation in the human left ventricle. *Circulation.* 1998;97:651-660
37. Shibata Y, Yamamoto T. Freeze-fracture studies of gap junctions in vertebrate cardiac muscle cells. *J Ultrastruct Res.* 1979;67:79-88
38. Green CR, Peters NS, Gourdie RG, Rothery S, Severs NJ. Validation of immunohistochemical quantification in confocal scanning laser microscopy: A comparative assessment of gap junction size with confocal and ultrastructural techniques. *J Histochem Cytochem.* 1993;41:1339-1349
39. Luke RA, Saffitz JE. Remodeling of ventricular conduction pathways in healed canine infarct border zones. *Journal of Clinical Investigation.* 1991;87:1594-1602
40. Peters NS, Green CR, Poole-Wilson PA, Severs NJ. Reduced content of connexin43 gap junctions in ventricular myocardium from hypertrophied and ischemic human hearts. *Circulation.* 1993;88:864-875
41. Smith JH, Green CR, Peters NS, Rothery S, Severs NJ. Altered patterns of gap junction distribution in ischemic heart disease. *American Journal of Pathology.* 1991;139:801-821

42. Jongsma HJ. Diversity of gap junctional proteins: Does it play a role in cardiac excitation? *J Cardiovasc Electrophysiol.* 2000;11:228-230
43. Wilders R, Verheijck EE, Kumar R, Goolsby WN, van Ginneken AC, Joyner RW, Jongsma HJ. Model clamp and its application to synchronization of rabbit sinoatrial node cells. *Am J Physiol.* 1996;271:H2168-2182
44. Joyner RW, van Capelle FJ. Propagation through electrically coupled cells. How a small sa node drives a large atrium. *Biophys J.* 1986;50:1157-1164
45. Zhang H, Holden AV, Boyett MR. Gradient model versus mosaic model of the sinoatrial node. *Circulation.* 2001;103:584-588
46. Davis LM, Kanter HL, Beyer EC, Saffitz JE. Distinct gap junction protein phenotypes in cardiac tissues with disparate conduction properties. *Journal of the American College of Cardiology.* 1994;24:1124-1132
47. Boyett MR, Honjo H, Kodama I. The sinoatrial node, a heterogeneous pacemaker structure. *Cardiovasc Res.* 2000;47:658-687
48. ten Velde I, de Jonge B, Verheijck EE, van Kempen MJ, Analbers L, Gros D, Jongsma HJ. Spatial distribution of connexin43, the major cardiac gap junction protein, visualizes the cellular network for impulse propagation from sinoatrial node to atrium. *Circ Res.* 1995;76:802-811
49. Rackauskas M, Kreuzberg MM, Pranevicius M, Willecke K, Verselis VK, Bukauskas FF. Gating properties of heterotypic gap junction channels formed of connexins 40, 43, and 45. *Biophys J.* 2007;92:1952-1965
50. Kirchhoff S, Nelles E, Hagendorff A, Kruger O, Traub O, Willecke K. Reduced cardiac conduction velocity and predisposition to arrhythmias in connexin40-deficient mice. *Curr Biol.* 1998;8:299-302
51. Simon AM, Goodenough DA, Paul DL. Mice lacking connexin40 have cardiac conduction abnormalities characteristic of atrioventricular block and bundle branch block. *Curr Biol.* 1998;8:295-298
52. Bagwe S, Berenfeld O, Vaidya D, Morley GE, Jalife J. Altered right atrial excitation and propagation in connexin40 knockout mice. *Circulation.* 2005;112:2245-2253
53. Tamaddon HS, Vaidya D, Simon AM, Paul DL, Jalife J, Morley GE. High-resolution optical mapping of the right bundle branch in connexin40 knockout mice reveals slow conduction in the specialized conduction system. *Circ Res.* 2000;87:929-936
54. Vanderbrink BA, Sellito C, Saba S, Link MS, Zhu W, Homoud MK, Estes NA, 3rd, Paul DL, Wang PJ. Connexin40-deficient mice exhibit atrioventricular nodal and infra-hisian conduction abnormalities. *J Cardiovasc Electrophysiol.* 2000;11:1270-1276
55. Verheule S, van Batenburg CA, Coenjaerts FE, Kirchhoff S, Willecke K, Jongsma HJ. Cardiac conduction abnormalities in mice lacking the gap junction protein connexin40. *J Cardiovasc Electrophysiol.* 1999;10:1380-1389
56. Bevilacqua LM, Simon AM, Maguire CT, Gehrman J, Wakimoto H, Paul DL, Berul CI. A targeted disruption in connexin40 leads to distinct atrioventricular conduction defects. *J Interv Card Electrophysiol.* 2000;4:459-467
57. Hagendorff A, Schumacher B, Kirchhoff S, Lüderitz B, Willecke K. Conduction disturbances and increased atrial vulnerability in connexin40 deficient mice analyzed by transeptal stimulation. *Circulation.* 1999;99:1508-1515
58. Kruger O, Maxeiner S, Kim JS, van Rijen HV, de Bakker JM, Eckardt D, Tiemann K, Lewalter T, Ghanem A, Luderitz B, Willecke K. Cardiac morphogenetic defects and conduction abnormalities in mice homozygously deficient for connexin40 and heterozygously deficient for connexin45. *J Mol Cell Cardiol.* 2006
59. Schrickel JW, Kreuzberg MM, Ghanem A, Kim JS, Linhart M, Andrie R, Tiemann K, Nickenig G, Lewalter T, Willecke K. Normal impulse propagation in the atrioventricular conduction system of cx30.2/cx40 double deficient mice. *J Mol Cell Cardiol.* 2009;46:644-652
60. Guerrero PA, Schuessler RB, Davis LM, Beyer EC, Johnson CM, Yamada KA, Saffitz JE. Slow ventricular conduction in mice heterozygous for a connexin43 null mutation. *Journal of Clinical Investigation.* 1997;99:1991-1998

61. Thomas SA, Schuessler RB, Berul CI, Beardslee MA, Beyer EC, Mendelsohn ME, Saffitz JE. Disparate effects of deficient expression of connexin43 on atrial and ventricular conduction: Evidence for chamber-specific molecular determinants of conduction. *Circulation*. 1998;97:686-691
62. Morley GE, Vaidya D, Samie FH, Lo C, Delmar M, Jalife J. Characterization of conduction in the ventricles of normal and heterozygous cx43 knockout mice using optical mapping. *J Cardiovasc Electrophysiol*. 1999;10:1361-1375
63. Gutstein DE, Morley GE, Tamaddon H, Vaidya D, Schneider MD, Chen J, Chien KR, Stuhlmann H, Fishman GI. Conduction slowing and sudden arrhythmic death in mice with cardiac-restricted inactivation of connexin43. *Circ Res*. 2001;88:333-339.
64. Eckardt D, Theis M, Degen J, Ott T, van Rijen HV, Kirchhoff S, Kim JS, de Bakker JM, Willecke K. Functional role of connexin43 gap junction channels in adult mouse heart assessed by inducible gene deletion. *J Mol Cell Cardiol*. 2004;36:101-110
65. Rohr S, Kucera JP, Fast VG, Kleber AG. Paradoxical improvement of impulse conduction in cardiac tissue by partial cellular uncoupling. *Science*. 1997;275:841-844
66. van der Velden HM, Ausma J, Rook MB, Hellemons AJ, van Veen TA, Allesie MA, Jongsma HJ. Gap junctional remodeling in relation to stabilization of atrial fibrillation in the goat. *Cardiovasc Res*. 2000;46:476-486.
67. Danik SB, Liu F, Zhang J, Suk HJ, Morley GE, Fishman GI, Gutstein DE. Modulation of cardiac gap junction expression and arrhythmic susceptibility. *Circ Res*. 2004;95:1035-1041
68. Kirchhoff S, Kim JS, Hagedorff A, Thonissen E, Kruger O, Lamers WH, Willecke K. Abnormal cardiac conduction and morphogenesis in connexin40 and connexin43 double-deficient mice [in process citation]. *Circ Res*. 2000;87:399-405
69. Kanagaratnam P, Rothery S, Patel P, Severs NJ, Peters NS. Relative expression of immunolocalized connexins 40 and 43 correlates with human atrial conduction properties. *J Am Coll Cardiol*. 2002;39:116-123
70. Beauchamp P, Yamada KA, Baertschi AJ, Green K, Kanter EM, Saffitz JE, Kleber AG. Relative contributions of connexins 40 and 43 to atrial impulse propagation in synthetic strands of neonatal and fetal murine cardiomyocytes. *Circ Res*. 2006;99:1216-1224
71. Bruzzone R, Haefliger JA, Gimlich RL, Paul DL. Connexin40, a component of gap junctions in vascular endothelium, is restricted in its ability to interact with other connexins. *Molecular Biology of the Cell*. 1993;4:7-20
72. Elfgang C, Eckert R, Lichtenberg-Fraté H, Butterweck A, Traub O, Klein RA, Hülser DF, Willecke K. Specific permeability and selective formation of gap junction channels in connexin-transfected hela cells. *Journal of Cell Biology*. 1995;129:805-817
73. Haubrich S, Schwarz HJ, Bukauskas F, Lichtenberg-Frate H, Traub O, Weingart R, Willecke K. Incompatibility of connexin 40 and 43 hemichannels in gap junctions between mammalian cells is determined by intracellular domains. *Mol Biol Cell*. 1996;7:1995-2006
74. Valiunas V, Weingart R, Brink PR. Formation of heterotypic gap junction channels by connexins 40 and 43. *Circ Res*. 2000;86:E42-49
75. Kanagaratnam P, Cherian A, Stanbridge RD, Glenville B, Severs NJ, Peters NS. Relationship between connexins and atrial activation during human atrial fibrillation. *J Cardiovasc Electrophysiol*. 2004;15:206-216
76. He DS, Jiang JX, Taffet SM, Burt JM. Formation of heteromeric gap junction channels by connexins 40 and 43 in vascular smooth muscle cells. *Proc Natl Acad Sci U S A*. 1999;96:6495-6500
77. Valiunas V, Gemel J, Brink PR, Beyer EC. Gap junction channels formed by coexpressed connexin40 and connexin43. *Am J Physiol Heart Circ Physiol*. 2001;281:H1675-1689
78. Cottrell GT, Burt JM. Heterotypic gap junction channel formation between heteromeric and homomeric cx40 and cx43 connexons. *Am J Physiol Cell Physiol*. 2001;281:C1559-1567
79. Fuster V, Ryden LE, Cannon DS, Crijns HJ, Curtis AB, Ellenbogen KA, Halperin JL, Le Heuzey JY, Kay GN, Lowe JE, Olsson SB, Prystowsky EN, Tamargo JL, Wann S. Acc/aha/esc 2006 guidelines for the management of patients with atrial fibrillation-executive summary: A report of the american college of cardiology/american heart association task force on practice guidelines and the european society of

- cardiology committee for practice guidelines (writing committee to revise the 2001 guidelines for the management of patients with atrial fibrillation). *Eur Heart J.* 2006;27:1979-2030
80. Duffy HS, Wit AL. Is there a role for remodeled connexins in af? No simple answers. *J Mol Cell Cardiol.* 2008;44:4-13
 81. Nattel S, Maguy A, Le Bouter S, Yeh YH. Arrhythmogenic ion-channel remodeling in the heart: Heart failure, myocardial infarction, and atrial fibrillation. *Physiol Rev.* 2007;87:425-456
 82. Nattel S, Shiroshita-Takeshita A, Brundel BJ, Rivard L. Mechanisms of atrial fibrillation: Lessons from animal models. *Prog Cardiovasc Dis.* 2005;48:9-28
 83. Severs NJ, Bruce AF, Dupont E, Rothery S. Remodelling of gap junctions and connexin expression in diseased myocardium. *Cardiovasc Res.* 2008;80:9-19
 84. Van Kempen MJA, Ten Velde I, Wessels A, Oosthoek PW, Gros D, Jongsma HJ, Moorman AFM, Lamers WH. Differential connexin expression accommodates cardiac function in different species. *Microscopy Research and Technique.* 1995;31:420-436
 85. Coppens SR, Severs NJ, Gourdie RG. Connexin45 (alpha 6) expression delineates an extended conduction system in the embryonic and mature rodent heart. *Dev Genet.* 1999;24:82-90
 86. van Rijen HV, van Veen TA, van Kempen MJ, Wilms-Schopman FJ, Potse M, Krueger O, Willecke K, Opthof T, Jongsma HJ, de Bakker JM. Impaired conduction in the bundle branches of mouse hearts lacking the gap junction protein connexin40. *Circulation.* 2001;103:1591-1598
 87. Van Rijen HV, van Veen AA, van Kempen MJ, Wilms-Schopman FJ, Potse M, Krueger O, Willecke K, Jongsma HJ, de Bakker JMT. Impaired conduction in the bundle branches of mouse hearts lacking the gap junction protein connexin40. *Circulation.* 2000;102:1748 Suppl. S
 88. Kruger O, Plum A, Kim JS, Winterhager E, Maxeiner S, Hallas G, Kirchhoff S, Traub O, Lamers WH, Willecke K. Defective vascular development in connexin 45-deficient mice. *Development.* 2000;127:4179-4193
 89. Kumai M, Nishii K, Nakamura K, Takeda N, Suzuki M, Shibata Y. Loss of connexin45 causes a cushion defect in early cardiogenesis. *Development.* 2000;127:3501-3512
 90. Kreuzberg MM, Schrickel JW, Ghanem A, Kim JS, Degen J, Janssen-Bienhold U, Lewalter T, Tiemann K, Willecke K. Connexin30.2 containing gap junction channels decelerate impulse propagation through the atrioventricular node. *Proc Natl Acad Sci U S A.* 2006;103:5959-5964
 91. Reaume AG, de Sousa PA, Kulkarni S, Langille BL, Zhu D, Davies TC, Juneja SC, Kidder GM, Rossant J. Cardiac malformation in neonatal mice lacking connexin43. *Science.* 1995;267:1831-1834
 92. Huang GY, Wessels A, Smith BR, Linask KK, Ewart JL, Lo CW. Alteration in connexin 43 gap junction gene dosage impairs conotruncal heart development. *Dev Biol.* 1998;198:32-44.
 93. Ya J, Erdtsieck-Ernste EBHW, de Boer PAJ, Van Kempen MJA, Jongsma HJ, Gros D, Moorman AFM, Lamers WH. Heart defects in connexin43-deficient mice. *Circ Res.* 1998;82:360-366
 94. Eloff BC, Lerner DL, Yamada KA, Schuessler RB, Saffitz JE, Rosenbaum DS. High resolution optical mapping reveals conduction slowing in connexin43 deficient mice. *Cardiovasc Res.* 2001;51:681-690
 95. Guerrero PA, Schuessler RB, Beyer EC, Saffitz JE. Mice heterozygous for a cx43 null mutation exhibit a cardiac conduction defect. *Circulation.* 1996;94 Suppl.1:8
 96. van Rijen HVM, Eckardt D, Degen J, Theis M, Ott T, Willecke K, Jongsma HJ, Opthof T, De Bakker JMT. Slow conduction and enhanced anisotropy increase the propensity for ventricular tachyarrhythmias in adult mice with induced deletion of connexin43. *Circulation.* 2004;109:1048-1055
 97. Thomas SP, Kucera JP, Bircher-Lehmann L, Rudy Y, Saffitz JE, Kleber AG. Impulse propagation in synthetic strands of neonatal cardiac myocytes with genetically reduced levels of connexin43. *Circ Res.* 2003;92:1209-1216
 98. Beauchamp P, Choby C, Desplantez T, de Peyer K, Green K, Yamada KA, Weingart R, Saffitz JE, Kleber AG. Electrical propagation in synthetic ventricular myocyte strands from germline connexin43 knockout mice. *Circ Res.* 2004;95:170-178
 99. Feil R, Brocard J, Mascrez B, LeMeur M, Metzger D, Chambon P. Ligand-activated site-specific recombination in mice. *Proc Natl Acad Sci U S A.* 1996;93:10887-10890
 100. Shaw RM, Rudy Y. Ionic mechanisms of propagation in cardiac tissue. Roles of the sodium and I-type calcium currents during reduced excitability and decreased gap junction coupling. *Circ Res.* 1997;81:727-741

101. Jongsma HJ, Wilders R. Gap junctions in cardiovascular disease. *Circ.Res.* 2000;86:1193-1197
102. Rohr S, Kucera JP, Kléber AG. Slow conduction in cardiac tissue,i. Effects of a reduction of excitability versus a reduction of electrical coupling on microconduction. *Circ Res.* 1998;83:781-794
103. Vaidya D, Tamaddon HS, Lo CW, Taffet SM, Delmar M, Morley GE, Jalife J. Null mutation of connexin43 causes slow propagation of ventricular activation in the late stages of mouse embryonic development. *Circ Res.* 2001;88:1196-1202.
104. Spach MS. Discontinuous cardiac conduction: Its origin in cellular connectivity with long-term adaptive changes that cause arrhythmias. In: Spooner PM, Joyner RW, Jalife J, eds. *Discontinuous conduction in the heart*. Armonk, NY: Futura Publishing Company Inc.; 1997.
105. Green CR, Severs NJ. Distribution and role of gap junctions in normal myocardium and human ischaemic heart disease. *Histochemistry.* 1993;99:105-120
106. Kostin S, Dammer S, Hein S, Klovekorn WP, Bauer EP, Schaper J. Connexin 43 expression and distribution in compensated and decompensated cardiac hypertrophy in patients with aortic stenosis. *Cardiovasc Res.* 2004;62:426-436
107. Kitamura H, Ohnishi Y, Yoshida A, Okajima K, Azumi H, Ishida A, Galeano EJ, Kubo S, Hayashi Y, Itoh H, Yokoyama M. Heterogeneous loss of connexin43 protein in nonischemic dilated cardiomyopathy with ventricular tachycardia. *J Cardiovasc Electrophysiol.* 2002;13:865-870
108. Kitamura H, Yoshida A, Ohnishi Y, Okajima K, Ishida A, Galeano EJ, Kubo S, Fukuzawa K, Takano T, Yokoyama M. Correlation of connexin43 expression and late ventricular potentials in nonischemic dilated cardiomyopathy. *Circ J.* 2003;67:1017-1021
109. Kostin S, Rieger M, Dammer S, Hein S, Richter M, Klovekorn WP, Bauer EP, Schaper J. Gap junction remodeling and altered connexin43 expression in the failing human heart. *Mol Cell Biochem.* 2003;242:135-144
110. Yamada KA, Rogers JG, Sundset R, Steinberg TH, Saffitz JE. Up-regulation of connexin45 in heart failure. *J Cardiovasc Electrophysiol.* 2003;14:1205-1212
111. Peters NS. New insights into myocardial arrhythmogenesis: Distribution of gap junctional coupling in normal ischemic and hypertrophied human hearts. *Clinical Science.* 1996;90:447-452
112. Peters NS, Coromilas J, Severs NJ, Wit AL. Disturbed connexin43 gap junction distribution correlates with the location of reentrant circuits in the epicardial border zone of healing canine infarcts that cause ventricular tachycardia. *Circulation.* 1997;95:988-996
113. van Rijen HV, de Bakker JM, van Veen TA. Hypoxia, electrical uncoupling, and conduction slowing: Role of conduction reserve. *Cardiovasc Res.* 2005;66:9-11
114. Stein M, Boulaklil M, Engelen MA, Van Veen AAB, Hauer RN, de Bakker JM, van Rijen HV. Conduction reserve and arrhythmias. *Netherlands Heart Journal.* 2006;14
115. van Rijen HV, van Veen TA, Gros D, Wilders R, de Bakker JM. Connexins and cardiac arrhythmias. *Adv Cardiol.* 2006;42:150-160
116. Ufret-Vincenty CA, Baro DJ, Lederer WJ, Rockman HA, Quinones LE, Santana LF. Role of sodium channel deglycosylation in the genesis of cardiac arrhythmias in heart failure. *J Biol Chem.* 2001;276:21211-21217
117. Borlak J, Thum T. Hallmarks of ion channel gene expression in end-stage heart failure. *FASEB J.* 2003;17:1592-1608
118. Valdivia CR, Chu WW, Pu J, Foell JD, Haworth RA, Wolff MR, Kamp TJ, Makielski JC. Increased late sodium current in myocytes from a canine heart failure model and from failing human heart. *J Mol Cell Cardiol.* 2005;38:475-483
119. La Vecchia L, Ometto R, Bedogni F, Finocchi G, Mosele GM, Bozzola L, Bevilacqua P, Vincenzi M. Ventricular late potentials, interstitial fibrosis, and right ventricular function in patients with ventricular tachycardia and normal left ventricular function. *Am J Cardiol.* 1998;81:790-792
120. Swynghedauw B. Molecular mechanisms of myocardial remodeling. *Physiol Rev.* 1999;79:215-262
121. Kawara T, Derksen R, de Groot JR, Coronel R, Tasseron S, Linnenbank AC, Hauer RN, Kirkels H, Janse MJ, de Bakker JM. Activation delay after premature stimulation in chronically diseased human myocardium relates to the architecture of interstitial fibrosis. *Circulation.* 2001;104:3069-3075
122. van Veen TA, Stein M, Royer A, Le Quang K, Charpentier F, Colledge WH, Huang CL, Wilders R, Grace AA, Escande D, de Bakker JM, van Rijen HV. Impaired impulse propagation in scn5a-knockout

- mice. Combined contribution of excitability, connexin expression, and tissue architecture in relation to aging. *Circulation*. 2005;112:1927-1935
123. Jansen JA, van Veen AA, Bosch AA, van der Nagel R, Vos MA, de Bakker JM, van Rijen HVM. Arrhythmia vulnerability of aged haploinsufficient cx43 mice is determined by heterogeneous downregulation of cx43 combined with increased fibrosis. *Circulation*. 2008;118:S494
124. Stein M, Van Veen TAB, Remme CA, Boulaksil M, van Stuijvenberg L, van der Nagel R, Bezzina CR, Hauer RNW, de Bakker JMT, van Rijen HVM. Combined reduction of intercellular coupling and membrane excitability differentially affects transverse and longitudinal cardiac conduction. *Cardiovasc Res*. 2009;83:52-60
125. Guerra JM, Everett TH, Lee KW, Wilson E, Olgin JE. Effects of the gap junction modifier rotigaptide (zp123) on atrial conduction and vulnerability to atrial fibrillation. *Circulation*. 2006;114:110-118
126. Haugan K, Miyamoto T, Takeishi Y, Kubota I, Nakayama J, Shimojo H, Hirose M. Rotigaptide (zp123) improves atrial conduction slowing in chronic volume overload-induced dilated atria. *Basic Clin Pharmacol Toxicol*. 2006;99:71-79
127. Xing D, Kjolbye AL, Nielsen MS, Petersen JS, Harlow KW, Holstein-Rathlou NH, Martins JB. Zp123 increases gap junctional conductance and prevents reentrant ventricular tachycardia during myocardial ischemia in open chest dogs. *J Cardiovasc Electrophysiol*. 2003;14:510-520
128. Wiegierinck RF, de Bakker JM, Opthof T, de Jonge N, Kirkels H, Wilms-Schopman FJ, Coronel R. The effect of enhanced gap junctional conductance on ventricular conduction in explanted hearts from patients with heart failure. *Basic Res Cardiol*. 2009;104:321-332
129. Dhein S, Weng S, Grover R, Tudyka T, Gottwald M, Schaefer T, Polontchouk L. Protein kinase calpha mediates the effect of antiarrhythmic peptide on gap junction conductance. *Cell Commun Adhes*. 2001;8:257-264
130. Weng S, Lauven M, Schaefer T, Polontchouk L, Grover R, Dhein S. Pharmacological modification of gap junction coupling by an antiarrhythmic peptide via protein kinase c activation. *Faseb J*. 2002;16:1114-1116
131. Quan XQ, Bai R, Liu N, Chen BD, Zhang CT. Increasing gap junction coupling reduces transmural dispersion of repolarization and prevents torsade de pointes in rabbit lqt3 model. *J Cardiovasc Electrophysiol*. 2007;18:1184-1189
132. Beardslee MA, Laing JG, Beyer EC, Saffitz JE. Rapid turnover of connexin43 in the adult rat heart. *Circ Res*. 1998;83:629-635
133. Beardslee MA, Lerner DL, Tadros PN, Laing JG, Beyer EC, Yamada KA, Kleber AG, Schuessler RB, Saffitz JE. Dephosphorylation and intracellular redistribution of ventricular connexin43 during electrical uncoupling induced by ischemia. *Circ Res*. 2000;87:656-662
134. Ai X, Pogwizd SM. Connexin 43 downregulation and dephosphorylation in nonischemic heart failure is associated with enhanced colocalized protein phosphatase type 2a. *Circ Res*. 2005;96:54-63
135. Yang B, Lin H, Xiao J, Lu Y, Luo X, Li B, Zhang Y, Xu C, Bai Y, Wang H, Chen G, Wang Z. The muscle-specific microRNA mir-1 regulates cardiac arrhythmogenic potential by targeting gja1 and kcnj2. *Nat Med*. 2007;13:486-491

Chapter 2 - Lysosome mediated Kir2.1 breakdown directly influences inward rectifier current density

John A Jansen, Teun P de Boer, Rianne Wolswinkel, Toon AB van Veen, Marc A Vos, Harold VM van Rijen, Marcel AG van der Heyden

Biochem Biophys Res Commun 2008;367:687-692

Lysosome mediated Kir2.1 breakdown directly influences inward rectifier current density

John A. Jansen¹; Teun P. de Boer¹; Rianne Wolswinkel¹; Toon A.B. van Veen¹; Marc A. Vos¹; Harold V.M. van Rijen¹; Marcel A.G. van der Heyden¹

1. Department of Medical Physiology, Division Heart and Lungs, University Medical Center Utrecht, The Netherlands

Abstract

The inward rectifier current generated by Kir2.1 ion channel proteins is primarily responsible for the stable resting membrane potential in various excitable cell types, like neurons and myocytes. Tight regulation of Kir2.1 functioning prevents premature action potential formation and ensures optimal repolarization times. While Kir2.1 forward trafficking has been addressed in a number of studies, its degradation pathways are thus far unknown. Using three different lysosomal inhibitors, NH₄Cl, chloroquine and leupeptin, we now demonstrate involvement of the lysosomal degradation pathway in Kir2.1 breakdown. Upon application of the inhibitors, increased steady state protein levels are detectable within few hours coinciding with intracellular granular Kir2.1 accumulation. Treatment for 24 hours with either chloroquine or leupeptin results in increased plasmamembrane originating inward rectifier current densities, while current-voltage characteristics remain unaltered. We conclude that the lysosomal degradation pathway contributes to Kir2.1 mediated inward rectifier current regulation.

Introduction

The formation of an action potential stands at the basis of many physiological processes. A number of distinct diseases of the cardiovascular system (atrial or ventricular fibrillation), the neuronal system (seizures, migraine) and the motor system (myotonia) can be related to ion channel malfunctioning¹. The action potential (AP) of excitable cells, such as neurons and myocytes, is the resultant of sequential and coordinated activity of a number of ion channels. Depolarizing currents are generally carried by sodium and calcium ions, while repolarizing currents result mainly from potassium fluxes. The inward rectifier potassium current (I_{K1}) is one of the few that operates between subsequent APs and is primarily responsible for generating and stabilizing the resting membrane potential at a rather negative level between -75 and -90 mV, and secondly for the initial depolarization (indirectly, opposing depolarizing currents) and fine tuning of final repolarization (directly, contributing repolarizing current) of the AP². In mammals, several different but closely related ion channel proteins constitute the cardiac ventricular I_{K1} . Of these, the KCNJ2 and KCNJ12 gene products Kir2.1 and Kir2.2 are the main determinants. To function as an ion channel, Kir2.x proteins form either homotypic or heterotypic tetramers defined by specific sequence domains³. Several studies indicate that manipulating I_{K1} by means of null mutation⁴, overexpression⁵⁻⁷ or dominant negative expression of Kir2.1^{6, 8} elucidates the importance of Kir2.1 mediated I_{K1} for normal action potential formation and control of sinus rhythm. The ultimate expression level of Kir2.1 may influence the eventual arrhythmogenic outcome. In humans, loss-of-function mutations in Kir2.1 leads to Andersen-Tawil syndrome which is characterized by potentially lethal ventricular arrhythmias, periodic paralysis and dysmorphic features, further emphasizing the pleiotropic action of Kir2.1 in development and adult physiology⁹.

Trafficking of potassium channels involves a large number of subsequent steps, all of which are subject to tight regulation¹⁰. Several elegant studies have addressed molecular mechanisms of Kir2.x trafficking towards and anchoring at the plasma membrane. This disclosed several Kir2.x intracellular N- and C-terminal domains and interacting proteins involved in endoplasmic reticulum retention, forward trafficking and plasma membrane targeting¹¹⁻¹⁷. Several human KCNJ2 mutations that display trafficking defects have been identified^{18, 19}, but interestingly these mutations are not in the previously mentioned export signal sequences. Finally, celastrol, a bioactive compound with strong antioxidant characteristics, inhibits Kir2.1 trafficking towards the plasmamembrane in HEK293 cells^{20, 21}. As demonstrated by Tong et al., tyrosine242 of Kir2.1 is involved in clathrin mediated endocytosis, by a tyrosine kinase dependent mechanism²². However, beyond endocytosis no experimental evidence has been described on the pathways involved in Kir2.x degradation thus far. In this study we focused on the lysosomal degradation pathway by using three different inhibitors of lysosomal breakdown²³. The lysosomal degradation pathway starts in endosomes containing trapped membrane proteins, followed by fusion with early lysosomes which results in mature lysosomes (for reviews see^{24, 25}). The acid environment in the lysosomes is required for protein digestion by acidic hydrolases. We

used the lysosomal protease inhibitors chloroquine, ammoniumchloride (NH₄Cl) and leupeptin. Chloroquine, an antimalarial drug, and NH₄Cl are weak bases, increasing the lysosomal pH and thereby prohibiting the breakdown of proteins by hydrolases. Furthermore, both chemicals inhibit the transport of hydrolases to the lysosomes. Leupeptin, on the other hand, acts directly as an inhibitor of the hydrolases. Interestingly, leupeptin appears to affect only the lysosomes, whereas NH₄Cl and chloroquine influence both the lysosome and the endosomes. In this study we demonstrate that inhibition of lysosomal protein breakdown results in increased steady state level and intracellular accumulation of Kir2.1 protein, and elevated I_{K1} current densities.

Materials and Methods

Cell culture and pharmacological treatment

HEK-KWGF cells stably expressing wildtype murine Kir2.1-GFP fusion protein were generated and cultured as described previously²⁶. HEK-HsKir2.1 cells stably express non-tagged human Kir2.1 from a pcDNA3 (Invitrogen, Breda, The Netherlands) based expression vector. For lysosomal degradation pathway inhibition, NH₄Cl (BHD, Poole, UK), chloroquine (Sigma, St. Louis, MO, USA) and leupeptin (Sigma) were added to the culture medium to obtain final concentrations of 1 mM, 10 μM and 5 μg/mL respectively for the indicated time at the end of the experiment until harvesting or electrophysiological recording.

Western Blotting

HEK-KWGF cells were lysed in RIPA buffer (20mM Tris-HCl, pH 7.4, 150mM NaCl, 10mM Na₂HPO₄, 1% (v/v) Triton X-100, 1% (w/v) Na-deoxycholate, 0.1% (w/v) SDS, 1mM EDTA, 50 mM NaF, 2mM PMSF and 14 μg/ml aprotinin). Lysates were clarified by centrifugation at 14000rpm for 10' at 4°C and mixed with loading buffer. Twenty micrograms of proteins were separated by 10% SDS-PAGE and blotted onto nitrocellulose membrane (Bio-Rad, Veenendaal, The Netherlands). Blots were incubated with GFP (cat. no. Sc-9996; Santa Cruz Biotechnology, Santa Cruz, CA, USA) and Pan-Cadherin (cat. no. C1821; Sigma) primary antibodies and peroxidase-conjugated secondary antibody (Jackson ImmunoResearch, West Grove, PA, USA). Standard ECL procedure was used as final detection (Amersham Bioscience, Buckinghamshire, UK).

Immunofluorescence microscopy

HEK-KWGF or HEK-HsKir2.1 cells cultured on 11mm Ø glass cover slips (Smethwick, Warley, UK) were fixed using 4% paraformaldehyde. After permeabilization with 0.2% Triton X-100 (BDH) in PBS, cells were pre-incubated with 2% BSA. Next, cells were incubated overnight with either anti-GFP or anti-Kir2.1 (cat. no. Sc-18708; Santa Cruz Biotechnology, Santa Cruz, CA, USA) primary antibody for HEK-KWGF and HEK-HsKir2.1 cells respectively, followed by incubation with anti-mouse or anti-goat FITC conjugated secondary antibody (Jackson ImmunoResearch) for 2h. Cover slips were mounted with Vectashield (Vector Laboratories Inc, Burlingame, CA, USA) and imaged using a Nikon Optiphot-2 microscope equipped for epifluorescence.

Electrophysiology

I_{K1} -currents were recorded using the whole cell voltage clamp configuration in randomly chosen single HEK-KWGF cells using an Axopatch 200B amplifier (Molecular Devices, Toronto, Canada). Currents were low-pass filtered at 2 kHz and recorded at 4 kHz using a Apple PowerMac fitted with A/D card (National Instruments, Austin, TX, USA). From a holding potential of -40 mV, 750 ms long square test pulses to potentials ranging between -100 and +50 mV were applied to elicit membrane currents. Steady state currents at the end of the test pulse were normalized to membrane capacitance and plotted versus test potential. To obtain membrane conductances, the slope of I-V plot between -100 and -80 mV was determined using linear regression.

Experiments were done at 20°C using an extracellular solution containing (mmol/L) 140 NaCl, 17.5 NaCO₃, 15 HEPES, 6 glucose, 5.4 KCl, 1.8 CaCl₂ and 1 MgCl₂ in H₂O (pH 7.20, NaOH). Patch pipettes were filled with an internal solution containing (mmol/L) 125 potassium gluconate, 10 KCl, 5 HEPES, 5 EGTA, 4 Na₂ATP, 2 MgCl₂ and 0.6 CaCl₂ in H₂O (pH 7.20, KOH) and had resistances ranging between 2 and 5 MΩ. Liquid junction potential was calculated using pClamp (Molecular Devices) and used for offline correction.

Statistics

All data are presented as mean ± SEM. Differences among groups were evaluated using one-way ANOVA and a post-hoc Holm-Sidak test, significance was assumed if $p < 0.05$.

Results

Inhibition of lysosomal breakdown pathways increases Kir2.1 steady state levels

HEK-KWGF cells were incubated with either 1 mM NH_4Cl , 10 μM chloroquine or 5 $\mu\text{g}/\text{mL}$ leupeptin for 6 and 24 hours respectively. Subsequently, expression level of Kir2.1-GFP fusion protein was analyzed by Western blotting. As depicted in Fig.1A, chloroquine rapidly increased Kir2.1-GFP expression levels within 6 hours which was even more pronounced after 24 hours. Leupeptin resulted in enhanced Kir2.1-GFP following 6 and 24 hours of incubation. Only modest increased Kir2.1-GFP levels were observed by NH_4Cl application. Following the strong upregulation due to chloroquine or leupeptin treatment, an additional signal is observed at ~ 70 kDa. Since the fusion protein is detected by an antibody directed against the C-terminal fused GFP, this product most likely represents a protein product that results from N-terminal Kir2.1 cleavage. To further elucidate the kinetics of Kir2.1 upregulation, HEK-KWGF cells were treated with 10 μM chloroquine for 1, 2, 3, 4, 6 and 24 hours respectively (Fig. 1B). Increased expression levels of full-length Kir2.1-GFP were observed already after one hour of treatment. Furthermore, the presumed ~ 70 kDa degradation product becomes detectable following three hours of chloroquine treatment. These data indicate that the lysosomal degradation pathway is involved in Kir2.1-GFP breakdown, and that Kir2.1-GFP turnover takes place at a time scale of only a few hours.

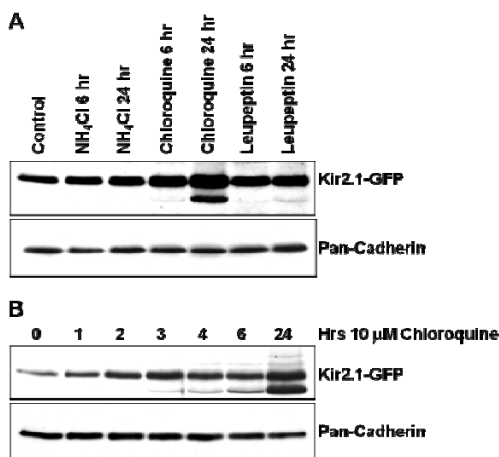
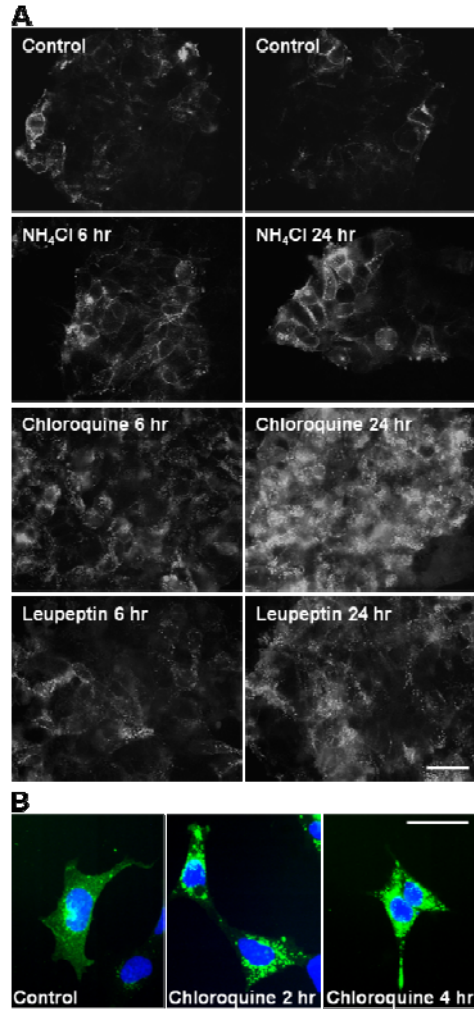


Figure 1 - Effect of lysosomal degradation inhibitors on Kir2.1-GFP steady state expression levels. (A) Kir2.1-GFP protein expression levels in HEK-KWGF cells increase upon treatment with different lysosomal inhibitors. HEK-KWGF cell cultures were treated with 1 mM NH_4Cl , 10 μM chloroquine or 5 $\mu\text{g}/\text{mL}$ leupeptin for 6 and 24 hours respectively. Kir2.1-GFP protein level in total cell lysates was detected using GFP antibody. (B) Kinetics of Kir2.1-GFP upregulation following treatment with 10 μM Chloroquine. Cadherin expression levels were identical to total protein levels as detected by Ponceau S staining prior to immunodetection (not shown), and are regarded as loading control using a pan-cadherin antibody.

Figure 2 - Intracellular Kir2.1-GFP accumulation upon treatment of HEK-KWGF cells with lysosomal inhibitors. (A) Cell cultures were treated as in Fig. 1. Subsequently, Kir2.1-GFP was detected in fixed cells using anti-GFP as primary and Fitc-labeled secondary antibody. Scale bar represents 40 μm . (B) Intracellular accumulation of non-tagged Kir2.1 (green) upon treatment of HEK-HsKir2.1 cells with 10 μM chloroquine for 2 and 4 hours respectively. Kir2.1 was detected by anti-Kir2.1 antibody, nuclei are stained with DAPI (blue). Scale bar represents 20 μm .



Lysosomal inhibition results in granular intracellular Kir2.1 accumulation

Next, we assessed Kir2.1-GFP localization following application of the different inhibitors for 6 and 24 hours. In non-treated cells, Kir2.1-GFP is mainly localized at the plasmamembrane. Chloroquine incubation leads to strong intracellular accumulation (Fig. 2A). Similar results were obtained using non-tagged Kir2.1 (Fig. 2B). Like for chloroquine, incubation with leupeptin or NH_4Cl results in intracellular accumulation of Kir2.1-GFP and appeared to increase plasmamembrane staining (Fig. 2A). We conclude that the strong increase in Kir2.1-GFP levels in chloroquine, and to a lesser extend leupeptin and NH_4Cl , treated cells substantially results from intracellular granular accumulation, presumably in late endosomes and/or lysosomes²³.

Inhibition of lysosomal mediated Kir2.1 breakdown results in increased I_{K1} densities

To see whether the increased protein levels as observed by Western blotting and intracellular accumulation would also result in enhanced functional Kir2.1-GFP expression at the plasmamembrane, HEK-KWGF cells treated with chloroquine or leupeptin were analyzed for I_{K1} current densities (Fig. 3A). As depicted in Fig. 3A and B, chloroquine significantly increased the inward component of I_{K1} at membrane potentials between -114 and -94 mV, while both chloroquine and leupeptin significantly increased the outward component of I_{K1} between membrane potentials of -50 and -65 mV (Fig. 3C). Furthermore, the reversal potential was not changed, which was reflected by a lack of difference in membrane potential (-75.2 ± 0.5 , -75.5 ± 0.5 and -74.9 ± 0.6 mV for control, chloroquine and leupeptin respectively).

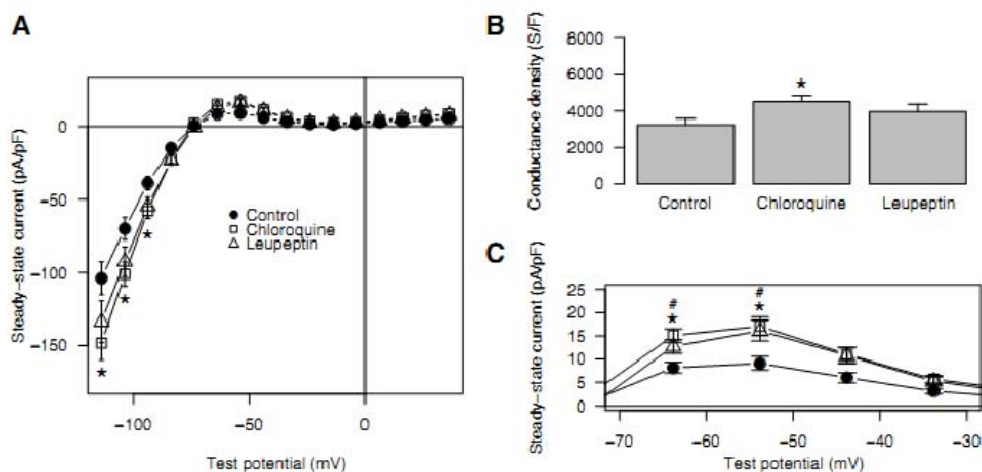


Figure 3 - Quantification of functional membrane expression of Kir2.1 using the whole cell voltage clamp technique. (A) Diagram depicting the relation between steady state I_{K1} current and test potential. Compared to controls, inward I_{K1} currents are larger in chloroquine and leupeptin treated HEK-KWGF cell cultures. Asterisk indicates a significant difference between control and chloroquine ($p < 0.05$). (B) Steady state conductance density negative to E_k were significantly increased in chloroquine treated cultures, underscoring increased membrane localization of Kir2.1 channels ($p < 0.05$). (C) Detail of outward currents depicted in panel A; legend as in panel A. Both chloroquine and leupeptin treated cultures show significantly increased outward current (* and #, $p < 0.05$).

Discussion

In the current study we provide biochemical, immunofluorescence and electrophysiological evidence for involvement of the lysosomal degradation pathway in Kir2.1 breakdown. Results of Tong et al.,²² suggest that Kir2.1 channels enter the degradation pathway via clathrin mediated endocytosis. Whether all Kir2.1 channels are subsequently degraded via the lysosomal pathway is unknown. Alternatively, internalized channels may become targeted to proteasome mediated degradation or recycle to the plasmamembrane. Biochemical analysis displayed increased steady state expression levels within 1 hour of treatment with lysosomal inhibitors (Fig. 1B). This implicates a relatively rapid turnover, within hours, of the Kir2.1 ion channel protein in HEK293 cells. Furthermore, lysosomal inhibition results in intracellular Kir2.1 protein accumulation as depicted in Fig. 2 within two hours, however this does not necessarily imply a retarded internalization from the plasmamembrane. Apparently, our 24 hour treatment with chloroquine and leupeptin results in saturation of the Kir2.1 degradation pathway which likely affects internalization capacity of the functional Kir2.1 channels, culminating in increased I_{K1} densities. Preliminary studies indicated that NH_4Cl did not result in a significant increase in I_{K1} densities, which is in line with the biochemical results. Furthermore, chloroquine and NH_4Cl display the same mechanism of action with respect to lysosomal degradation inhibition although with different efficiencies. In contrast to our results, transiently transfected Kir6.2 channels in COS cells do not display increased cell surface expression upon 6 or 12 hours of chloroquine treatment²⁷. This may be due to different methodology between their (chemiluminescence) and our (patch clamp) study to detect ion channel expression at the plasmamembrane. On the other hand, Kir6.2 channels may be degraded by a different pathway or multiple pathways, or at a different time scale. Finally, Kv1.5 voltage gated channel is degraded via the proteasomal pathway instead of the lysosomal pathway and blocking this degradation pathway results in increased $I_{K_{irr}}$ current densities²⁸. Obviously, no universal potassium ion channel protein degradation pathway seems to exist.

Chloroquine and leupeptin treatment yields a product that is approximately 10 kDa less in molecular weight than full-length Kir2.1-GFP. Since GFP is fused to the C-terminus of Kir2.1, we reason that this product is the result of N-terminal cleavage. It might have a much shorter half-life than full length protein and therefore only becomes detectable following maximal inhibition of degradation. N-terminal cleavage might be the first step in Kir2.1 degradation.

Chloroquine has a long clinical history as an antimalarial drug and is associated with cardiac rhythm and conduction disturbances that can evolve in life-threatening arrhythmias²⁹. In feline purkinje and ventricular cardiomyocytes, acute application of chloroquine results in block of various cardiac ion channels including the I_{K1} channel.³⁰ In our studies, chloroquine acts at a completely different cellular level as a lysosomal inhibitor displaying opposite biological effects, i.e. an increase in I_{K1} current densities. Our electrophysiological measurements were performed in the absence of the drug and thereby exclude the acute

effect of chloroquine on Kir2.1 based ion channels. These data indicate that chloroquine can display a dual effect on inward rectifier currents, directly by blocking the channel, and indirectly by inhibition of channel degradation. The resultant of long term exposure to chloroquine in a complex system as the intact cardiomyocyte or heart, however, is difficult to predict and requires a comprehensive analysis of spatial and functional expression of Kir2.x isoforms.

Acknowledgements

This work was supported by the Netherlands Heart Foundation (2005B170) and the Prof. Dr. R.L.J. van Ruyven Foundation (RW).

References

1. Ashcroft FM. From molecule to malady. *Nature*. 2006;440:440-447
2. Dharmoon AS, Jalife J. The inward rectifier current (ik1) controls cardiac excitability and is involved in arrhythmogenesis. *Heart Rhythm*. 2005;2:316-324
3. Tinker A, Jan YN, Jan LY. Regions responsible for the assembly of inwardly rectifying potassium channels. *Cell*. 1996;87:857-868
4. Zaritsky JJ, Redell JB, Tempel BL, Schwarz TL. The consequences of disrupting cardiac inwardly rectifying k(+) current (i(k1)) as revealed by the targeted deletion of the murine kir2.1 and kir2.2 genes. *J Physiol*. 2001;533:697-710
5. Li J, McLerie M, Lopatin AN. Transgenic upregulation of ik1 in the mouse heart leads to multiple abnormalities of cardiac excitability. *Am J Physiol Heart Circ Physiol*. 2004;287:H2790-2802
6. Miake J, Marban E, Nuss HB. Functional role of inward rectifier current in heart probed by kir2.1 overexpression and dominant-negative suppression. *J Clin Invest*. 2003;111:1529-1536
7. Piao L, Li J, McLerie M, Lopatin AN. Transgenic upregulation of ik1 in the mouse heart is proarrhythmic. *Basic Res Cardiol*. 2007;102:416-428
8. McLerie M, Lopatin AN. Dominant-negative suppression of i(k1) in the mouse heart leads to altered cardiac excitability. *J Mol Cell Cardiol*. 2003;35:367-378
9. Plaster NM, Tawil R, Tristani-Firouzi M, Canun S, Bendahhou S, Tsunoda A, Donaldson MR, Iannaccone ST, Brunt E, Barohn R, Clark J, Deymeer F, George AL, Jr., Fish FA, Hahn A, Nitu A, Ozdemir C, Serdaroglu P, Subramony SH, Wolfe G, Fu YH, Ptacek LJ. Mutations in kir2.1 cause the developmental and episodic electrical phenotypes of andersen's syndrome. *Cell*. 2001;105:511-519
10. Steele DF, Eldstrom J, Fedida D. Mechanisms of cardiac potassium channel trafficking. *J Physiol*. 2007;582:17-26
11. Ma D, Zerangue N, Lin YF, Collins A, Yu M, Jan YN, Jan LY. Role of er export signals in controlling surface potassium channel numbers. *Science*. 2001;291:316-319
12. Stockklauser C, Ludwig J, Ruppertsberg JP, Klocker N. A sequence motif responsible for er export and surface expression of kir2.0 inward rectifier k(+) channels. *FEBS Lett*. 2001;493:129-133
13. Stockklauser C, Klocker N. Surface expression of inward rectifier potassium channels is controlled by selective golgi export. *J Biol Chem*. 2003;278:17000-17005
14. Hofherr A, Fakler B, Klocker N. Selective golgi export of kir2.1 controls the stoichiometry of functional kir2.X channel heteromers. *J Cell Sci*. 2005;118:1935-1943
15. Leonoudakis D, Conti LR, Anderson S, Radeke CM, McGuire LM, Adams ME, Froehner SC, Yates JR, 3rd, Vandenberg CA. Protein trafficking and anchoring complexes revealed by proteomic analysis of inward rectifier potassium channel (kir2.X)-associated proteins. *J Biol Chem*. 2004;279:22331-22346
16. Grishin A, Li H, Levitan ES, Zaks-Makhina E. Identification of gamma-aminobutyric acid receptor-interacting factor 1 (trak2) as a trafficking factor for the k+ channel kir2.1. *J Biol Chem*. 2006;281:30104-30111
17. Sampson LJ, Leyland ML, Dart C. Direct interaction between the actin-binding protein filamin-a and the inwardly rectifying potassium channel, kir2.1. *J Biol Chem*. 2003;278:41988-41997
18. Bendahhou S, Donaldson MR, Plaster NM, Tristani-Firouzi M, Fu YH, Ptacek LJ. Defective potassium channel kir2.1 trafficking underlies andersen-tawil syndrome. *J Biol Chem*. 2003;278:51779-51785
19. Ballester LY, Benson DW, Wong B, Law IH, Mathews KD, Vanoye CG, George AL, Jr. Trafficking-competent and trafficking-defective kcnj2 mutations in andersen syndrome. *Hum Mutat*. 2006;27:388
20. Sun H, Liu X, Xiong Q, Shikano S, Li M. Chronic inhibition of cardiac kir2.1 and herg potassium channels by celastrol with dual effects on both ion conductivity and protein trafficking. *J Biol Chem*. 2006;281:5877-5884
21. van der Heyden MA, Smits ME, Vos MA. Drugs and trafficking of ion channels: A new proarrhythmic threat on the horizon? *Br J Pharmacol*. 2008;153:406-409

22. Tong Y, Brandt GS, Li M, Shapovalov G, Slimko E, Karschin A, Dougherty DA, Lester HA. Tyrosine decaging leads to substantial membrane trafficking during modulation of an inward rectifier potassium channel. *J Gen Physiol.* 2001;117:103-118
23. Seglen PO, Grinde B, Solheim AE. Inhibition of the lysosomal pathway of protein degradation in isolated rat hepatocytes by ammonia, methylamine, chloroquine and leupeptin. *Eur J Biochem.* 1979;95:215-225
24. Hershko A, Ciechanover A. Mechanisms of intracellular protein breakdown. *Annu Rev Biochem.* 1982;51:335-364
25. Pillay CS, Elliott E, Dennison C. Endolysosomal proteolysis and its regulation. *Biochem J.* 2002;363:417-429
26. de Boer TP, van Veen TA, Houtman MJ, Jansen JA, van Amersfoort SC, Doevendans PA, Vos MA, van der Heyden MA. Inhibition of cardiomyocyte automaticity by electrotonic application of inward rectifier current from kir2.1 expressing cells. *Med Biol Eng Comput.* 2006;44:537-542
27. Taschenberger G, Mougey A, Shen S, Lester LB, LaFranchi S, Shyng SL. Identification of a familial hyperinsulinism-causing mutation in the sulfonylurea receptor 1 that prevents normal trafficking and function of katp channels. *J Biol Chem.* 2002;277:17139-17146
28. Kato M, Ogura K, Miake J, Sasaki N, Taniguchi S, Igawa O, Yoshida A, Hoshikawa Y, Murata M, Nanba E, Kurata Y, Kawata Y, Ninomiya H, Morisaki T, Kitakaze M, Hisatome I. Evidence for proteasomal degradation of kv1.5 channel protein. *Biochem Biophys Res Commun.* 2005;337:343-348
29. White NJ. Cardiotoxicity of antimalarial drugs. *Lancet Infect Dis.* 2007;7:549-558
30. Sanchez-Chapula JA, Salinas-Stefanon E, Torres-Jacome J, Benavides-Haro DE, Navarro-Polanco RA. Blockade of currents by the antimalarial drug chloroquine in feline ventricular myocytes. *J Pharmacol Exp Ther.* 2001;297:437-445

Chapter 3 - Reduced Cx43 expression triggers increased fibrosis due to enhanced fibroblast activity

John A. Jansen; Toon A.B. van Veen; Sanne de Jong; Roel van der Nagel; Leonie van Stuijvenberg; Helen Driessen; Ronald Labzowski; Carolin M. Oefner; Astrid A. Bosch; Tri Q. Nguyen; Roel Goldschmeding; Marc A. Vos; Jacques M.T. de Bakker; Harold V.M. van Rijen

Submitted to 'Circulation Arrhythmia and Electrophysiology'

Reduced Cx43 expression triggers increased fibrosis due to enhanced fibroblast activity

John A. Jansen¹; Toon A.B. van Veen¹; Sanne de Jong¹; Roel van der Nagel¹; Leonie van Stuijvenberg¹; Helen Driessen¹; Ronald Labzowski¹; Carolin M. Oefner¹; Astrid A. Bosch¹; Tri Q. Nguyen,²; Roel Goldschmeding²; Marc A. Vos¹; Jacques M.T. de Bakker,^{1,3}; Harold V.M. van Rijen¹

1. Department of Medical Physiology, Division Heart and Lungs, University Medical Center Utrecht, The Netherlands
2. Department of Pathology, University Medical Center Utrecht, Utrecht, The Netherlands
3. Interuniversity Cardiology Institute of the Netherlands, Utrecht, The Netherlands

Abstract

Background - Arrhythmogenic ventricular remodeling is hallmarked by both reduced gap junction expression and increased collagen deposition. We hypothesized that reduced Cx43 expression is responsible for enhanced fibrosis in the remodeled heart, resulting in an arrhythmogenic substrate. Therefore, we investigated the effect of normal or reduced Cx43 expression on the formation of fibrosis in a physiological (aging) and pathophysiological (Transverse Aortic Constriction, TAC) mouse model.

Method and Results - Cx43^{fl/fl} and Cx43^{Cre-ER(T)/fl} mice were aged to 18-21 months, or at the age of 3 months either TAC- or Sham-operated and sacrificed after 16 weeks. Epicardial activation mapping of right (RV) and left (LV) ventricle was performed on Langendorff perfused hearts. Sustained ventricular arrhythmias were induced in 0/11 aged Cx43^{fl/fl} and 10/15 Cx43^{Cre-ER(T)/fl} mice ($p < 0.01$). Cx43 expression was reduced by half in aged Cx43^{Cre-ER(T)/fl} compared to aged Cx43^{fl/fl} mice, whereas collagen deposition was significantly increased from 1.1 ± 0.2 to $7.4 \pm 1.3\%$. Aged Cx43^{Cre-ER(T)/fl} mice with arrhythmias had significantly higher levels of fibrosis and conduction heterogeneity than aged Cx43^{Cre-ER(T)/fl} mice without arrhythmias. TAC-operation significantly increased fibrosis in control compared to Sham (0.4 ± 0.06 vs $4.0 \pm 1.2\%$, respectively), but this increase was significantly higher in Cx43^{Cre-ER(T)/fl} mice ($10.8 \pm 1.4\%$). DDR-2 expression, indicative for the amount of fibroblasts, was unchanged, but pro-collagen peptide I and III expression and COL1A2 mRNA levels were higher in TAC-operated Cx43HZ mice.

Conclusions - Reduced cellular coupling results in more excessive collagen deposition during aging or pressure overload in mice due to enhanced fibroblast activity, leading to increased conduction inhomogeneity and pro-arrhythmia.

Introduction

In the heart, the highly orchestrated propagation of the electrical impulse balances on the delicate interplay between excitability, cell-to-cell coupling and architecture of myocardial tissue. An important aspect of the myocardial architecture is interstitial collagen (fibrosis), which together with connexin43 (Cx43) determines cell-to-cell coupling in ventricular myocardium. Under normal physiological conditions the amount of collagen between the cardiomyocytes is low (< 1% of total tissue volume) but contributes to the structural organization of the heart and the anisotropic character of impulse propagation. We recently showed that in senescent mouse hearts collagen content was increased (200%) and Cx43 expression decreased (50%), changes that were associated with increased inducibility of ventricular tachycardias¹. On the other hand, when the excessive deposition of fibrosis was prevented through long term inhibition of the Renin-Angiotensin-Aldosterone system, the normal pattern of Cx43 expression was preserved and arrhythmia vulnerability strongly reduced².

In addition to those observations during physiological aging, a decreased Cx43 expression in concert with increased collagen content (interstitial and reactive fibrosis) is also found under various pathophysiological conditions³⁻⁸. These alterations have been shown to impair conduction velocity (CV) of the cardiac impulse, by increasing the anisotropic ratio and heterogeneity of conduction. In concert this predisposes the vulnerable heart to an increased risk for fatal arrhythmias that may partly account for the high incidence of sudden cardiac death in patients with remodeled hearts⁹⁻¹¹.

Up till now it is unknown if, and if so, how increased collagen deposition and the accompanied decrease in Cx43 expression are related. In Arrhythmogenic Right Ventricular Dysplasia / Cardiomyopathy (ARVD/C), decreased Cx43 levels are found already in the early stages, whereas fibrosis becomes more abundant during the progression of the disease^{12, 13}. This suggests a possible role of reduced Cx43 expression levels in the deposition of collagen in vulnerable hearts. A supportive recent *in vitro* study suggested increased proliferation of cardiac fibroblasts, the primary source of cells responsible for production of interstitial collagen, once the intercellular communication was inhibited¹⁴.

Other studies suggest a possible role for the interplay between decreased Cx43 expression and increased collagen content in arrhythmia vulnerability. In adult mice (age 12-17 months), interstitial fibrosis increased, but Cx43 expression was similar compared to young (3-4 months) animals¹⁵. Despite increased collagen content, arrhythmias could not be induced in the adult hearts. Another study showed that arrhythmias could not be induced in hearts without fibrosis but with reduced (50%) Cx43 expression¹⁶. These data suggest that a combination of reduced Cx43 expression and increased collagen content is required to increase arrhythmogenicity.

In the present study, we hypothesized that: (1) reduced Cx43 expression triggers enhanced fibrosis in the pathologically and physiologically remodeled heart, (2) the combination of

excessive fibrosis and reduced Cx43 levels results in impaired cardiac impulse conduction and a high arrhythmia-susceptibility. To investigate the potential role of a reduced Cx43 expression in triggering collagen deposition in hearts under physiological- and pathophysiological conditions, an aged (physiologic model 1) and a TAC-operated mouse model (pathophysiologic model 2) were used. In model 1, mice with 100% (Cx43^{fl/fl}) or 50% Cx43 expression (Cx43^{Cre-ER(T)/fl})^{17, 18}, were aged until 18-21 months. A previous study revealed that at this age interstitial fibrosis is highly increased¹. In model 2, three months old mice of the same strain (Cx43^{fl/fl} and Cx43^{Cre-ER(T)/fl}) received Transverse Aortic Constriction (TAC, induced pressure overload) or Sham-surgery and were sacrificed 16 weeks post-surgery. Epicardial mapping was performed on Langendorff perfused hearts to assess impulse conduction and arrhythmia inducibility, and tissue was subsequently analyzed for Cx43 expression and fibrosis. Finally, fibroblast proliferation and activity were determined.

Our data showed that both physiological (aging) and pathophysiological (TAC) stress leads to more excessive fibrosis in mice with a 50% reduced expression of Cx43 (Cx43^{Cre-ER(T)/fl} mice) compared to controls (Cx43^{fl/fl} mice), and that this was related to an increased activity of fibroblasts rather than an increased proliferation of these cells. Together with a heterogeneous reduced expression of Cx43, this resulted in dispersed conduction and pro-arrhythmia.

Materials and Methods

Animals

Cx43^{fl/fl} and Cx43^{Cre-ER(T)/fl} mice were generated as described previously¹⁶. For the experiments on aged animals, 18-21 months old Cx43^{fl/fl} (n=11) and Cx43^{Cre-ER(T)/fl} (n=15) mice were used. No abnormalities in phenotype were found, and HW/BW ratios, age and gender distribution were similar in the two groups (Table 1).

Three months old Cx43^{fl/fl} (n=11) and Cx43^{Cre-ER(T)/fl} (n=9) mice were TAC-operated as described previously¹⁹. A gradient of ~50% was confirmed by Doppler echocardiography. Sham-operated Cx43^{fl/fl} (n=12) and Cx43^{Cre-ER(T)/fl} (n=10) mice were used as control. Animal experiments were performed in accordance with institutional guidelines for animal use in research.

Preparation of the Hearts and Ventricular Conduction

Mice were anesthetized by 2.5% isoflurane in oxygen. A 3-lead electrocardiogram was recorded and analyzed off-line as described previously²⁰. Afterwards, the heart was excised, prepared and connected to a Langendorff perfusion setup as described previously

Table 1 - Statistics of heart and body weight, age and gender-distribution of aged and sham or TAC operated animals.

	BW (g)	HW (mg)	HW/BW (%)	age (months)	male (%)
Aged Cx43 ^{fl/fl}	33.9±1.1	219±13	0.68±0.06	20.1±0.7	55
Aged Cx43 ^{Cre-ER(T)/fl}	33.9±1.4	202±16	0.61±0.03	20.7±0.5	46

Cx43 ^{fl/fl} sham	25.0±1.1	142±10	0.58±0.02	6.6±0.1	42
Cx43 ^{Cre-ER(T)/fl} sham	26.0±0.5	154±6	0.59±0.02	6.5±0.2	50
Cx43 ^{fl/fl} TAC	29.1±1.4	262±21*	0.90±0.05*	6.7±0.4	55
Cx43 ^{Cre-ER(T)/fl} TAC	25.8±1.1	251±21*	0.97±0.08*	6.5±0.2	63

*BW, body weight; HW, heart weight. Data are mean ± SEM. * P<0.05 vs Cx43^{fl/fl} and Cx43^{Cre-ER(T)/fl} sham.*

²¹⁻²³. The hearts were continuously perfused with carbogen-gassed buffer of 37°C, composed of (in mmol/L): NaCl 116, KCl 5, MgSO₄ 1.1, NaH₂PO₄ 0.35, NaHCO₃ 27, glucose 10, mannitol 16 and CaCl₂ 1.8.

Extracellular electrograms were recorded using a 208-point multiterminal electrode (16x13 grid, 0.5-mm spacing) of both the left and right ventricle of the heart as described previously ²¹. Recordings were made during stimulation (1 ms pulse duration, 2x diastolic stimulation threshold) from the center of the grid at a basic cycle length (BCL) of 150 ms. The effective refractory period (ERP), the longest coupling interval of the premature stimulus that failed to activate the entire heart, was determined for each ventricle separately. Every sixteenth stimulus was followed by 1 premature stimulus. Starting at 140 ms, the coupling interval of the premature stimulus was reduced in steps of 10 ms until the ERP.

If spontaneous arrhythmias were absent, susceptibility for arrhythmias was provoked by programmed stimulation in the following sequence. First, 16 basic stimuli followed by 1 or 3 premature stimuli 5 ms longer than the locally determined ERP were applied. Next, if 1 or 3 premature stimuli failed to induce arrhythmias, 2-second burst pacing at the shortest possible cycle length was applied. Arrhythmias in mice were classified as sustained (>15 complexes followed stimulation), according to Lambeth Conventions ²⁴.

Data Analysis

The moment of maximal negative dV/dt in the unipolar electrograms was selected as the time of local activation and determined with custom written software based on MatLab (2006, The MathWorks Inc., Natick, MA) ²⁵. Activation times were used to construct activation maps. Conduction velocities parallel (CV_L) and perpendicular (CV_T) to fiber orientation were determined from activation maps generated from BCL-pacing. Activation times of at least 4 consecutive electrode terminals along lines perpendicular to intersecting isochronal lines were used to calculate CVs. Anisotropic ratio was defined as CV_L/CV_T . Dispersion of conduction was assessed for both LV and RV using the method described by Lammers et al ²⁶.

Immunohistochemistry and Histology

After electrophysiological measurements, hearts were rapidly frozen in liquid nitrogen and stored at -80°C . Coronal (4-chamber view) sections with a thickness of $10\mu\text{m}$ were taken from different levels of the hearts. After immunolabeling, sections were mounted in Vectashield (Vector Laboratories) and examined with a classic light microscope with epifluorescence equipment (Nikon Optiphot-2). To evaluate the presence of fibrosis, sections were fixed with 4% paraformaldehyde (in PBS, 30 minutes at room temperature), stained with Picosirius Red and examined by light microscopy.

The amount of fibrosis and Cx43, P1NP and P3NP immuno-signals were determined using at least 6 randomly chosen pictures of each heart at 200x magnification. Blinded operators calculated Cx43, P1NP and P3NP expression as percentage of the total tissue using Image J 1.40g (2008, NIH, Bethesda, MD). Photomicrographs were transformed into RGB (i.e. Red Green Blue) stack, and true Cx43, P1NP or P3NP pixels were defined in the 256-leveled green channel using a minimal cut-off level. For fibrosis quantification, a comparable procedure was used, but now the range between 90 and 190 in the red channel was defined as true fibrotic tissue.

Heterogeneity of Cx43 expression was determined using MatLab. Photomicrographs were transformed into 8-bit black (Cx43) and white (background) pictures (256 levels) with a cut-off level of 60. A custom written script in MatLab was used to assess for each black pixel the shortest distance to the next black pixel in a virtual circle around that pixel. The standard deviation of all shortest distances of all pixels was used as a measure of Cx43 heterogeneity ¹⁹.

Western blotting

Total cellular protein was isolated from 3 hearts of each group as described previously²², and pooled. Equal amounts of protein (25µg/lane) of each sample were separated on 10% SDS-polyacrylamide gels and transferred by electrophoresis to nitrocellulose membrane (Biorad). Equality of protein transfer was assessed by Ponceau S staining. After first and second antibody incubation, immuno-reactivity was detected using the ECL chemiluminescence kit (Amersham).

To quantify Cx43 protein expression, differences in specific protein concentrations were determined as follows. Processed films and Ponceau Red staining (gray scale scanned) were imported into ImageQuant software to measure separate protein band intensity. Unequal protein loading was corrected against total separated protein; the ratio Cx43/Ponceau Red signal intensity represents the actual Cx43 protein concentration of the different lanes.

Antibodies

The following antibodies were used: mouse monoclonal antibodies against Cx43 (1:250, Transduction Laboratories, used for Western blotting), N-cadherin (1:800, Sigma, Aldrich), α -actinin (1:1000, Sigma, Aldrich) and P1NP (1:250, DSHB, University of Iowa); rabbit polyclonal antibodies against Cx43 (1:250, Zymed, Invitrogen, used for immunohistochemistry) and P3NP (1:100, Millipore); a goat polyclonal antibody against DDR2 (1:100, Santa Cruz); Texas Red- and FITC-conjugated anti mouse or rabbit whole IgG (1:100, Jackson Laboratories) as secondary antibodies for immunohistochemistry; anti mouse or goat peroxidase (1:7000, Biorad) as secondary antibodies for Western blotting.

Quantitative PCR

Total RNA was isolated from frozen ventricular tissue using the Trizol procedure and subsequently treated with DNase I as described before²⁷. First strand cDNA was prepared from 1 µg of RNA with Superscript II reverse transcriptase (Invitrogen) at 42 °C for 1h, using 6.7 µM oligo dT and 0.25 µg of random hexamers (Promeda) as starting primers.

After cDNA synthesis, expression of mouse collagen type 1 α 2 (COL1A2) was assessed by quantitative real-time PCR using TaqMan Gene Expression Assays with pre-designed probe and primers (Applied Biosystems). Glyceraldehyde 3-phosphate dehydrogenase (GAPDH) was used as internal reference.

Statistics

Two-group comparisons were performed using an unpaired t-test, multiple group comparisons using a 1-way analysis of variance (ANOVA) with Bonferroni post hoc analysis. Arrhythmia vulnerability was compared by a fisher exact test. Values are given as mean \pm SEM. $P \leq 0.05$ was considered as statistically significant. Data were analyzed using SPSS 15.0 (2006, SPSS Inc, Chicago, IL) software.

Table 2 - Electrophysiological and tissue characteristics of aged mice

	Cx43 ^{fl/fl}	Cx43 ^{Cre-ER(T)/fl}	VT-	VT+
Arrhythmias (%)	0	67	0	100
LV CV _L (cm/s)	58.8 \pm 5.0	57.9 \pm 3.1	59.6 \pm 4.9	56.2 \pm 4.3
RV CV _L (cm/s)	58.6 \pm 1.0	58.3 \pm 2.3	58.9 \pm 4.9	57.7 \pm 0.4
LV CV _T (cm/s)	35.8 \pm 4.0	32.2 \pm 0.8	32.9 \pm 0.4	31.6 \pm 1.5
RV CV _T (cm/s)	42.7 \pm 1.0	36.5 \pm 1.3	39.4 \pm 1.1	33.7 \pm 0.7**§
LV AR (CV _L /CV _T)	1.68 \pm 0.13	1.79 \pm 0.08	1.81 \pm 0.15	1.77 \pm 0.07
RV AR (CV _L /CV _T)	1.38 \pm 0.10	1.63 \pm 0.14*	1.56 \pm 0.10	1.70 \pm 0.05*
QRS duration (ms)	11.2 \pm 0.29	11.2 \pm 0.18	11.1 \pm 0.37	11.3 \pm 0.20
LV CV Disp Index	1.38 \pm 0.05	2.11 \pm 0.33	1.58 \pm 0.15	2.65 \pm 0.54*
RV CV Disp Index	1.48 \pm 0.02	1.81 \pm 0.13	1.50 \pm 0.00	2.13 \pm 0.13***§§
LV ERP (ms)	82.7 \pm 5.9	64.7 \pm 5.5*	54.0 \pm 9.3*	70.0 \pm 6.5
RV ERP (ms)	77.3 \pm 5.6	53.3 \pm 2.9**	52.0 \pm 6.6*	54.0 \pm 3.1*
Cx43 expression (%)	2.98 \pm 0.80	1.54 \pm 0.27	1.50 \pm 0.36	1.56 \pm 0.40
Cx43 heterogeneity	23.7 \pm 1.49	31.6 \pm 2.26*	31.9 \pm 4.89	31.4 \pm 2.96
Fibrosis (%)	1.10 \pm 0.21	7.38 \pm 1.27*	4.77 \pm 1.77	8.69 \pm 0.91*

LV, left ventricle; RV, right ventricle; CV_L, longitudinal conduction velocity; CV_T, transversal conduction velocity; AR, anisotropic ratio; CV Disp, dispersion of conduction velocity; ERP, effective refractory period; VT-, Cx43^{Cre-ER(T)/fl} mice without arrhythmias; VT+, Cx43^{Cre-ER(T)/fl} mice with arrhythmias. Values are \pm SEM. * $p < 0.05$ vs Cx43^{fl/fl}; ** $p < 0.005$ vs Cx43^{fl/fl}; § $p < 0.05$ vs VT-; §§ $p < 0.005$ vs VT-.

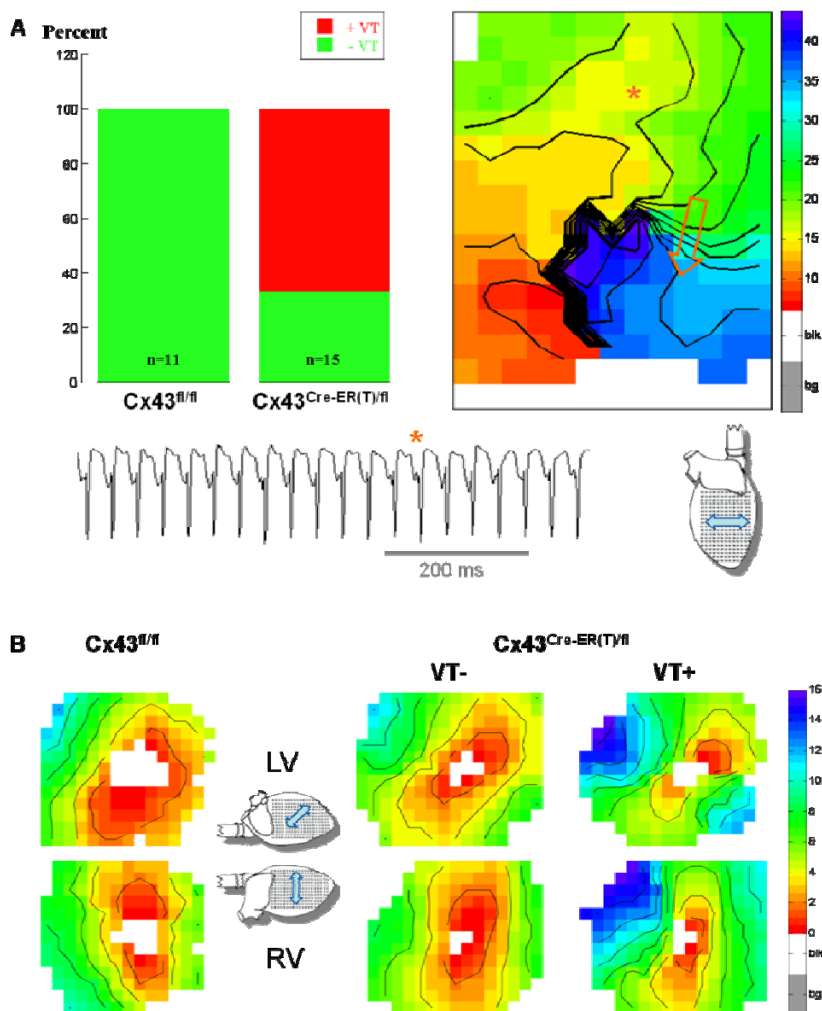


Figure 1 – Ventricular conduction and arrhythmias in aged mice. The bar-plot in panel A shows inducibility of ventricular tachycardias in aged Cx43^{fl/fl} and aged Cx43^{Cre-ER(T)/fl} mice. The right panel shows an activation map of an induced sustained monomorphic ventricular tachycardia, based on anisotropic reentry, with local slow transverse to the fiber direction (open arrow). Black lines are isochronal lines at distances of 2 ms. The epicardial electrogram recorded at the asterisk, showing a monomorphic tachycardia, is shown in the lower panel. Panel B shows typical epicardial activation patterns of LV and RV of aged Cx43^{fl/fl} and aged Cx43^{Cre-ER(T)/fl} mice without (VT-) and with (VT+) inducible arrhythmias. Stimulation was performed from the center of the grid at a BCL of 150 ms, resulting in anisotropic conduction. The blue arrows in the schematics of the heart indicate fiber direction. Colors indicate areas activated within the same time interval and are comparable for each map. Lines are isochronal lines at distances of 2 ms.

Results

Aged mice with reduced Cx43 expression

The majority of hearts of aged Cx43^{Cre-ER(T)/fl} mice were susceptible for monomorphic ventricular tachyarrhythmias (10 out of 15 mice), in sharp contrast to aged Cx43^{fl/fl} mice, in which no arrhythmias were inducible (0 out of 11 mice, $P < 0.01$, Figure 1A). Most arrhythmias were provoked in the RV (9 out of 10), indicating a higher arrhythmia vulnerability of the RV. Figure 1A shows a typical example of a sustained monomorphic VT in a RV induced after burst pacing. The activation map of this VT (right panel) shows anisotropic reentry: impulse propagation occurred around a zone of conduction block, with slow conduction perpendicular to the fiber direction towards the apex of the heart in a localized area (open arrow).

QRS duration was comparable between aged Cx43^{fl/fl} and Cx43^{Cre-ER(T)/fl} mice (11.20 ± 0.29 ms vs 11.24 ± 0.18 ms respectively, Table 2). Representative epicardial activation maps of aged Cx43^{fl/fl} and Cx43^{Cre-ER(T)/fl} mice of both LV and RV during stimulation at a BCL of 150 ms are shown in Figure 1B. Stimulation from the center of the grid resulted in anisotropic activation patterns determined by the fiber direction. Longitudinal conduction velocities in both LV and RV were equal between aged Cx43^{fl/fl} and aged Cx43^{Cre-ER(T)/fl} mice. In the transverse direction, conduction velocity (CV_T) was significantly slower in RV of aged Cx43^{Cre-ER(T)/fl} mice compared to aged Cx43^{fl/fl} mice (Table 2). Concomitantly, the anisotropic ratio was significantly higher in RV of aged Cx43^{Cre-ER(T)/fl} mice.

Interestingly, CV_T in RV was significantly slower in Cx43^{Cre-ER(T)/fl} mice with arrhythmias (VT+) compared to non-arrhythmogenic aged Cx43^{Cre-ER(T)/fl} mice (VT-), which can be appreciated in Figure 1B. The effective refractory period was decreased in both LV and RV of Cx43^{Cre-ER(T)/fl} mice, but not different between VT+ and VT- (Table 2). Typically, activation maps of VT+ mice showed a higher heterogeneous activation pattern with regions of local slow conduction. This was quantified as ‘dispersion of conduction index’²⁶. The dispersion index was higher in VT+ mice, compared to VT- mice, which was only significant in RV. Values in VT- mice were similar to Cx43^{fl/fl} mice (Table 2).

As expected, Cx43^{Cre-ER(T)/fl} hearts expressed about half of the amount of Cx43 compared to control, as determined by immunohistochemistry (52% of Cx43^{fl/fl}, Fig 2A and Table 2) and Western blot (42% of Cx43^{fl/fl}, Fig 2C). Cx43 expression levels were not different between VT+ and VT- (Fig 2A&C, Table 2).

The expression pattern of Cx43 was heterogeneous in Cx43^{Cre-ER(T)/fl} hearts. Regions of low Cx43 were found adjacent to regions of normal Cx43 expression (Figure 2D left panel), while the expression of N-cadherin remained homogenous, indicating intact intercalated discs (Fig 2D right panel). Cx43 heterogeneity, a relative value indicating variation in local expression of Cx43 over the sections was determined. Aged Cx43^{Cre-ER(T)/fl} hearts had

significantly higher heterogeneity-values than aged Cx43^{fl/fl} hearts. Heterogeneity in Cx43 expression was not different between VT+ and VT- (Table 2).

The presence of ventricular fibrosis was evaluated by histochemical analysis with Picrosirius Red staining. Age-related interstitial fibrosis was present in aged Cx43^{fl/fl} hearts (Figure 2A). Interestingly, the amount of fibrosis was significantly higher in aged Cx43^{Cre-ER(T)/fl} hearts compared to Cx43^{fl/fl} hearts (Figure 2B, Table 2). Moreover, the percentage of fibrosis in Cx43^{Cre-ER(T)/fl} VT+ hearts was almost twofold higher than in the VT- group (Figure 2B), albeit statistically not significant (p=0.10).

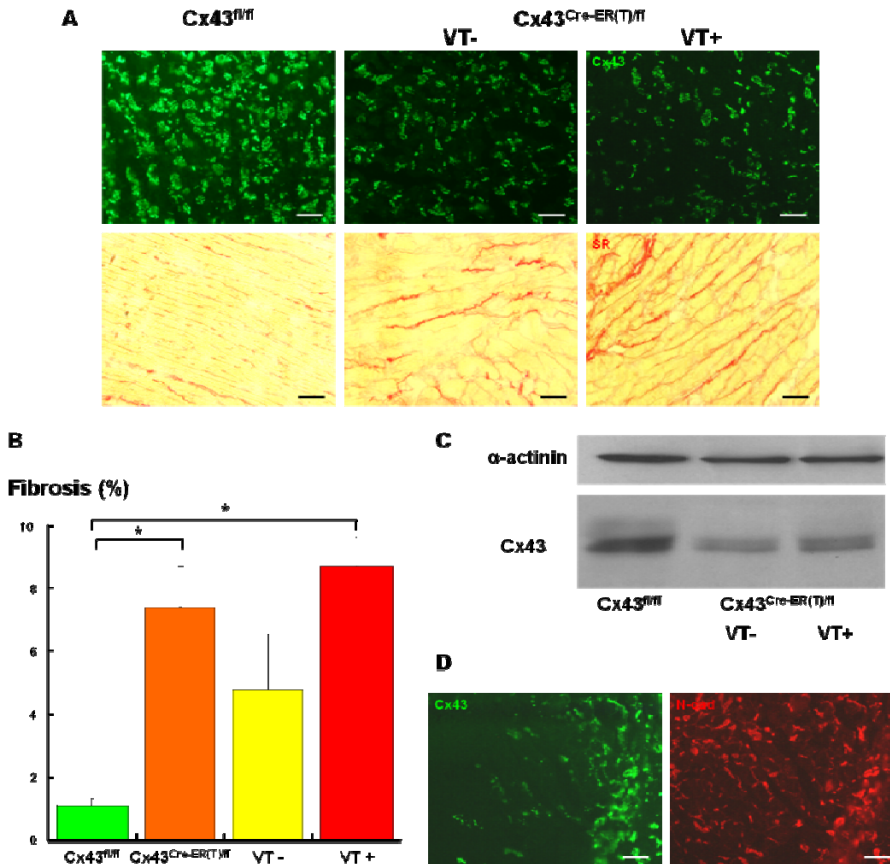


Figure 2 – Cx43 expression and fibrosis in aged mice. Panel A shows typical pictures of Cx43 expression (upper pictures) and fibrosis (lower pictures) in aged Cx43^{fl/fl} and Cx43^{Cre-ER(T)/fl} VT- and VT+ hearts. The amount of collagen in aged hearts is quantified in panel B. Panel C shows Western blot data on α -actinin and Cx43 of aged Cx43^{fl/fl} and Cx43^{Cre-ER(T)/fl} VT- and VT+ mice. Panel D shows local depletion of Cx43 (left picture) with N-cadherin staining on the same spot (right panel), which was found specifically in aged Cx43^{Cre-ER(T)/fl} hearts. Bars represent 50 μ m.

Pressure overloaded mice with reduced Cx43

In the model of physiological aging, the presence of reduced Cx43 resulted in excessive formation of fibrosis and arrhythmias, suggestive that enhanced collagen deposition is caused by reduced Cx43 expression under circumstances of cardiac stress. Therefore, Cx43^{fl/fl} and Cx43^{Cre-ER(T)/fl} mice were subjected to TAC- or Sham-operation to quantify the effect of pathological stress and reduced Cx43 expression (in young animals) on the formation of fibrosis.

Sustained polymorphic ventricular tachycardias were induced in 2/11 (18%) TAC-operated Cx43^{fl/fl} hearts and 3/9 TAC-operated (33%) Cx43^{Cre-ER(T)/fl} hearts (Figure 3, n.s.). No arrhythmias were induced in Sham-operated Cx43^{fl/fl} and Cx43^{Cre-ER(T)/fl} hearts. An example of a sustained polymorphic VT is shown in Figure 3. All electrophysiological characteristics are summarized in Table 3.

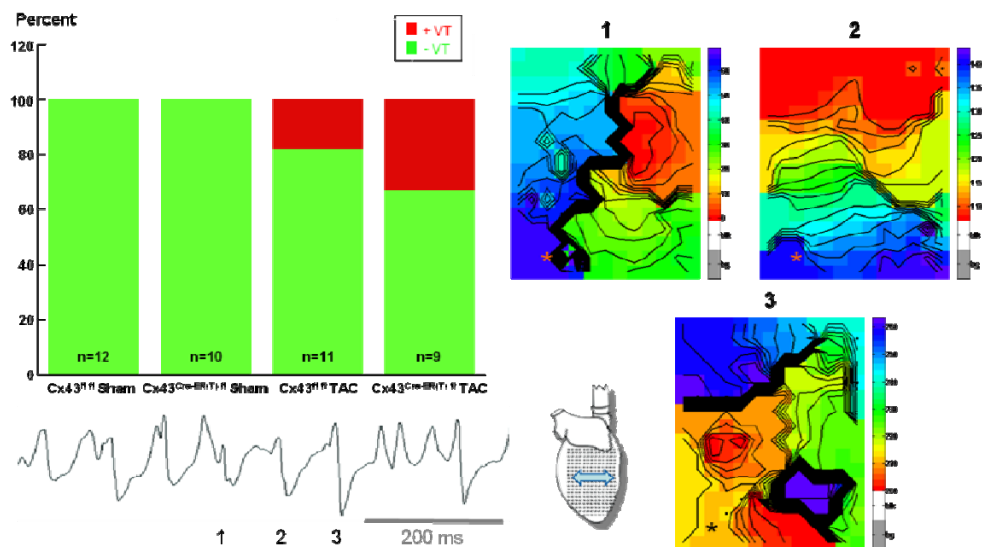


Figure 3 – Arrhythmias in Sham- and TAC-operated mice. The bar-plot shows inducibility of ventricular tachycardias in Sham- and TAC-operated Cx43^{fl/fl} and aged Cx43^{Cre-ER(T)/fl} mice. The lower panel shows the epicardial electrogram, showing a sustained polymorphic tachycardia, recorded at the asterisks. The right panel shows activation maps of 3 consecutive beats, as numbered in the electrogram. Colors indicate areas activated within the same time interval in each individual map, as indicated by the different time axes. Black lines are isochronal lines at distances of 2 ms. The blue arrows in the schematics of the heart indicate fiber direction.

Table 3 - Electrophysiological and tissue characteristics of Sham- and TAC-operated mice

	Cx43 ^{fl/fl} Sham	Cx43 ^{Cre-ER(T)/fl} Sham	Cx43 ^{fl/fl} TAC	Cx43 ^{Cre-ER(T)/fl} TAC
Arrhythmias (%)	0	0	18	36
LV CV _L (cm/s)	70.4±2.1	70.7±1.7	62.1±2.3* [#]	55.8±0.9** ^{##}
RV CV _L (cm/s)	71.5±2.3	70.2±3.0	60.0±1.5* [#]	54.2±3.6** ^{##}
LV CV _T (cm/s)	35.5±1.8	34.0±2.0	30.6±1.7	26.6±2.8
RV CV _T (cm/s)	42.2±2.1	42.3±3.2	36.3±1.9	31.5±3.2*
LV AR (CV _L /CV _T)	1.98±0.09	2.10±0.10	2.00±0.15	2.09±0.27
RV AR (CV _L /CV _T)	1.70±0.08	1.66±0.07	1.68±0.10	1.79±0.22
QRS duration (ms)	9.9±0.14	10.2±0.15	12.6±0.69** ^{##}	12.5±0.37** ^{##}
LV CV Disp Index	1.11±0.11	1.19±0.19	1.43±0.21	1.68±0.10
RV CV Disp Index	1.01±0.01	1.06±0.06	1.36±0.12	1.50±0.19* [#]
LV ERP (ms)	60.0±5.0	62.5±7.0	73.3±5.3	70.0±4.5
RV ERP (ms)	57.3±6.6	57.8±6.2	67.5±8.4	66.7±4.2
Cx43 expression (%)	4.34±0.60	2.14±0.25*	3.88±0.63	0.66±0.14** ^{§§}
Cx43 heterogeneity	24.4±0.72	27.9±0.56	27.4±1.33	32.4±1.40** [§]
Fibrosis (%)	0.42±0.06	0.41±0.04	4.01±1.23	10.77±1.41** ^{##} ^{§§}
P1NP (%)	1.73±0.76	1.68±0.40	4.23±1.78	10.20±3.63* [#]
P3NP (%)	0.67±0.16	1.01±0.14	1.58±0.35	2.62±0.65* [#]
COL1A2	1.00±0.14	1.13±0.22	2.39±0.42	3.34±0.93* [#]

LV, left ventricle; *RV*, right ventricle; *CV_L*, longitudinal conduction velocity; *CV_T*, transversal conduction velocity; *AR*, anisotropic ratio; *CV Disp*, dispersion of conduction velocity; *ERP*, effective refractory period. Values are ± SEM. * $p < 0.05$ vs Cx43^{fl/fl} sham; ** $p < 0.005$ vs Cx43^{fl/fl} sham; # $p < 0.05$ vs Cx43^{Cre-ER(T)/fl} sham; ## $p < 0.005$ vs Cx43^{Cre-ER(T)/fl} sham; § $p < 0.05$ vs Cx43^{fl/fl} TAC; §§ $p < 0.005$ vs Cx43^{fl/fl} TAC.

Typical examples of Cx43-immunolabeled sections of Sham- or TAC-operated Cx43^{fl/fl} and Cx43^{Cre-ER(T)/fl} hearts are shown in Figure 4A. As expected, Cx43 expression was significantly lower (~50%) in Sham-operated Cx43^{Cre-ER(T)/fl} hearts compared to Sham-operated Cx43^{fl/fl} hearts. TAC-operation did not affect Cx43 expression in Cx43^{fl/fl} hearts, but significantly decreased Cx43 expression in Cx43^{Cre-ER(T)/fl} hearts (Table 3), which was confirmed by Western blot (Figure 4C).

Hearts of Sham-operated Cx43^{fl/fl} and Cx43^{Cre-ER(T)/fl} mice displayed only low amounts of interstitial fibrosis (Figure 4A&B). Pressure overload by TAC-surgery resulted in a significant increase in fibrosis in Cx43^{fl/fl} hearts (Figure 4B). However, in TAC-operated Cx43^{Cre-ER(T)/fl} hearts a significantly higher amount of fibrosis was detected (Figure 4A&B), indicating that pressure overload in the background of reduced Cx43 leads to enhanced fibrosis.

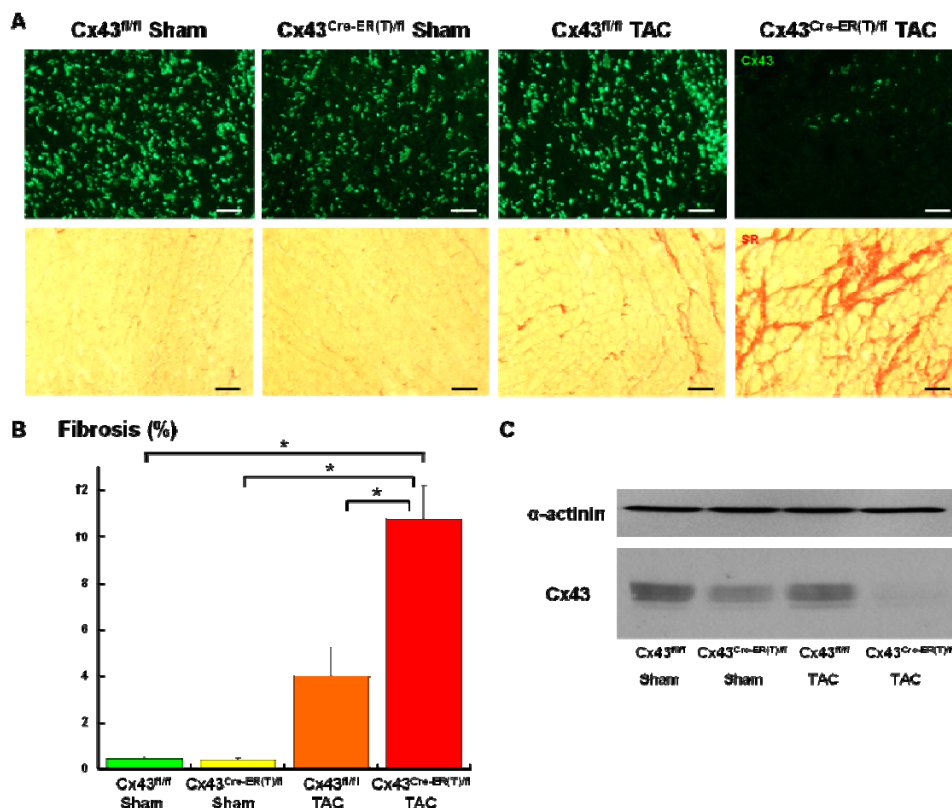


Figure 4 – Cx43 expression and fibrosis in Sham- and TAC-operated mice. Panel A shows typical pictures of Cx43 expression (upper pictures) and fibrosis (lower pictures) in Sham- and TAC-operated Cx43^{fl/fl} and Cx43^{Cre-ER(T)/fl} hearts. Bars represent 50 μ m. The amount of collagen in Sham- and TAC-operated hearts is quantified in panel B. Panel C shows Western blot data on α -actinin and Cx43 of Sham- and TAC-operated Cx43^{fl/fl} and Cx43^{Cre-ER(T)/fl} mice.

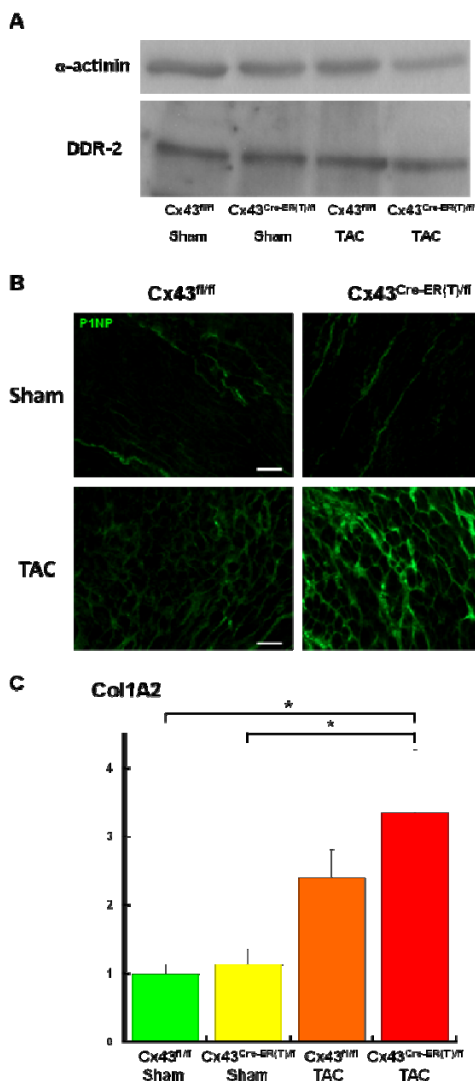


Figure 5 – Fibroblast proliferation and activity. Panel A shows Western blot data with comparable DDR2 expression in Sham- and TAC-operated Cx43^{fl/fl} and Cx43^{Cre-ER(T)/fl} hearts. Immunofluorescent pictures in panel B show low P1NP expression in Sham-operated Cx43^{fl/fl} and Cx43^{Cre-ER(T)/fl} hearts (upper pictures), which was slightly increased after TAC-operation in Cx43^{fl/fl} hearts, but much more pronounced and only significantly in TAC-operated Cx43^{Cre-ER(T)/fl} hearts. Bars represent 50 μ m. Panel C shows that COL1A2 mRNA expression was significantly increased in TAC-operated Cx43^{Cre-ER(T)/fl} hearts compared to Sham-operated Cx43^{fl/fl} and Cx43^{Cre-ER(T)/fl} hearts. Values are relative increases compared to expression in Sham-operated Cx43^{fl/fl} hearts.

Fibroblast proliferation and activity

Both aged and TAC-operated Cx43^{Cre-ER(T)/fl} hearts showed more pronounced fibrosis compared to aged and TAC-operated Cx43^{fl/fl} hearts. Enhanced fibrosis is due to enhanced collagen deposition, which may be caused by either enhanced fibroblast proliferation, enhanced fibroblast activity, or both. Therefore, we analyzed fibroblast proliferation and activity of TAC- and Sham-operated Cx43^{fl/fl} and Cx43^{Cre-ER(T)/fl} hearts. Discoidin domain receptor 2 (DDR2) expression, specifically present at the cell membrane of fibroblasts in cardiac tissue, was evaluated by Western blotting. Figure 5A shows that DDR2 expression

was equal between Cx43^{fl/fl} and Cx43^{Cre-ER(T)/fl} hearts, and that TAC-operation did not change DDR2 expression, indicating that the number of fibroblasts remained unchanged.

Subsequently, activity of fibroblasts was determined by expression of the procollagen peptide P1NP. Figure 5B shows low P1NP expression in Sham-operated Cx43^{fl/fl} and Cx43^{Cre-ER(T)/fl} hearts, respectively. TAC-operation did not statistically alter P1NP expression in Cx43^{fl/fl} hearts, although the expression tended to be somewhat more intense. However, P1NP expression was significantly increased in Cx43^{Cre-ER(T)/fl} hearts after TAC-surgery when compared to Sham-operated hearts (Table 3). Comparable results were obtained for P3NP, another procollagen peptide (Table 3).

Finally, we performed a qPCR on COL1A2, the gene encoding for the alpha-2 chain of collagen type 1. Figure 5C shows that COL1A2 mRNA levels were comparable between Sham-operated Cx43^{fl/fl} and Cx43^{Cre-ER(T)/fl} hearts. However, TAC-operation significantly increased COL1A2 mRNA levels in Cx43^{Cre-ER(T)/fl} hearts.

Discussion

The main and novel finding of this study is that reduced expression of Cx43 leads to more excessive fibrosis during both physiological (aging) and pathophysiological (TAC) stress in mice due to an increased activity of fibroblasts rather than an increased proliferation. Furthermore, heterogeneously reduced Cx43 expression in concert with enhanced fibrosis leads to an arrhythmogenic substrate due to dispersed conduction.

Fibroblast proliferation and activity

The increased collagen deposition during aging or after pressure-overload is in agreement with previous results^{15, 19, 28}. Interestingly, we showed that this increase in fibrosis is more prominent in Cx43^{Cre-ER(T)/fl} compared to Cx43^{fl/fl} hearts. In order to unravel the mechanism for the enhanced fibrosis in stressed hearts with reduced Cx43 levels, we hypothesized that reduced Cx43 levels may alter cardiomyocytes/fibroblast and fibroblast/fibroblast communication, leading to increased fibroblast proliferation and/or activity. Previously, Zhang et al showed that in cultures of isolated adult murine ventricular fibroblasts, proliferation of fibroblasts was increased upon decreasing levels of Cx43 expression¹⁴. Using DDR2 as a selective marker for fibroblasts in the heart²⁹, our data showed that DDR2 expression was similar between Cx43^{Cre-ER(T)/fl} and Cx43^{fl/fl} hearts, and that TAC-surgery did not affect DDR2 levels, indicating that the number of fibroblasts was equal among the groups. Apparently, the effect of decreased Cx43 expression on fibroblast proliferation *in vivo* differs from *in vitro* studies, possibly due to the presence of cardiomyocytes and/or contact inhibition.

To determine the activity of fibroblasts, we first measured expression of P1NP and P3NP, the propeptides of procollagen type I and III, respectively. The data showed a significant increase in P1NP and P3NP expression after TAC-operation, specifically in Cx43^{Cre-ER(T)/fl} hearts. Furthermore, the COL1A2 mRNA level, encoding for the pro- α 2 chain of procollagen type I, was significantly increased in Cx43^{Cre-ER(T)/fl} hearts after TAC-operation. These data indicate that an increased fibroblast activity, rather than an increased proliferation, accounts for the enhanced fibrosis in challenged Cx43^{Cre-ER(T)/fl} hearts.

Decreased Cx43 expression leads to enhanced fibrosis and arrhythmias.

Arrhythmogenic remodeled hearts are commonly hallmarked by a combined decrease in Cx43 and increase in collagen deposition³⁻⁸. It is not clear however whether Cx43 expression and fibrosis are related, and if so, whether decreased Cx43 expression precedes the formation of fibrosis, or is the resultant of fibrosis. In a previous study, we aged mice to 15 months. These mice had slightly increased levels of fibrosis with normal levels of Cx43¹⁵. The resultant was an electrically stable heart with moderate conduction slowing. However, when we aged mice further, i.e. to 22 months¹, reduced Cx43 expression and further enhanced fibrosis was found, leading to moderate conduction slowing, but with a high incidence of arrhythmias. In the current study, genetically induced reduction of Cx43 resulted in strong enhancement of fibrosis after aging or aortic stenosis. These observations strongly suggest that reduced levels of Cx43 trigger enhanced fibrosis and not *vice versa*. This viewpoint is further supported by the finding that our aged 22 months old Cx43^{fl/fl} control mice have lower levels of Cx43 compared to 5 months old Cx43^{fl/fl} mice, resulting in increased levels of fibrosis in the aged mice (not shown). Secondly, we and others have shown that chronic inhibition of the renin-angiotensin-aldosterone system of aging mice², cardiomyopathic hamsters³⁰ and TAC mice³¹, prevents gap junction remodeling and leads to reduced levels of fibrosis. The general mechanistic view is that enhanced interstitial fibrosis leads to separation of the myocardial fibers with subsequent reduction of gap junction plaques. However, Qu and coworkers showed that treatment of TAC-mice with the aldosterone antagonist Spironolactone after gap junction remodeling and the formation of fibrosis, resulted in reversal of gap junction expression, but not to reversal of fibrosis. Furthermore, CV was normalized, while only gap junction expression was normalized. Two important conclusions with regard to our current study can be drawn: 1. gap junction remodeling precedes the process of collagen remodeling and in the case of reversal, gap junction remodeling precedes the reduction of fibrosis. 2. Both reduced Cx43 expression and increased fibrosis are needed for conduction slowing.

A strong argument supporting the first conclusion is found in Arrhythmogenic Right Ventricular Dysplasia/Cardiomyopathy. The overt state of this disease is hallmarked by reduced Cx43 expression and prominent fibrosis, leading to arrhythmias. However, the temporal evolution of the disease in the concealed phase clearly starts with reduced

expression of Cx43, resulting from reduced desmosomal integrity, clearly before the formation of fibrosis^{12,13}. The results of this study imply that, potentially also in ARVD/C, reduced expression of Cx43 triggers enhanced expression of collagen by the fibroblasts and thereby progressing the course of ARVD/C. Then, the combination of reduced Cx43, together with enhanced fibrosis will lead to the formation of the arrhythmogenic substrate (conclusion 2).

Arrhythmogeneity

Aged mice

In aged mice, ventricular tachycardias could only be induced in Cx43^{Cre-ER(T)/fl} hearts. Tachycardias were monomorphic and based on anisotropic reentry. Several factors may be in favor of the high incidence of the reentry-based arrhythmias in the aged Cx43^{Cre-ER(T)/fl} hearts: a heterogeneously reduced Cx43 expression with increased fibrosis, resulting in slower transverse conduction preferentially in RV, increased dispersed conduction, and a decreased ERP.

TAC-operated mice

In TAC operated mice induced ventricular tachycardias were always polymorphic. The mechanism of the arrhythmias is not completely clear, but previous studies suggest that they are based on triggered activity¹⁹. Increased ERP, indicative of prolonged action potential durations, and reduced cell-to-cell coupling are in favor of triggered activity. Whereas a slowed and dispersed conduction, due to fibrosis and/or a heterogeneous reduction of Cx43, considerably increases the susceptibility for monomorphic ventricular tachycardias, based on anisotropic reentry, it hardly affects the vulnerability to triggered activity³². This may explain why arrhythmia vulnerability was comparable between TAC-operated Cx43^{Cre-ER(T)/fl} and Cx43^{fl/fl} hearts.

Clinical relevance

This study shows that reduced levels of Cx43 promote the formation of fibrosis in stressed hearts. In several cardiac diseases, such as ARVD/C, gap junctional remodeling is already found in early stages, whereas fibrosis becomes more abundant during progression of the disease. Our data suggest that early normalization of Cx43 expression might partly prevent fibrosis formation, reducing the susceptibility to fatal arrhythmias.

Acknowledgements

The P1NP antibody developed by Dr Heinz Furthmayr was obtained from the Developmental Studies Hybridoma Bank developed under the auspices of the NICHD and maintained by the University of Iowa, Department of Biology, Iowa City, IA 52242.

This study was supported by the Netherlands Heart Foundation, grant 2005B170.

References

1. Stein M, Noorman M, van Veen TA, Herold E, Engelen MA, Boulaksil M, Antoons G, Jansen JA, van Oosterhout MF, Hauer RN, de Bakker JM, van Rijen HV. Dominant arrhythmia vulnerability of the right ventricle in senescent mice. *Heart Rhythm*. 2008;5:438-448
2. Stein M, Boulaksil M, Jansen JA, Herold E, Noorman M, Joles JA, van Veen TA, Houtman MJ, Engelen MA, Hauer RN, de Bakker JM, van Rijen HV. Reduction of fibrosis-related arrhythmias by chronic renin-angiotensin-aldosterone system inhibitors in an aged mouse model. *Am J Physiol Heart Circ Physiol*. 2010;299:H310-321
3. Peters NS. New insights into myocardial arrhythmogenesis: Distribution of gap-junctional coupling in normal, ischaemic and hypertrophied human hearts. *Clin Sci (Lond)*. 1996;90:447-452
4. Kaprielian RR, Gunning M, Dupont E, Sheppard MN, Rothery SM, Underwood R, Pennell DJ, Fox K, Pepper J, Poole-Wilson PA, Severs NJ. Downregulation of immunodetectable connexin43 and decreased gap junction size in the pathogenesis of chronic hibernation in the human left ventricle. *Circulation*. 1998;97:651-660
5. Kostin S, Rieger M, Dammer S, Hein S, Richter M, Klovekorn WP, Bauer EP, Schaper J. Gap junction remodeling and altered connexin43 expression in the failing human heart. *Mol Cell Biochem*. 2003;242:135-144
6. La Vecchia L, Ometto R, Bedogni F, Finocchi G, Mosele GM, Bozzola L, Bevilacqua P, Vincenzi M. Ventricular late potentials, interstitial fibrosis, and right ventricular function in patients with ventricular tachycardia and normal left ventricular function. *Am J Cardiol*. 1998;81:790-792
7. Swynghedauw B. Molecular mechanisms of myocardial remodeling. *Physiol Rev*. 1999;79:215-262
8. Kawara T, Derksen R, de Groot JR, Coronel R, Tasseron S, Linnenbank AC, Hauer RN, Kirkels H, Janse MJ, de Bakker JM. Activation delay after premature stimulation in chronically diseased human myocardium relates to the architecture of interstitial fibrosis. *Circulation*. 2001;104:3069-3075
9. Winterton SJ, Turner MA, O'Gorman DJ, Flores NA, Sheridan DJ. Hypertrophy causes delayed conduction in human and guinea pig myocardium: Accentuation during ischaemic perfusion. *Cardiovasc Res*. 1994;28:47-54
10. McIntyre H, Fry CH. Abnormal action potential conduction in isolated human hypertrophied left ventricular myocardium. *J Cardiovasc Electrophysiol*. 1997;8:887-894
11. Levy D, Anderson KM, Savage DD, Balkus SA, Kannel WB, Castelli WP. Risk of ventricular arrhythmias in left ventricular hypertrophy: The framingham heart study. *Am J Cardiol*. 1987;60:560-565
12. Saffitz JE. Arrhythmogenic cardiomyopathy and abnormalities of cell-to-cell coupling. *Heart Rhythm*. 2009;6:S62-65
13. Oxford EM, Everitt M, Coombs W, Fox PR, Kraus M, Gelzer AR, Saffitz J, Taffet SM, Moise NS, Delmar M. Molecular composition of the intercalated disc in a spontaneous canine animal model of arrhythmogenic right ventricular dysplasia/cardiomyopathy. *Heart Rhythm*. 2007;4:1196-1205
14. Zhang Y, Kanter EM, Laing JG, Aprhys C, Johns DC, Kardami E, Yamada KA. Connexin43 expression levels influence intercellular coupling and cell proliferation of native murine cardiac fibroblasts. *Cell Commun Adhes*. 2008;15:289-303
15. van Veen TA, Stein M, Royer A, Le Quang K, Charpentier F, Colledge WH, Huang CL, Wilders R, Grace AA, Escande D, de Bakker JM, van Rijen HV. Impaired impulse propagation in scn5a-knockout mice: Combined contribution of excitability, connexin expression, and tissue architecture in relation to aging. *Circulation*. 2005;112:1927-1935
16. van Rijen HV, Eckardt D, Degen J, Theis M, Ott T, Willecke K, Jongsma HJ, Opthof T, de Bakker JM. Slow conduction and enhanced anisotropy increase the propensity for ventricular tachyarrhythmias in adult mice with induced deletion of connexin43. *Circulation*. 2004;109:1048-1055
17. Eckardt D, Theis M, Degen J, Ott T, van Rijen HV, Kirchhoff S, Kim JS, de Bakker JM, Willecke K. Functional role of connexin43 gap junction channels in adult mouse heart assessed by inducible gene deletion. *J Mol Cell Cardiol*. 2004;36:101-110

18. Feil R, Brocard J, Mascres B, LeMeur M, Metzger D, Chambon P. Ligand-activated site-specific recombination in mice. *Proc Natl Acad Sci U S A*. 1996;93:10887-10890
19. Boulaksil M, Winckels SK, Engelen MA, Stein M, van Veen TA, Jansen JA, Linnenbank AC, Bierhuizen MF, Groenewegen WA, van Oosterhout MF, Kirkels JH, de Jonge N, Varro A, Vos MA, de Bakker JM, van Rijen HV. Heterogeneous connexin43 distribution in heart failure is associated with dispersed conduction and enhanced susceptibility to ventricular arrhythmias. *Eur J Heart Fail*. 2010;12:913-921
20. Royer A, van Veen TA, Le Bouter S, Marionneau C, Griol-Charhbili V, Leoni AL, Steenman M, van Rijen HV, Demolombe S, Goddard CA, Richer C, Escoubet B, Jarry-Guichard T, Colledge WH, Gros D, de Bakker JM, Grace AA, Escande D, Charpentier F. Mouse model of scn5a-linked hereditary lenegre's disease: Age-related conduction slowing and myocardial fibrosis. *Circulation*. 2005;111:1738-1746
21. van Rijen HV, van Veen TA, van Kempen MJ, Wilms-Schopman FJ, Potse M, Krueger O, Willecke K, Opthof T, Jongsma HJ, de Bakker JM. Impaired conduction in the bundle branches of mouse hearts lacking the gap junction protein connexin40. *Circulation*. 2001;103:1591-1598
22. van Veen TA, van Rijen HV, Wiegerinck RF, Opthof T, Colbert MC, Clement S, de Bakker JM, Jongsma HJ. Remodeling of gap junctions in mouse hearts hypertrophied by forced retinoic acid signaling. *J Mol Cell Cardiol*. 2002;34:1411-1423
23. Alcolea S, Jarry-Guichard T, de Bakker J, Gonzalez D, Lamers W, Coppens S, Barrio L, Jongsma H, Gros D, van Rijen H. Replacement of connexin40 by connexin45 in the mouse: Impact on cardiac electrical conduction. *Circ Res*. 2004;94:100-109
24. Walker MJ, Curtis MJ, Hearse DJ, Campbell RW, Janse MJ, Yellon DM, Cobbe SM, Coker SJ, Harness JB, Harron DW, et al. The lambeth conventions: Guidelines for the study of arrhythmias in ischaemia infarction, and reperfusion. *Cardiovasc Res*. 1988;22:447-455
25. Potse M, Linnenbank AC, Grimbergen CA. Software design for analysis of multichannel intracardial and body surface electrocardiograms. *Comput Methods Programs Biomed*. 2002;69:225-236
26. Lammers WJ, Schalijs MJ, Kirchhof CJ, Allesie MA. Quantification of spatial inhomogeneity in conduction and initiation of reentrant atrial arrhythmias. *Am J Physiol*. 1990;259:H1254-1263
27. Teunissen BE, Jansen AT, Mutsaers NA, Vuerhard MJ, Vos MA, Bierhuizen MF. Primary structure, organization, and expression of the rat connexin45 gene. *DNA Cell Biol*. 2007;26:108-115
28. Xia Y, Lee K, Li N, Corbett D, Mendoza L, Frangogiannis NG. Characterization of the inflammatory and fibrotic response in a mouse model of cardiac pressure overload. *Histochem Cell Biol*. 2009;131:471-481
29. Goldsmith EC, Hoffman A, Morales MO, Potts JD, Price RL, McFadden A, Rice M, Borg TK. Organization of fibroblasts in the heart. *Dev Dyn*. 2004;230:787-794
30. De Mello WC, Specht P. Chronic blockade of angiotensin ii at1-receptors increased cell-to-cell communication, reduced fibrosis and improved impulse propagation in the failing heart. *J Renin Angiotensin Aldosterone Syst*. 2006;7:201-205
31. Qu J, Volpicelli FM, Garcia LI, Sandeep N, Zhang J, Marquez-Rosado L, Lampe PD, Fishman GI. Gap junction remodeling and spironolactone-dependent reverse remodeling in the hypertrophied heart. *Circ Res*. 2009;104:365-371
32. Wit AL, Dillon SM. Anisotropic reentry. *Cardiac Mapping, Chapter 8*. 1993

Chapter 4 - Progressive AV-block in a mouse-model of Lev / Lenègre disease

John A. Jansen; Sanne de Jong; Carol Ann Remme; Toon A.B. van Veen; Roel van der Nagel; Ronald Labzowski; Marc A. Vos; Connie Bezzina; Jacques M.T. de Bakker; Harold V.M. van Rijen

In preparation

Progressive AV-block in a mouse-model of Lev / Lenègre disease

John A. Jansen¹; Sanne de Jong¹; Carol Ann Remme²; Toon A.B. van Veen¹; Roel van der Nagel¹; Ronald Labzowski¹; Marc A. Vos¹; Connie Bezzina²; Jacques M.T. De Bakker^{1,3}; Harold V.M. van Rijen¹

1. Department of Medical Physiology, Division Heart and Lungs, University Medical Center Utrecht, The Netherlands
2. Department of Experimental Cardiology, Heart Failure Research Center, Academic Medical Center, Amsterdam, The Netherlands
3. Interuniversity Cardiology Institute of the Netherlands, Utrecht, The Netherlands

Abstract

Background - Lev / Lenègre disease is a progressive cardiac conduction defect, characterized by fibrosis and degeneration of the conduction system. It is also associated with mutations in Scn5a, encoding the cardiac sodium channel. Clinical manifestation occurs after cardiac events such as coronary sclerosis or aortic stenosis. To mimic aortic stenosis, we investigated the effect of Transverse Aortic Constriction (TAC) on transgenic Scn5a^{1798insD/+} mice.

Method and Results - Wild-type (WT) and Scn5a^{1798insD/+} (HET) mice were either TAC- or Sham-operated. Between the 5th and 14th day after TAC-surgery 8 out of 19 HET TAC mice died, in contrast to none of the WTs or Shams. 24-h Telemetry recording showed progressively increased PR- and RR-intervals in HET TAC mice, finally resulting in AV-block and death, while in surviving HET TAC animals, PR- and RR-intervals were only moderately increased. Epicardial conduction during S1S1 pacing (120ms), atrioventricular (AV) conduction and arrhythmia susceptibility were determined on Langendorff-perfused hearts. AV-delay was significantly increased in HET TAC mice during S1S1 pacing (58.3ms vs 43-45.5ms in the other groups), which strongly increased at shorter coupling-intervals. AV nodal refractory period and Wenckebach periodicity were increased in HET TAC mice. Longitudinal conduction velocity was slightly lower in both MUT Sham and TAC animals, resulting in a small increase in QRS-duration, but no ventricular arrhythmias could be induced. Cx43 expression was decreased in MUT TAC mice, with increased levels of fibrosis.

Conclusions - Aortic stenosis in the background of abnormal sodium channel function resulted in disturbed AV-conduction, typical for Lev / Lenègre disease.

Introduction

Lev or Lenègre disease, also known as progressive cardiac conduction defect, is an age-related conduction disturbance in the heart. It is characterized by a senile degeneration of the His-Purkinje conduction system with right or left bundle branch block and increased QRS-duration^{1, 2}. Eventually, it can result in complete atrioventricular block and Stoke-Adams syncope, justifying pacemaker implantation, but ventricular tachyarrhythmias are absent³. Originally, the degeneration of the conduction system was completely attributed to increased fibrosis and calcification in the His bundle and bundle branches. More recently, loss-of-function mutations in the *Scn5a* gene, encoding for the cardiac sodium channel, have been associated with Lev / Lenègre disease⁴.

In 1999, Bezzina et al showed that a single human *Scn5a* mutation (1795insD) can cause long-QT 3 (LQT₃), Brugada syndrome and Conduction disease (CD)⁵. An overlap syndrome of these pathologies was found in transgenic mice carrying the mouse equivalent (1798insD) of the mutation; these *Scn5a*^{1798insD/+} mice showed decreased peak sodium current with an increased persistent current, resulting in bradycardia, conduction slowing and QT-prolongation⁶. Aged haploinsufficient *Scn5a*^{+/-} mice showed progressively increased QRS- and PR-intervals with extensive fibrosis, typical for Lev / Lenègre disease⁷. Recently, the 1795insD mutation has also been linked to progressive CD⁸.

The original paper of Lenègre in 1964 describes the high prevalence of several cardiac pathologies, such as coronary sclerosis and aortic stenosis, in post-mortem hearts of Lev / Lenègre patients¹. This observation suggests that besides a mutated cardiac sodium channel, a secondary cardiac defect is required for, or at least accelerates, the process towards clinical manifestation. Therefore, we hypothesized that challenging the hearts of mice with abnormal cardiac sodium channel function (*Scn5a*^{1798insD/+} mice, HET) would result in a Lev / Lenègre phenotype in a short time span. For this purpose, we investigated the effect of Transverse Aortic Constriction (TAC), to mimic aortic stenosis, on three months old HET or wild-type (WT) mice. Continuous telemetry ECG recordings were acquired of a subset of TAC-operated mice. All mice were sacrificed 2 weeks post-surgery to perform epicardial activation mapping on Langendorff-perfused hearts, and afterwards Cx43 expression and fibrosis was determined.

Our data showed that within 2 weeks after TAC-surgery, 42% of HET mice developed first degree AV-block (increased PR-interval) with decreased heart rates, ultimately leading to third degree AV-block and death, in contrast to WT and Sham-operated mice. Epicardial mapping in surviving TAC-operated HET mice revealed increased AV-conduction delay with increased AV nodal refractory period and Wenckebach periodicity. Tissue analysis showed that Cx43 expression was decreased, the amount of collagen increased. These data indicate that aortic stenosis in the background of abnormal sodium channel function resulted in a typical Lev / Lenègre phenotype.

Materials and Methods

Animals and Transverse Aortic Constriction (TAC) Procedure

Heterozygous $Scn5a^{1798insD/+}$ (HET) and homozygous $Scn5a^{+/+}$ (WT) mice were generated as described previously ⁶. At the age of three months, HET (n=19) and WT (n=13) mice were TAC-operated as described previously ⁹. A gradient of ~50mm Hg across the aortic valve was confirmed by Doppler echocardiography. Sham-operated HET (n=9) and WT (n=10) mice were used as control. Gender distribution and body weight (BW) were comparable among the 4 groups, however heart weight / body weight ratio (HW/BW) was increased in TAC-operated WT and HET mice (Table 1). Animal experiments were performed in accordance with institutional guidelines for animal use in research.

Telemetry ECG Measurements

In a subset of HET and WT mice that received TAC-surgery, a radiotelemetry transmitter (model EA-F20, Data Sciences International, St. Paul, Minnesota) was surgically inserted into the peritoneal cavity, with 1 lead placed subcutaneously at the right shoulder, and the other subcutaneously ~1cm left of the xiphoid process. After 2 days of recovery, ECGs were measured continuously until 2 weeks after TAC-operation or death. Custom made signal-acquisition software was used to store ECG-data digitally. ECG-data were analyzed using Labchart 7 Pro (AD-instruments).

Table 1 - Statistics of body and heart weight, gender distribution and mortality

	WT Sham	$Scn5a^{1798insD/+}$ Sham	WT TAC	$Scn5a^{1798insD/+}$ TAC
BW (g)	26.3±1.3	27.7±1.4	25.9±0.7	26.3±0.9
HW/BW (%)	0.59±0.02	0.61±0.04	0.79±0.03**###	0.80±0.03**###
Male (%)	50	56	54	63
† (%)	0	0	0	42*#§

*BW, body weight; HW/BW, heart weight / body weight ratio; †, mortality-rate in the first 2 weeks after surgery. Values are ± SEM. * $p < 0.05$ vs WT Sham; ** $p < 0.005$ vs WT Sham; # $p < 0.05$ vs $Scn5a^{1798insD/+}$ Sham; ### $p < 0.005$ vs $Scn5a^{1798insD/+}$ Sham; § $p < 0.05$ vs WT TAC; §§ $p < 0.005$ vs WT TAC.*

Epicardial Mapping

Two weeks after TAC- or Sham-surgery, mice were anesthetized by 2.5% isoflurane in oxygen. A 3-lead electrocardiogram was recorded and analyzed off-line as described previously⁷. Afterwards, the heart was excised and connected to a Langendorff perfusion system as described previously¹⁰⁻¹², where it was continuously perfused with carbogen-gassed buffer of 37°C, composed of (in mmol/L): NaCl 116, KCl 5, MgSO₄ 1.1, NaH₂PO₄ 0.35, NaHCO₃ 27, glucose 10, mannitol 16 and CaCl₂ 1.8.

Extracellular electrograms were recorded using a 247-point multiterminal electrode (19x13 grid, 0.3-mm spacing) of both ventricles and atria as described previously¹¹. Recordings were made during stimulation (1 ms pulse, 2x diastolic stimulation threshold) from the center of the grid at a basic cycle length (BCL) of 120 ms. The effective refractory period (ERP), the longest coupling interval of the premature stimulus that failed to activate the entire heart, and arrhythmia susceptibility were determined as described previously¹³.

Wenckebach periodicity (WBP) was determined by > 2s pacing at the left atrium. Starting at 150 ms, the cycle length was reduced in steps of 10ms until a single stimulation failed to activate the ventricles. For the AV nodal refractory period (AVNRP), the same protocol was used as for the ERP. The intrinsic sinus rate (SR) was measured without stimulation using at least 8 consecutive beats.

Data Analysis

QT-intervals were corrected for heart rate using a mouse equivalent of the Bazett's formula, as described previously¹⁴.

The times of local activation in the unipolar electrograms were determined with custom written software based on MatLab (2006, The MathWorks Inc., Natick, MA)¹⁵. Conduction velocities parallel (CV_L) and perpendicular (CV_T) to fiber orientation and anisotropic ratios (CV_L/CV_T) were determined during BCL-pacing as described previously¹³. Atrial-ventricular delay (AV-delay) was determined by stimulation from the left atrium (LA), by calculating the averaged temporal difference between the signal, corresponding to LA-activation, and the remote signal that corresponds to ventricular activation (Figure 2A).

Statistics

Multiple group comparisons were performed using a 1-way analysis of variance (ANOVA) with Bonferroni post hoc analysis. Values are given ± SEM. P≤0.05 was considered as statistically significant. Data were analyzed using SPSS 17.0 (2008, SPSS Inc, Chicago, IL) software.

Immunohistochemistry and Histology

After electrophysiological measurements, hearts were rapidly frozen in liquid nitrogen and stored at -80°C . Coronal (4-chamber view) sections with a thickness of $10\ \mu\text{m}$ were taken from different levels of the hearts. Sections were immuno-labeled with a rabbit polyclonal antibody against Cx43 (1:250, Zymed, Invitrogen) and a FITC-conjugated anti rabbit whole IgG (1:100, Jackson Laboratories) afterwards. Then, sections were mounted in Vectashield (Vector Laboratories) and examined with a classic light microscope with epifluorescence equipment (Nikon Optophot-2). To evaluate the presence of fibrosis, sections were fixed with 4% paraformaldehyde (in PBS, 30' at RT), stained with Picosirius Red and examined by light microscopy. The quantification and heterogeneity of Cx43 immuno-signal and fibrosis was performed as described previously¹³. Five hearts of each group were analyzed for Cx43 expression and fibrosis.

Results

ECG Measurements

TAC-surgery in HET mice resulted in a mortality-rate of 42% (8 out of 19) in the first 2 weeks after TAC-surgery, in sharp contrast to 0% in TAC-operated WT and Sham-operated mice (Table 1). Survival after surgery is plotted in Figure 1A, showing that spontaneous death in HET TAC mice occurs from day 5. To gain more insight in the cause of death of TAC-operated HET mice, telemetry transmitters were implanted in 2 WT and 6 HET TAC-operated mice. Figure B shows HR (solid lines) and PR-interval (dotted lines) course measured 3.5 to 0.5 days before the end of the experiment (day 14) of WT and surviving HET TAC mice. For deceased HET TAC mice, the moment of death was used as $t = 0$. Overall, HET TAC mice had slower heart rates and prolonged PR-intervals compared to WT TAC mice. Whereas HR and PR were stable in both WT and surviving HET TAC mice, HR progressively decreased and PR increased starting at day 2.5 before death in deceased HET TAC mice. An example of 24h telemetry recordings of an HET mouse that died 7 days after TAC-surgery is shown in Figure 1C. No irregularities were found in ECG-traces 3 days before death (left trace). However, 2 hours before death the ECG shows extreme bradycardia with very long PR-intervals (middle trace). Two hours later, the first episode of AV-block was observed (right trace), after which the mouse died within 2 minutes.

Figure 1D shows surface ECG traces of anesthetized mice, recorded 2 weeks after Sham- or TAC-surgery. In general, HET mice had a slower HR compared to WT mice, although not significantly (Table 2). PR-interval and QRS-duration were increased in HET mice compared to WT mice, but similar between Sham- and (surviving) TAC-operated mice. Fractionated P-waves were found specifically in TAC-operated HET mice (Fig. 1D, lower

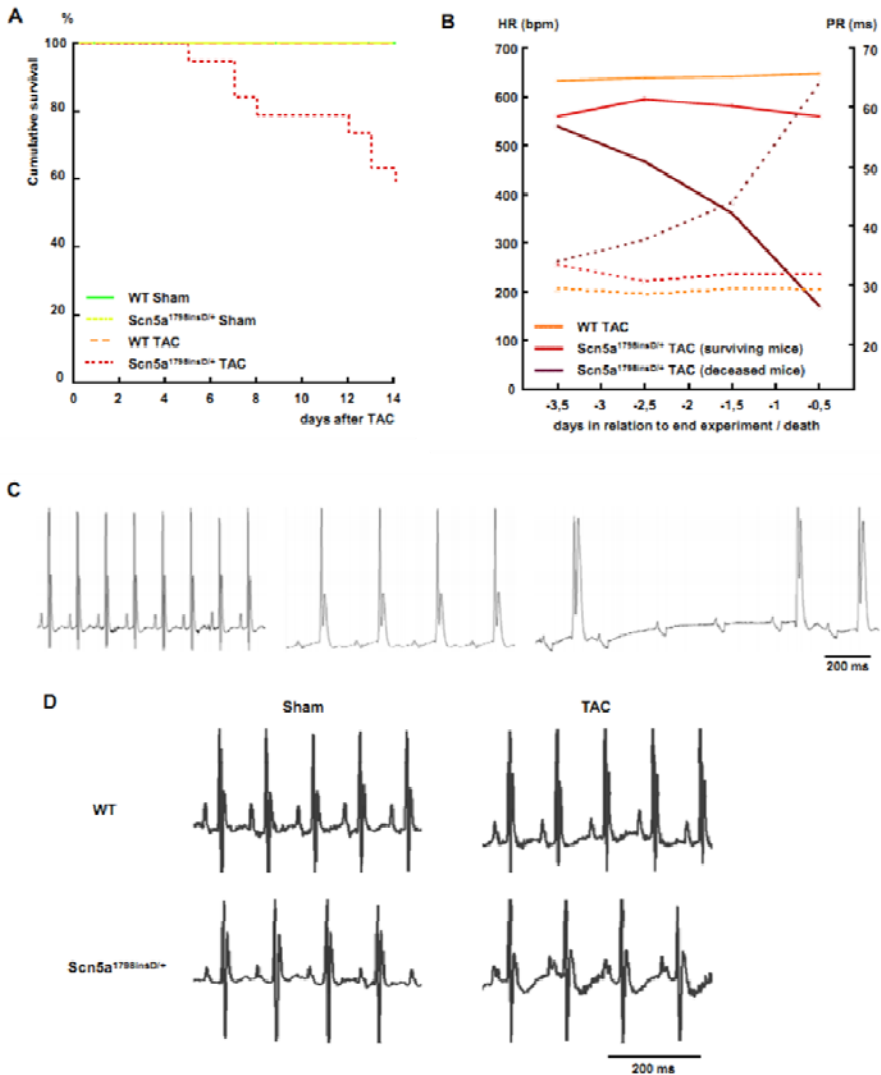


Figure 1 - ECG measurements. Panel A shows a Kaplan-Meier curve of Sham- and TAC-operated WT and HET mice. In panel B, the progression of heart-rate (solid lines) and PR-interval (dotted lines) is plotted of telemetry-analyzed TAC-operated WT and HET mice. $t = 0$ corresponds to day 14 after TAC-surgery for WT and surviving HET mice and to the moment of death in deceased TAC-operated HET mice. An example of telemetry recordings of a deceased TAC-operated HET mouse, measured 3 days (left trace), 2 hours (middle trace) and 2 minutes (right trace) before death, is shown in panel C. Panel D shows typical surface ECGs of anesthetized Sham- and TAC-operated WT and HET mice.

right panel), which could explain the prolonged P-wave. No significant differences were found in QT_c-intervals (Table 2).

Table 2 - Surface ECG measurements

	WT Sham	Scn5a ^{1798insD/+} Sham	WT TAC	Scn5a ^{1798insD/+} TAC
HR (bpm)	562±19	538±23	548±8	512±16
PR-interval (ms)	31.0±0.6	35.6±0.7**§§	30.8±0.5	35.6±0.4**§§
QRS duration (ms)	10.0±0.2	11.2±0.3*§§	10.0±0.1	11.8±0.4**§§
P duration (ms)	10.9±0.4	11.4±0.3	11.5±0.3	14.0±0.3*##§
QTc (ms)	40.0±2.2	45.0±1.7	44.0±1.3	46.9±1.7

HR, heart rate; bpm, beats per minute; QT_c, QT-interval, corrected for HR. Values are ± SEM. * $p < 0.05$ vs WT Sham; ** $p < 0.005$ vs WT Sham; # $p < 0.05$ vs Scn5a^{1798insD/+} Sham; ## $p < 0.005$ vs Scn5a^{1798insD/+} Sham; § $p < 0.05$ vs WT TAC; §§ $p < 0.005$ vs WT TAC.

Epicardial Mapping

After surface ECG measurements, the hearts were prepared for epicardial activation mapping. Ventricular mapping showed that the longitudinal conduction velocity (CV_L) was significantly lower in HET compared to WT mice in both the left (LV) and right (RV) ventricle (Table 3). Transverse conduction velocities (CV_T) were similar between HET and WT mice. Concomitantly, anisotropic ratios were decreased in HET compared to WT mice, although not significantly. Two weeks of pressure overload did not affect ventricular conduction in both HET and WT mice.

The effective refractory period (ERP) was comparable among the 4 groups in both LV and RV, although it tended to be increased in HET compared to WT mice. Ventricular arrhythmias could not be induced in any of the mice (Table 3).

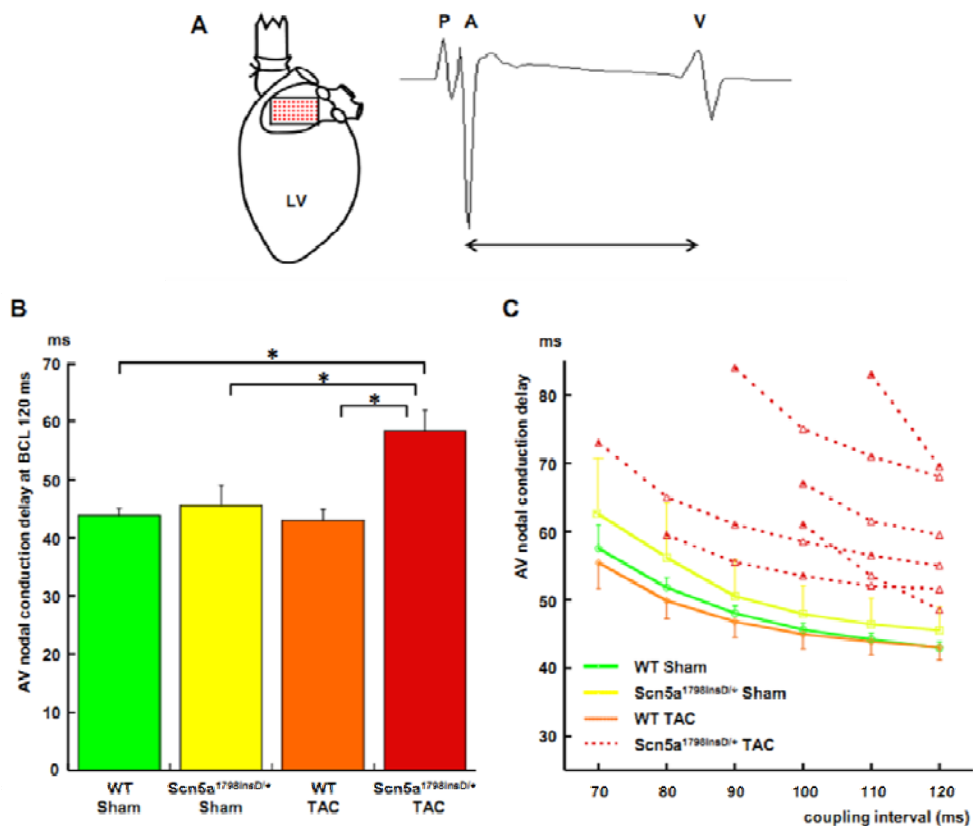


Figure 2 - Langendorff experiments. Panel A – After pacing (P) at the left atrium, both atrial activation (A) and remote activation of the ventricles (V) were recorded. The time between A and V was calculated as measure for AV nodal conduction delay (arrow). The AV nodal conduction delay at a BCL of 120 ms for Sham- and TAC-operated WT and HET mice is plotted in panel B. Panel C shows AV nodal conduction delay curves at decremental coupling intervals, starting at 120 ms. Averaged data are shown of Sham-operated mice and TAC-operated WT mice, curves of TAC-operated HET mice are plotted individually.

AV nodal conduction delay was determined by pacing the left atrium (LA) and calculating the temporal difference between atrial and ventricular activation (Figure 2A). Figure 2B displays AV nodal conduction delays in animals of the 4 groups at BCL 120 ms, demonstrating that this delay is increased specifically in HET TAC hearts. Plots of AV nodal conduction delay at decremental coupling intervals are shown in plot 2C. No significant differences were found in the averaged curves of Sham-operated WT and HET and WT TAC mice. However, all curves of individual TAC-operated HET mice were

Table 3 - Epicardial Mapping

	WT Sham	Scn5a ^{1798insD/+} Sham	WT TAC	Scn5a ^{1798insD/+} TAC
Arrhythmias (%)	0	0	0	0
LV CV _L (cm/s)	81.2±1.6	68.1±1.8*	75.8±3.0	65.3±2.9**§
RV CV _L (cm/s)	69.5±2.4	57.0±1.5**§§	68.9±1.4	56.0±1.4**§§
LV CV _T (cm/s)	45.3±0.9	42.0±1.3	43.2±1.4	40.4±1.9
RV CV _T (cm/s)	45.0±1.1	43.0±1.5	43.8±2.2	39.9±2.3
LV AR (CV _L /CV _T)	1.80±0.07	1.63±0.07	1.76±0.07	1.64±0.10
RV AR (CV _L /CV _T)	1.55±0.08	1.34±0.06	1.61±0.09	1.41±0.07
LV ERP (ms)	70.0±4.9	74.3±6.5	60.0±3.0	65.0±4.2
RV ERP (ms)	50.0±3.7	70.0±6.9	55.0±4.0	66.7±5.3
AVNRP (ms)	57.1±4.2	55.0±9.6	58.6±2.6	90.0±8.2*#§
WBP (ms)	80.0±3.2	86.7±8.8	76.7±3.3	116.0±10.8*§
SR (bpm)	351±30	314±38	324±37	345±30

*LV, left ventricle; RV, right ventricle; CV_L, longitudinal conduction velocity; CV_T, transversal conduction velocity; AR, anisotropic ratio; ERP, effective refractory period; SR, intrinsic sinus rate; AVNRP, AV nodal refractory period; WBP, Wenckebach periodicity. Values are ± SEM. * p<0.05 vs WT Sham; ** p<0.005 vs WT Sham; # p<0.05 vs Scn5a^{1798insD/+} Sham; § p<0.05 vs WT TAC; §§ p<0.005 vs WT TAC.*

different from the curves of the other groups. The steepness of 4 out of 6 HET TAC curves was increased, indicative of an increased AV-delay at shorter coupling intervals. Besides, in virtually all TAC-operated HET hearts, the impulse was blocked at longer coupling intervals. Table 3 shows that the AV nodal refractory period (AVNRP) was significantly increased in HET TAC hearts compared to Sham-operated hearts and TAC-operated WT hearts. Furthermore, HET TAC hearts had an increased Wenckebach Periodicity (WBP) compared to WT mice.

The intrinsic sinus rate (SR) was determined for all Langendorff-perfused hearts. No differences were found in beating rate between Sham- and TAC-operated WT and HET hearts (Table 3).

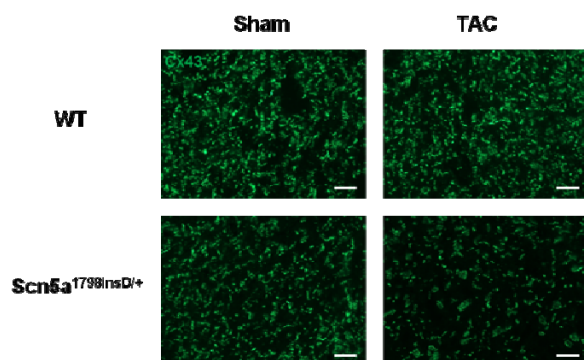


Figure 3 – Cx43 expression. Typical pictures of Cx43 expression in the left ventricle of Sham- and TAC-operated WT and HET hearts. Bars represent 50 μ m.

Cx43 expression and Fibrosis

Typical examples of Cx43-immunolabeled sections of LV of Sham- and TAC-operated WT and HET hearts are shown in Figure 3. In Sham-operated mice, Cx43 expression was equal between WT and HET hearts (Table 4). TAC-operation did not affect Cx43 expression in WT mice. However, Cx43 expression in TAC-operated HET hearts was reduced, which was significantly different compared to Sham- and TAC-operated WT hearts. No significant differences were found in the heterogeneity of Cx43 expression, although values were higher in both Sham- and TAC-operated HET hearts (Table 4).

Table 4 - Cx43 expression and fibrosis

	WT Sham	Scn5a ^{1798insD/+} Sham	WT TAC	Scn5a ^{1798insD/+} TAC
Cx43-expression (%)	3.81±0.34	3.06±0.31	3.64±0.66	1.84±0.26* [§]
Cx43 heterogeneity	23.1±1.18	27.0±1.27	24.4±2.48	28.7±0.87
Fibrosis LV (%)	0.29±0.09	0.21±0.07	0.53±0.27	2.49±0.96* [#]
Fibrosis septum (%)	1.90±0.57	1.62±0.33	1.13±0.38	2.92±1.58

Values are \pm SEM. * $p < 0.05$ vs WT Sham; [#] $p < 0.05$ vs Scn5a^{1798insD/+} Sham; [§] $p < 0.05$ vs WT TAC.

Finally, we performed Picrosirius Red staining to evaluate the presence of fibrosis (Figure 4). Hearts of Sham-operated WT and HET hearts showed only low amounts of collagen in the left ventricular free wall, and some collagen in the septum. Two weeks of pressure overload had no affect on the deposition of collagen in WT hearts. However, collagen staining was more intense in LV of TAC-operated HET hearts, and quantification showed that the amount of fibrosis was significantly higher than in WT and HET Sham hearts (Table 4). Figure 4 also shows increased fibrosis staining in the septum of TAC-operated HET hearts. However, this increased collagen deposition was not found in all TAC-operated HET hearts, and therefore no significant differences were present (Table 4).

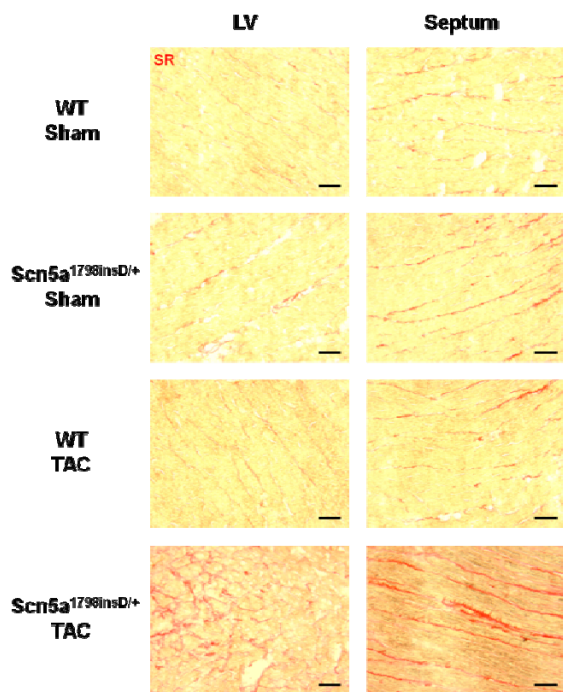


Figure 4 – Fibrosis. Typical pictures of fibrosis in the left ventricle (LV) and septum of Sham- and TAC-operated WT and HET hearts. Bars represent 50 μm .

Discussion

The present study shows that applying aortic stenosis to mice with a mutated cardiac sodium channel results in a typical Lev / Lenègre phenotype 2 weeks after surgery in 42% of the mice: progressively slowed impulse propagation through the specific conduction system, eventually evolving into AV-block. Although this pronounced phenotype was not found in surviving mice *in vivo*, these mice showed delayed AV-conduction *ex vivo*, as well as increased collagen deposition. Progressive AV-conduction slowing and increased fibrosis was not found in WT mice or in mice without aortic stenosis.

Lev / Lenègre disease

Lev / Lenègre disease is characterized as a senile degeneration of the His-Purkinje conduction system^{1,2}. Patients show progressively increased P-wave, PR-interval and QRS duration with a decreased HR¹⁶. In this study we have presented an accelerated model of Lev / Lenègre disease in mice with a combined aortic stenosis and Scn5a-mutation: (1) progressively slowed AV-conduction, eventually resulting in AV-block, (2) progressively decreased HR, (3) increased P-wave and QRS duration, without ventricular arrhythmias, and (4) increased fibrosis.

We have used transgenic mice carrying the 1798insD mutation, equivalent of the human cardiac sodium channel mutation 1795insD⁶. This mutation has been linked to LQT₃, Brugada syndrome and conduction disease, and recently also to Lev / Lenègre disease^{5, 8}. Nevertheless, the observed phenotype does not fit into either Brugada syndrome or LQT₃: ventricular arrhythmias were not observed (Brugada)¹⁷⁻¹⁹, and QT-interval was not prolonged (LQT₃)^{20, 21}. Other Scn5a mutations that can lead to both Brugada syndrome and Lev / Lenègre disease have been reported, indicating a close relation between these pathologies²². It is therefore not surprisingly that the 1795insD mutation has recently also been linked to Lev / Lenègre disease.

TAC-operated HET mice can be subdivided in 2 groups, based on the degree of Lev / Lenègre phenotype: (1) susceptible mice presenting with progressively increasing PR-intervals and decreasing HR *in vivo*, ultimately resulting in AV-block and death and (2) relatively resistant mice without progressive ECG-abnormalities *in vivo*. However, epicardial mapping on hearts of the latter group showed significant AV-conduction delay, with increased AV-nodal refractory period and Wenckebach periodicity. Furthermore, Cx43-expression was decreased with increased levels of fibrosis. This indicates that the process towards Lev / Lenègre disease was presumably ongoing in these mice, but yet without phenotypical alterations *in vivo*.

Figure 1B shows that the progressive increase in PR-interval in group (1) mice coincides with a decreased HR. This finding raised the question whether the PR-interval increase and HR decrease are unrelated processes, or that the increased PR-interval was secondary to the decreased HR. Although *in vivo* ECG-measurements could not elucidate this question, epicardial mapping experiments on Langendorff-perfused hearts strongly point towards the hypothesis that the PR-interval increase was an independent process: TAC-operated HET mice showed increased AV-conduction delay, AV nodal refractory period and Wenckebach periodicity, but sinus rhythm was unchanged, indicative of a normal intrinsic sinus node functioning.

Another interesting question is whether the increased PR-interval, or the resulting decreased HR, accounts for the high mortality-rate in TAC-operated HET mice. Our finding that the slowed AV-conduction eventually resulted in AV-block, after which the mice dead within several minutes, suggests a major role for the slowed AV-conduction on

the high mortality. However, we cannot rule out the possible role of a very slow HR (<200 bpm) on the high death rate. Sick Sinus Syndrome (SSS), characterized by sinus bradycardia and sinus arrest, has been correlated to mutations in *Scn5a*²³. Besides, Lev / Lenègre disease is associated with a high risk for Stoke-Adams syncope³. It is possible that the moment of death is actually the first episode of syncope, which is lethal in mice because of the high physiological HR. Finally, *Scn5a*-channels are also expressed in cardiac neurons, innervating the sinus node²⁴. A decreased sodium channel availability could explain the overall lower HR in HET mice compared to WT mice, which could become more prominent after stressing the hearts. Because neuronal innervation of the sinus node is absent during *ex vivo* measurements, this could explain why sinus rhythm was similar in all groups on Langendorff-perfused hearts.

Fibrosis

Previous studies have shown that 16 weeks of pressure overload increased fibrosis in WT mice^{9, 25}. Our data showed that 2 weeks after TAC-surgery the amount of collagen in the hearts of WT mice was not increased, indicating that the deposition of collagen after TAC-surgery is a relatively slow process. However, we showed that 2 weeks after TAC-surgery the amount of fibrosis was significantly increased in HET mice, pointing to an accelerated deposition of collagen. This increase in fibrosis was accompanied by a decreased Cx43 expression. Comparable results were found in our previous study using aged heterozygous *Scn5a*-knockout mice: decreased Cx43 expression together with increased fibrosis²⁶. Recently, we have shown that decreased Cx43 expression enhanced fibrosis in aged and TAC-operated hearts¹³. This would suggest that in stressed hearts an altered expression of the cardiac sodium channel promotes gap junctional remodeling, which then enhance the deposition of collagen. This hypothesis is strengthened by our data of Cx43 expression in Sham-operated HET hearts, which was less intense compared to WT hearts, although not significantly, without increased levels of fibrosis. This process could explain the increased collagen-deposition found in Lev / Lenègre disease, but also in other pathologies that are caused by mutated cardiac sodium channels, such as Brugada syndrome, which are strongly associated with fibrosis^{19, 27}.

In summary, we have shown that applying aortic stenosis to mice with a cardiac sodium channel mutation results in a Lev / Lenègre phenotype of progressive AV-conduction slowing, eventually resulting in AV-block. Our data support the hypothesis that a secondary cardiac defect, together with a cardiac sodium channel mutation, is required for a rapid development of Lev / Lenègre disease. Furthermore, this accelerated mouse-model of Lev / Lenègre disease could function as a useful tool for future intervention studies.

References

1. Lenegre J, Moreau P, Iris L. 2 cases of complete auriculo-ventricular block due to primary sarcoma of the heart. *Arch Mal Coeur Vaiss.* 1964;56:361-387
2. Lev M. Anatomic basis for atrioventricular block. *Am J Med.* 1964;37:742-748
3. Davies MJ. Pathology of chronic a-v block. *Acta Cardiol.* 1976;Suppl 21:19-30
4. Schott JJ, Alshinawi C, Kyndt F, Probst V, Hoorntje TM, Hulsbeek M, Wilde AA, Escande D, Mannens MM, Le Marec H. Cardiac conduction defects associate with mutations in *scn5a*. *Nat Genet.* 1999;23:20-21
5. Bezzina C, Veldkamp MW, van Den Berg MP, Postma AV, Rook MB, Viersma JW, van Langen IM, Tan-Sindhunata G, Bink-Boelkens MT, van Der Hout AH, Mannens MM, Wilde AA. A single *na(+)* channel mutation causing both long-qt and brugada syndromes. *Circ Res.* 1999;85:1206-1213
6. Remme CA, Verkerk AO, Nuyens D, van Ginneken AC, van Brunschot S, Belterman CN, Wilders R, van Roon MA, Tan HL, Wilde AA, Carmeliet P, de Bakker JM, Veldkamp MW, Bezzina CR. Overlap syndrome of cardiac sodium channel disease in mice carrying the equivalent mutation of human *scn5a-1795insd*. *Circulation.* 2006;114:2584-2594
7. Royer A, van Veen TA, Le Bouter S, Marionneau C, Griol-Charhbili V, Leoni AL, Steenman M, van Rijen HV, Demolombe S, Goddard CA, Richer C, Escoubet B, Jarry-Guichard T, Colledge WH, Gros D, de Bakker JM, Grace AA, Escande D, Charpentier F. Mouse model of *scn5a*-linked hereditary lenegre's disease: Age-related conduction slowing and myocardial fibrosis. *Circulation.* 2005;111:1738-1746
8. Postema PG, Van den Berg M, Van Tintelen JP, Van den Heuvel F, Grundeken M, Hofman N, Van der Roest WP, Nannenberg EA, Krapels IP, Bezzina CR, Wilde A. Founder mutations in the netherlands: *Scn5a 1795insd*, the first described arrhythmia overlap syndrome and one of the largest and best characterised families worldwide. *Neth Heart J.* 2009;17:422-428
9. Boulaksil M, Winkels SK, Engelen MA, Stein M, van Veen TA, Jansen JA, Linnenbank AC, Bierhuizen MF, Groenewegen WA, van Oosterhout MF, Kirkels JH, de Jonge N, Varro A, Vos MA, de Bakker JM, van Rijen HV. Heterogeneous connexin43 distribution in heart failure is associated with dispersed conduction and enhanced susceptibility to ventricular arrhythmias. *Eur J Heart Fail.* 2010;12:913-921
10. Alcolea S, Jarry-Guichard T, de Bakker J, Gonzalez D, Lamers W, Coppen S, Barrio L, Jongsma H, Gros D, van Rijen H. Replacement of connexin40 by connexin45 in the mouse: Impact on cardiac electrical conduction. *Circ Res.* 2004;94:100-109
11. van Rijen HV, van Veen TA, van Kempen MJ, Wilms-Schopman FJ, Potse M, Krueger O, Willecke K, Opthof T, Jongsma HJ, de Bakker JM. Impaired conduction in the bundle branches of mouse hearts lacking the gap junction protein connexin40. *Circulation.* 2001;103:1591-1598
12. van Veen TA, van Rijen HV, Wiegerinck RF, Opthof T, Colbert MC, Clement S, de Bakker JM, Jongsma HJ. Remodeling of gap junctions in mouse hearts hypertrophied by forced retinoic acid signaling. *J Mol Cell Cardiol.* 2002;34:1411-1423
13. Jansen J, van Veen T, de Jong S, van der Nagel R, Driessen H, Labzowski R, Vos M, de Bakker J, van Rijen H. Reduced Cx43 expression leads to increased fibrosis and arrhythmias due to enhanced fibroblast activity in aged and pressure overloaded mice. *Circulation Arrhythmia and Electrophysiology. Submitted*
14. Mitchell GF, Jeron A, Koren G. Measurement of heart rate and q-t interval in the conscious mouse. *Am J Physiol.* 1998;274:H747-751
15. Potse M, Linnenbank AC, Grimbergen CA. Software design for analysis of multichannel intracardial and body surface electrocardiograms. *Comput Methods Programs Biomed.* 2002;69:225-236
16. Probst V, Kyndt F, Potet F, Trochu JN, Miallet G, Demolombe S, Schott JJ, Baro I, Escande D, Le Marec H. Haploinsufficiency in combination with aging causes *scn5a*-linked hereditary lenegre disease. *J Am Coll Cardiol.* 2003;41:643-652

17. Brugada P, Brugada J. Right bundle branch block, persistent st segment elevation and sudden cardiac death: A distinct clinical and electrocardiographic syndrome. A multicenter report. *J Am Coll Cardiol.* 1992;20:1391-1396
18. Brugada J, Brugada P. What to do in patients with no structural heart disease and sudden arrhythmic death? *Am J Cardiol.* 1996;78:69-75
19. Coronel R, Casini S, Koopmann TT, Wilms-Schopman FJ, Verkerk AO, de Groot JR, Bhuiyan Z, Bezzina CR, Veldkamp MW, Linnenbank AC, van der Wal AC, Tan HL, Brugada P, Wilde AA, de Bakker JM. Right ventricular fibrosis and conduction delay in a patient with clinical signs of brugada syndrome: A combined electrophysiological, genetic, histopathologic, and computational study. *Circulation.* 2005;112:2769-2777
20. Wang Q, Shen J, Splawski I, Atkinson D, Li Z, Robinson JL, Moss AJ, Towbin JA, Keating MT. Scn5a mutations associated with an inherited cardiac arrhythmia, long qt syndrome. *Cell.* 1995;80:805-811
21. Bennett PB, Yazawa K, Makita N, George AL, Jr. Molecular mechanism for an inherited cardiac arrhythmia. *Nature.* 1995;376:683-685
22. Kyndt F, Probst V, Potet F, Demolombe S, Chevallier JC, Baro I, Moisan JP, Boisseau P, Schott JJ, Escande D, Le Marec H. Novel scn5a mutation leading either to isolated cardiac conduction defect or brugada syndrome in a large french family. *Circulation.* 2001;104:3081-3086
23. Benson DW, Wang DW, Dymment M, Knilans TK, Fish FA, Strieper MJ, Rhodes TH, George AL, Jr. Congenital sick sinus syndrome caused by recessive mutations in the cardiac sodium channel gene (scn5a). *J Clin Invest.* 2003;112:1019-1028
24. Scornik FS, Desai M, Brugada R, Guerchicoff A, Pollevick GD, Antzelevitch C, Perez GJ. Functional expression of "cardiac-type" nav1.5 sodium channel in canine intracardiac ganglia. *Heart Rhythm.* 2006;3:842-850
25. Xia Y, Lee K, Li N, Corbett D, Mendoza L, Frangogiannis NG. Characterization of the inflammatory and fibrotic response in a mouse model of cardiac pressure overload. *Histochem Cell Biol.* 2009;131:471-481
26. van Veen TA, Stein M, Royer A, Le Quang K, Charpentier F, Colledge WH, Huang CL, Wilders R, Grace AA, Escande D, de Bakker JM, van Rijen HV. Impaired impulse propagation in scn5a-knockout mice: Combined contribution of excitability, connexin expression, and tissue architecture in relation to aging. *Circulation.* 2005;112:1927-1935
27. Ohkubo K, Watanabe I, Okumura Y, Takagi Y, Ashino S, Kofune M, Sugimura H, Nakai T, Kasamaki Y, Hirayama A, Morimoto S. Right ventricular histological substrate and conduction delay in patients with brugada syndrome. *Int Heart J.* 51:17-23

Chapter 5 - Reduced heterogeneous expression of Cx43 combined with decreased Nav1.5 expression account for arrhythmia vulnerability in conditional Cx43 Knockout mice

John A. Jansen; Maartje Noorman; Mèra Stein; Sanne de Jong; Roel van der Nagel; Thomas J. Hund; Peter J. Mohler; Toon A.B. van Veen; Jacques M.T. de Bakker; Harold V.M. van Rijen

Submitted to 'Heart Rhythm'

Reduced heterogeneous expression of Cx43 combined with decreased Nav1.5 expression account for arrhythmia vulnerability in conditional Cx43 Knockout mice

John A. Jansen¹; Maartje Noorman¹; Mèra Stein²; Sanne de Jong¹; Roel van der Nagel¹; Thomas J. Hund³; Peter J. Mohler⁴; Toon A.B. van Veen¹; Jacques M.T. de Bakker⁵; Harold V.M. van Rijen

1. Department of Medical Physiology, University Medical Center Utrecht, The Netherlands
2. Department of Cardiology, University Medical Center Utrecht, The Netherlands
3. Dorothy M. Davis Heart and Lung Research Institute, Departments of Biomedical Engineering and Internal Medicine, Ohio State University Medical Center, Columbus, OH, USA
4. Dorothy M. Davis Heart and Lung Research Institute, Departments of Internal Medicine and Physiology, Ohio State University Medical Center, Columbus, OH, USA
5. Interuniversity Cardiology Institute of the Netherlands, Utrecht, The Netherlands

Abstract

Background – Reduced Cx43 levels are associated with an increased vulnerability to arrhythmias. We hypothesized that induced Cx43 downregulation of conditional Cx43 KO mice results in more severe and heterogeneous reduction of Cx43, together with decreased Nav1.5 expression, in mice with spontaneous and induced ventricular arrhythmias. For this purpose, we determined electrophysiological and (immuno)histological characteristics of inducible Cx43 KO mice and compared arrhythmogenic (VT+) with non-arrhythmogenic (VT-) mice.

Methods and Results – Cx43 downregulation was induced with Tamoxifen in Cx43^{Cre-ER(T)/fl} mice. Animals were sacrificed 2 weeks after induction. Epicardial activation mapping was performed on Langendorff-perfused hearts, and arrhythmia vulnerability was tested. Mice were subdivided in VT+ (n=13) and VT- (n=10) animals and heart tissue was analyzed for Cx43, Nav1.5 and fibrosis. VT+ mice had decreased Cx43 expression with increased macroscopic, but not microscopic, heterogeneity of Cx43, compared to VT- mice. In addition, Nav1.5 expression was reduced in VT+ versus VT- mice, whereas the amount of fibrosis was comparable. QRS-duration was increased and epicardial activation was more dispersed in VT+ mice than in VT- mice. The effective refractory period (ERP) was similar between both groups. Premature stimulation resulted in a more severe conduction slowing in VT+ compared to VT- hearts in the right ventricle.

Conclusions – In induced conditional Cx43 KO mice, arrhythmogenic animals have a more severe reduction in Cx43, more macroscopic heterogeneity of Cx43 expression and decreased Nav1.5 expression compared to induced animals without arrhythmias. The alterations in reduced and dispersed cell-to-cell coupling together with reduced excitability allows for the occurrence of ventricular arrhythmias.

Introduction

A reduced expression of the main ventricular gap junction in the heart, Connexin43 (Cx43), is commonly found in a variety of cardiac pathologies, such as ischemia, hypertrophy and heart failure¹⁻³. Together with increased collagen deposition and a decreased expression of the cardiac sodium channel Nav1.5, this may impair proper conduction of the electrical impulse, increasing the risk for ventricular arrhythmias⁴⁻¹⁰. Besides a decreased expression, a more heterogeneous distribution of Cx43 has been found in remodeled hearts, resulting in a more dispersed conduction, which is also correlated with an increased susceptibility for arrhythmias¹¹⁻¹⁴.

We have previously shown that a 50% reduction in Cx43 expression in Cx43^{Cre-ER(T)/fl} mice did not affect impulse conduction. However, Tamoxifen-induction in these conditional Cx43 KO mice further reduced Cx43 levels to ~5%, which resulted in a high vulnerability for arrhythmias due to slowed and dispersed conduction. In that paper, we suggested that a heterogeneous expression of Cx43, combined with decreased Cx43 protein levels, allowed for the occurrence of ventricular arrhythmias¹⁵.

Despite the fact that the genetic tools allow for specific downregulation of Cx43, recent studies have shown that the intercalated disc (ID) is a highly dynamic structure with interaction between the different proteins that determine impulse conduction. A regulatory mechanism for Nav1.5 was shown to be localized at the ID, and Nav1.5 and Cx43 can be coprecipitated, suggesting an interaction at the level of the ID^{16, 17}. Furthermore, *in vitro* experiments on cultured cardiomyocytes have shown that loss of Plakophilin-2 results in both Cx43 remodeling and decreased sodium currents^{18, 19}. These studies point to a close relationship between Cx43 and Nav1.5, suggesting that proper expression and functioning of one protein is essential for the other.

In the present study, we focused on the factors that are responsible for the vulnerability to arrhythmias in mice with low (~5%) Cx43 expression. We hypothesized that in arrhythmogenic animals, expression levels of Cx43 after induction are lower than in animals without arrhythmias, with regions completely devoid of Cx43, resulting in slow and dispersed conduction. Secondly, we hypothesized that diminished Cx43 protein levels decrease Nav1.5 levels in these animals, further contributing to conduction disturbances. For this purpose, we subdivided Tamoxifen-induced Cx43^{Cre-ER(T)/fl} mice into arrhythmogenic (VT+) and non-arrhythmogenic (VT-) animals, and compared conduction parameters and tissue characteristics. Our data show that VT+ mice have a more severe reduction in Cx43 protein levels compared to VT- mice, which is accompanied by a global, but not local, heterogeneity in Cx43 expression. Furthermore, Nav1.5 expression was reduced in VT+ compared to VT- mice, whereas collagen content was comparable. Together, these concerted changes resulted in dispersed conduction and severe conduction slowing during premature stimulation, making the heart very prone to arrhythmias.

Materials and Methods

Animals

Cx43^{Cre-ER(T)/fl} (n = 17) mice were generated as described previously¹⁵ and injected intraperitoneally with 3-4 mg Tamoxifen (Sigma), dissolved in 100 μ l plant oil for 5 consecutive days. Electrophysiological experiments were performed 13-15 days after the first injection. Extended analysis of previous data (n=15) of van Rijen et al, Circulation 2004, on similar Tamoxifen-induced Cx43^{Cre-ER(T)/fl} mice, were included in this study¹⁵. Animal experiments were performed in accordance with institutional guidelines for animal use in research.

Preparation of the Hearts and Ventricular Conduction

Mice were anesthetized by 2.5% isoflurane in oxygen. A 3-lead electrocardiogram was recorded and analyzed off-line as described previously²⁰. Afterwards, the heart was excised, prepared and connected to a Langendorff perfusion setup as described previously²¹⁻²³. The hearts were continuously perfused with carbogen-gassed buffer of 37°C, composed of (in mmol/L): NaCl 116, KCl 5, MgSO₄ 1.1, NaH₂PO₄ 0.35, NaHCO₃ 27, glucose 10, mannitol 16 and CaCl₂ 1.8.

Extracellular electrograms were recorded using a 247-point multiterminal electrode (19x13 grid, 0.3-mm spacing) of both the left and right ventricle of the heart as described previously²¹. Recordings were made during stimulation (1 ms pulse duration, 2x diastolic stimulation threshold) from the center of the grid at a basic cycle length (BCL) of 120 ms. The effective refractory period (ERP), the longest coupling interval of the premature stimulus that failed to activate the entire heart, was determined for each ventricle separately as described previously²⁴. If spontaneous arrhythmias were absent, susceptibility for arrhythmias was provoked by programmed stimulation in the following sequence. First, 16 basic stimuli followed by 1 or 3 premature stimuli 5 ms longer than the locally determined ERP were applied. Next, if 1 or 3 premature stimuli failed to induce arrhythmias, 2-second burst pacing at the shortest possible cycle length was applied. Arrhythmias in mice were classified as sustained (>15 complexes followed stimulation), according to Lambeth Conventions²⁵.

Data Analysis

The moment of maximal negative dV/dt in the unipolar electrograms was selected as the time of local activation and determined with custom written software based on MatLab (2006, The MathWorks Inc., Natick, MA)²⁶. Activation times were used to construct activation maps. Conduction velocities parallel (CV_L) and perpendicular (CV_T) to fiber

orientation were determined from activation maps generated from BCL-pacing. Activation times of at least 4 consecutive electrode terminals along lines perpendicular to intersecting isochronal lines were used to calculate CVs. Anisotropic ratio was defined as CV_L/CV_T . Dispersion of conduction was assessed for both LV and RV using the method described by Lammers et al.²⁷.

Statistics

Two-group comparisons were performed using an unpaired t-test. A Fisher exact test was performed to compare gender-distribution. Ranked pictures of Nav1.5 expression were compared using a Wilcoxon Rank Sum test. Values are given as mean \pm SEM. $P \leq 0.05$ was considered as statistically significant. Data were analyzed using SPSS 17.0 (2008, SPSS Inc, Chicago, IL) software.

Immunohistochemistry and Histology

After electrophysiological measurements, hearts were rapidly frozen in liquid nitrogen and stored at -80°C . Coronal (4-chamber view) sections with a thickness of $10\mu\text{m}$ were taken from different levels of the hearts. Sections were double immuno-labeled with a rabbit polyclonal antibody against Cx43 (1:250, Zymed, Invitrogen) or Nav1.5 (1:100, custom made) and a mouse monoclonal antibody against N-cadherin (1:800, Sigma, Aldrich). Afterwards, sections were incubated with FITC-conjugated anti rabbit whole IgG and Texas Red-conjugated anti mouse whole IgG, mounted in Vectashield (Vector Laboratories) and examined with a classic light microscope with epifluorescence equipment (Nikon Optiphot-2). To evaluate the presence of fibrosis, sections were fixed with 4% paraformaldehyde (in PBS, 30 minutes at room temperature), stained with Picrosirius Red and examined by light microscopy.

The amount of fibrosis and Cx43 immuno-signals were determined in at least 5 hearts of each group. At least 8 randomly chosen pictures of both LV and RV of each heart were analyzed at 200x magnification. Blinded operators calculated Cx43 expression as percentage of the total tissue using Image J 1.43u (2010, NIH, Bethesda, MD). Photomicrographs were transformed into RGB (i.e. Red Green Blue) stack, and true Cx43 pixels were defined in the 256-leveled green channel using a minimal cut-off level of 50. For fibrosis quantification, a comparable procedure was used, but now the range between 90 and 190 in the red channel was defined as true fibrotic tissue.

Heterogeneity of Cx43 expression was determined using MatLab. Photographs were transformed into 8-bit white (Cx43) and black (background) pictures and a background subtraction with a rolling ball radius of 250 was performed. Each picture was subdivided in

140 equal squares and total intensity of the white-signal was measured for each square. Afterwards, the mean intensity of the squares and the standard deviation of the intensity among the squares were determined for each photograph separately. Micro heterogeneity, a relative value for the local heterogeneity in Cx43 expression, was defined as the standard deviation divided by the mean. An average value of all pictures of one ventricle of a heart was calculated.

To determine global heterogeneity of Cx43 expression, we determined the intensity of the total picture and measured the average intensity and the standard deviation among these intensities of all pictures of each ventricle of the heart. This macro heterogeneity was defined as this standard deviation divided by the average intensity of the pictures.

For Nav1.5 quantification, at least 5 hearts of both groups were used. Of each heart, 3-5 randomly taken pictures were analyzed. Three blinded observers individually ranked all 45 pictures from high to low expression. Statistical analysis was performed on every ranking separately.

Results

Arrhythmogeneity

We included 32 Tamoxifen-induced Cx43^{Cre-ER(T)/fl} mice in the study, of which 9 died within 2 weeks after induction. Of the remaining 23 mice, 13 mice were susceptible to arrhythmias during Langendorff-perfusion (57%). Five mice showed spontaneous arrhythmias and in 8 other isolated hearts, arrhythmias were induced by either premature stimulation or burst pacing (Figure 1C). The majority of arrhythmias (10 out of 13) were sustained (> 15 complexes either occurring spontaneously or following stimulation) and were found on both LV and RV. The other arrhythmias were non-sustained (8 complexes following stimulation in 1 heart) or premature beats (2 hearts). In the remaining 10 Tamoxifen-induced Cx43^{Cre-ER(T)/fl} mice, no spontaneous or induced arrhythmias were observed.

Figure 1A shows a typical example of the onset of a spontaneous polymorphic ventricular tachycardia (pVT). The activation maps of this pVT (lower panels) reveal fibrillatory conduction. In contrast, epicardial electrograms of an induced arrhythmia in another heart showed a monomorphic ventricular tachycardia, with repetitive activation patterns of consecutive beats (Figure 1B).

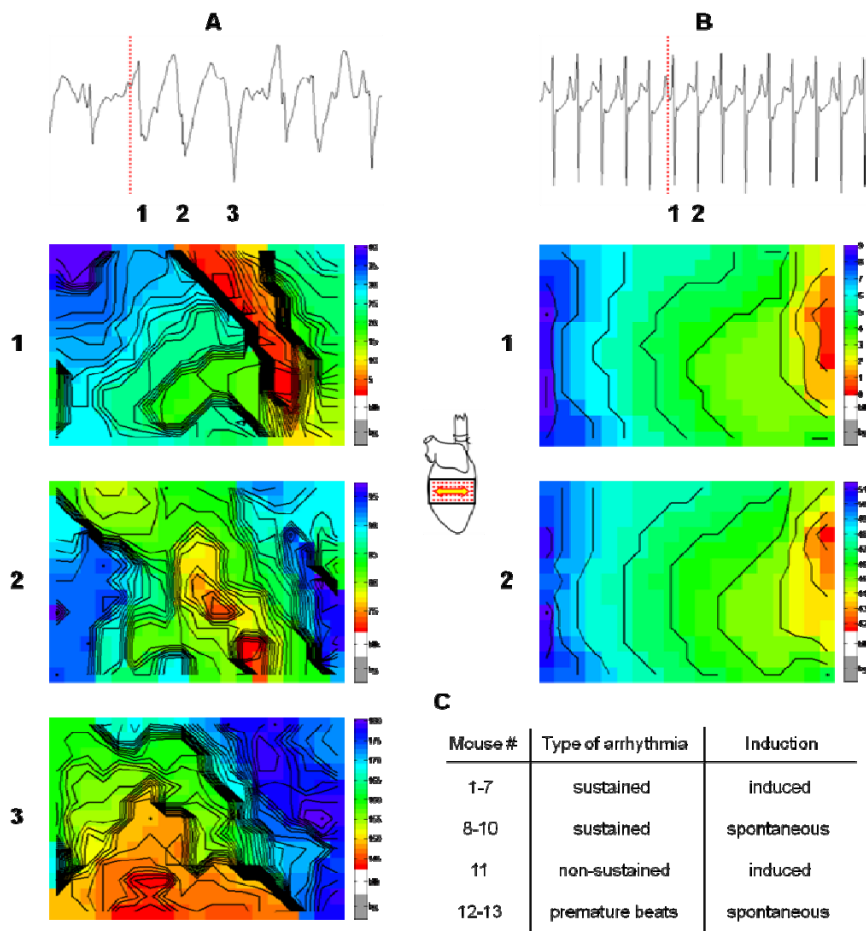


Figure 1 – Ventricular tachycardias. Panel A shows an epicardial electrogram (upper panel) of a sustained polymorphic tachycardia. The corresponding activation maps of the 3 numbered consecutive beats are presented below, showing fibrillatory conduction. The upper panel in B shows an epicardial electrogram of a sustained monomorphic tachycardia, with comparable activation maps of 2 consecutive beats (lower panels). The yellow arrow in the schematics of the heart indicates fiber direction. Colors indicate areas activated within the same time interval and are comparable for each map of one arrhythmia. Lines are isochronal lines at distances of 1 ms. The red dotted lines correspond to $t=0$ in the activation maps. Panel C overviews the induction and type of arrhythmia of individual susceptible mice.

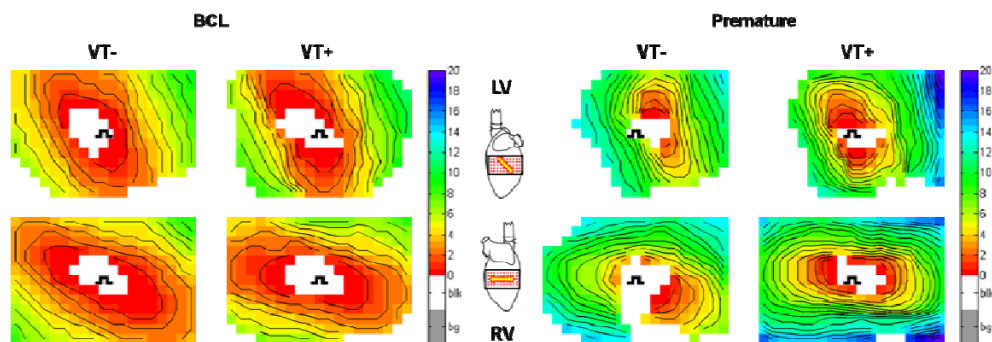


Figure 2 – Activation maps. Typical epicardial activation patterns of LV (upper panels) and RV (lower panels) of $Cx43^{Cre-ER(T)fl}$ mice without (VT-) and with (VT+) arrhythmias during BCL (120 ms, left panels) or premature stimulation (ERP + 5ms, right panels). The pacing site is shown in the center of each activation map, resulting in anisotropic conduction. The yellow arrows in the schematics of the heart indicate fiber direction. Colors indicate areas activated within the same time interval and are comparable for each map. Lines are isochronal lines at distances of 1 ms.

Ventricular conduction

Mice were divided in arrhythmogenic (13 mice, VT+) and non-arrhythmogenic (10 mice, VT-) animals to determine factors that are associated with the susceptibility for arrhythmias. No differences in induction-time, heart weight / body weight (HW/BW) ratio or gender distribution were found between the two groups (Table 1).

Table 1 - Statistics of induction-time, heart weight / body weight ratio and gender-distribution

	Induction-time (days)	HW/BW (%)	Male (%)
VT- (n=10)	13.8±0.6	0.72±0.03	60
VT+ (n=13)	13.5±0.3	0.77±0.14	38

VT-, $Cx43^{Cre-ER(T)fl}$ mice without arrhythmias; VT+, $Cx43^{Cre-ER(T)fl}$ mice with arrhythmias; induction-time, time from start Tamoxifen-induction to Langendorff experiments; HW/BW, heart weight / body weight ratio;. Values are ± SEM. * $p < 0.05$ vs VT-.

QRS-duration was prolonged in VT+ compared to VT- mice (15.4 ± 1.1 ms vs 12.1 ± 0.3 ms respectively, Table 2). The left panel in Figure 2 shows representative epicardial activation maps of Cx43^{Cre-ER(T)/fl} VT- and VT+ hearts of both LV and RV during stimulation at a BCL of 120 ms. Stimulation from the center of the grid resulted in anisotropic activation patterns determined by the fiber direction. No significant differences in impulse conduction velocity longitudinal (CV_L) and transverse (CV_T) to the fiber orientation were found between the groups, although conduction was generally a bit slower in VT+ compared to VT-. Concomitantly, the anisotropic ratio (CV_L/CV_T) in LV and RV were not different between both groups (Table 2). However, VT+ hearts showed regions with crowding of isochrones, indicative of local conduction slowing. Therefore, we determined the dispersion of conduction index²⁷. We found higher values of dispersion in VT+ compared to VT- mice, which was only significant in RV with a near-significant similar trend in LV ($p=0.058$).

Table 2 - Electrophysiology

	VT-	VT+
Arrhythmias (%)	0	100
LV CV_L (cm/s)	54.6 ± 4.3	45.7 ± 7.1
RV CV_L (cm/s)	47.2 ± 4.2	40.9 ± 6.2
LV CV_T (cm/s)	26.1 ± 2.1	21.1 ± 1.6
RV CV_T (cm/s)	27.7 ± 1.6	22.5 ± 2.8
LV AR (CV_L/CV_T)	2.11 ± 0.08	2.23 ± 0.22
RV AR (CV_L/CV_T)	1.72 ± 0.13	1.82 ± 0.15
LV CV Disp Index	1.41 ± 0.15	1.90 ± 0.19
RV CV Disp Index	1.41 ± 0.17	$2.31 \pm 0.36^*$
LV ERP (ms)	70.0 ± 10.1	75.6 ± 7.3
RV ERP (ms)	47.0 ± 3.4	46.1 ± 4.1
QRS-duration (ms)	12.1 ± 0.3	$15.4 \pm 1.1^*$
LV CV_L extra (cm/s)	41.0 ± 4.4	34.4 ± 6.7
RV CV_L extra (cm/s)	39.1 ± 6.2	$22.2 \pm 2.1^*$
LV CV_T extra (cm/s)	22.0 ± 2.5	17.1 ± 2.1
RV CV_T extra (cm/s)	21.6 ± 2.4	$13.4 \pm 1.1^*$
LV AR extra	1.88 ± 0.06	1.92 ± 0.20
RV AR extra	1.75 ± 0.18	1.64 ± 0.05

LV, left ventricle; RV, right ventricle; CV_L , longitudinal conduction velocity; CV_T , transversal conduction velocity; AR, anisotropic ratio; CV Disp, dispersion of conduction velocity; ERP, effective refractory period; VT-, Cx43^{Cre-ER(T)/fl} mice without arrhythmias; VT+, Cx43^{Cre-ER(T)/fl} mice with arrhythmias. Values are \pm SEM. * $p < 0.05$ vs VT-.

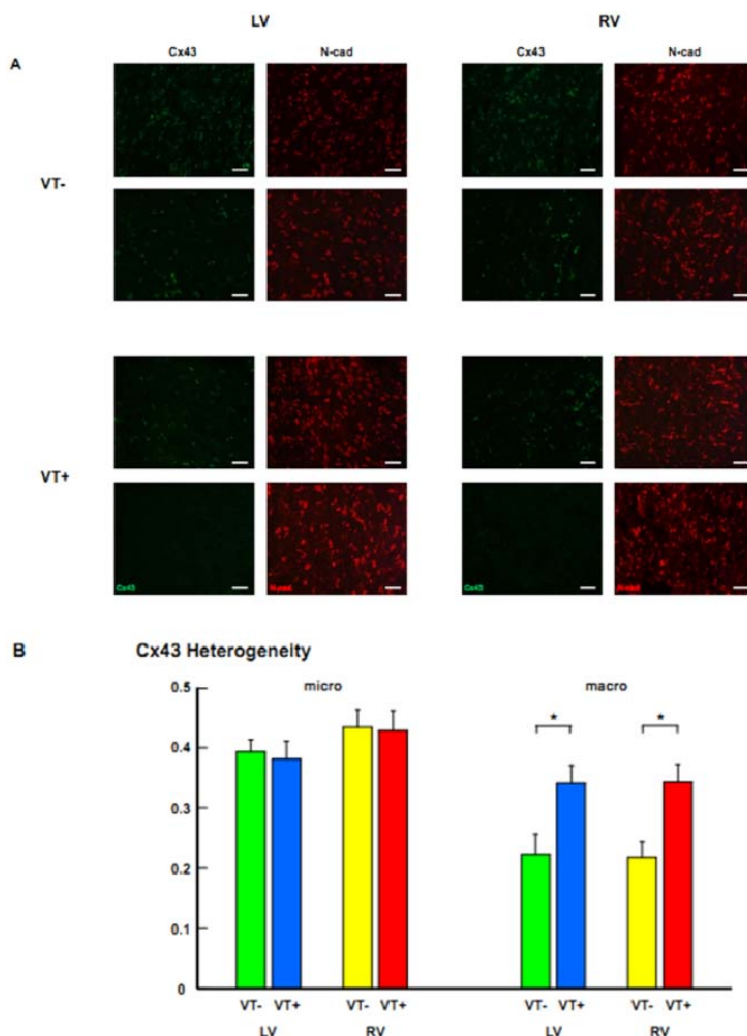


Figure 3 – Cx43 expression and heterogeneity. Panel A shows typical pictures of Cx43 expression with corresponding N-cadherin staining of LV (left panels) and RV (right panels) of $Cx43^{Cre-ER(T)/fl}$ mice without (VT-) and with (VT+) arrhythmias. Bars represent 50 μ m. Heterogeneity of Cx43 expression both at the micro and at the macro level is quantified in panel B.

The right panel in Figure 2 shows epicardial activation after premature stimulation (ERP + 5 ms). Conduction slowing both longitudinal and transverse to the fiber direction was more prominent in VT+ compared to VT- hearts, which was significant for CV_L and CV_T in RV (Table 2). The effective refractory period (ERP) was similar in both LV and RV for $Cx43^{Cre-ER(T)/fl}$ hearts VT- and VT+ (Table 2).

Cx43 expression and heterogeneity

Figure 3A shows typical examples of Cx43-immunolabeled sections of Tamoxifen-induced Cx43^{Cre-ER(T)/fl} VT- and VT+ hearts. As expected, Tamoxifen-induction resulted in a low Cx43 expression in both LV and RV, while N-cadherin (a highly stable component of the adherens junction in the ID) was still abundantly present at the intercalated discs. Whereas Cx43 was detectable throughout the ventricles in VT- mice, large areas in VT+ hearts showed a complete depletion of Cx43 expression (lower panels VT+ in Figure 3A), with some local spots, positive for Cx43 (upper panels VT+ in Figure 3A). As a result, total Cx43-immunosignal was decreased in VT+ compared to VT- hearts in both LV and RV (Table 3).

Next, we checked whether expression of Cx43 was more inhomogeneous in VT+ compared to VT- hearts. We first analyzed local Cx43 heterogeneity by quantifying intensity differences in Cx43 expression within pictures. Figure 3B shows that this micro heterogeneity of Cx43 expression was comparable between VT+ and VT- hearts in both LV and RV. However, macro heterogeneity of Cx43 expression, which quantifies the differences among regions of one complete ventricle of a heart, was significantly increased in both LV and RV in VT+ compared to VT- hearts (Figure 3B, Table 3).

Table 3 - Tissue characteristics

	VT-	VT+
Cx43-exp LV (%)	0.25±0.06	0.05±0.04*
Cx43-exp RV (%)	0.22±0.07	0.03±0.02*
Cx43-het micro LV	0.39±0.02	0.38±0.03
Cx43-het micro RV	0.43±0.03	0.43±0.03
Cx43-het macro LV	0.22±0.03	0.34±0.03*
Cx43-het macro RV	0.22±0.03	0.34±0.03*
Nav1.5-exp (rank obs. #1)	15.48	30.86**
Nav1.5-exp (rank obs. #2)	15.96	30.36**
Nav1.5-exp (rank obs. #3)	15.70	30.64**
Fibrosis LV (%)	0.48±0.12	0.81±0.32
Fibrosis RV (%)	0.54±0.09	0.81±0.32

Cx43-exp, Cx43 expression; *Cx43-het*, Cx43 heterogeneity; *Nav1.5-exp*, Nav1.5 expression; *rank obs. #1*, average rank of observer 1; *VT-*, Cx43^{Cre-ER(T)/fl} mice without arrhythmias; *VT+*, Cx43^{Cre-ER(T)/fl} mice with arrhythmias. Values are ± SEM. * $p < 0.05$ vs *VT-*; ** $p < 0.005$ vs *VT-*.

Nav1.5 expression and fibrosis

We further analyzed the cardiac tissue on other determinants of conduction, and stained for the cardiac sodium channel Nav1.5. As can be appreciated from Figure 4A, Nav1.5 expression was reduced in VT+ compared to VT- hearts, while again N-cadherin staining was normal. To quantify these differences, three blinded observers ranked all pictures from high to low expression, and three independent Wilcoxon Rank Sum tests were performed. Table 3 shows that the average rank of pictures of VT- hearts was significantly higher compared to pictures of VT+ hearts for all observers ($p < 0.001$ for each individual ranking, average ranking of the three observers was 15.71 ± 0.14 vs 30.62 ± 0.14 , respectively), showing quantitatively that Nav1.5 expression was decreased in VT+ compared to VT- hearts.

Finally, we determined the presence of fibrosis by histochemical analysis with Picrosirius Red staining. Figure 4B shows low amounts of interstitial collagen in both VT- and VT+ hearts. Quantification revealed no significant differences in collagen content between VT- and VT+ hearts (Table 3).

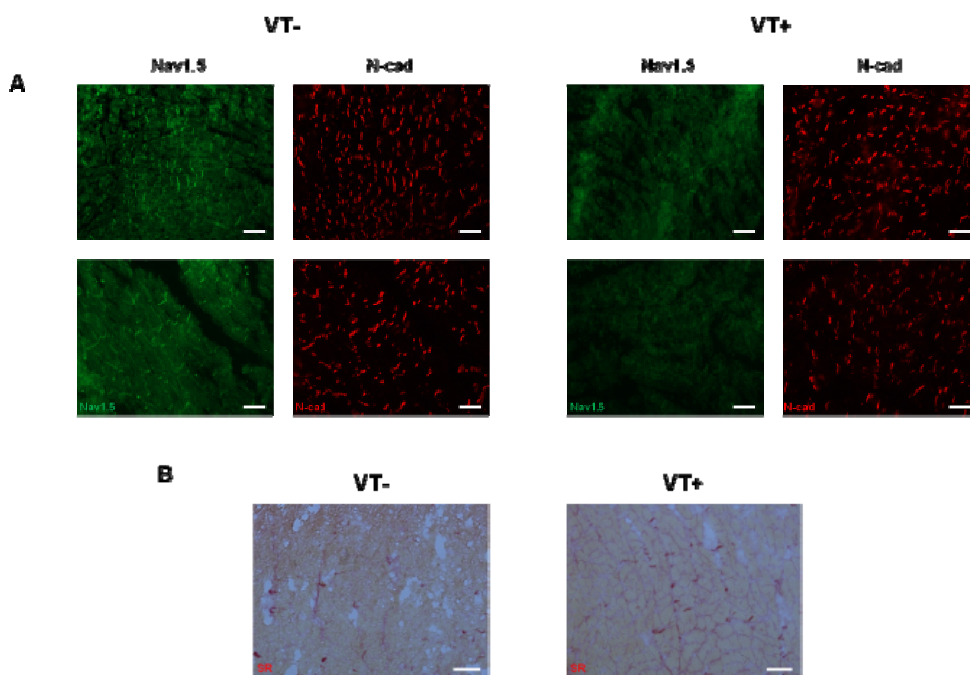


Figure 4 – Nav1.5 expression and fibrosis. Panel A shows typical pictures of Nav1.5 expression with corresponding N-cadherin staining of Cx43^{Cre-ER(T)/fl} mice without (VT-) and with (VT+) arrhythmias. Typical pictures of Picrosirius Red staining of Cx43^{Cre-ER(T)/fl} mice without (VT-) and with (VT+) arrhythmias are shown in panel B. Bars represent 50 μ m.

Discussion

Two weeks after induction of Cx43 depletion by Tamoxifen in Cx43^{Cre-ER(T)/fl} mice, ventricular tachycardias occur in about half of the animals. The main finding of this study is that in tachycardia prone animals, the arrhythmia vulnerability was associated with lower Cx43 expression and higher macroscopic Cx43 heterogeneity in concert with lower Nav1.5 expression compared to animals without arrhythmias.

Cx43 expression and heterogeneity

The very low Cx43 expression levels in Cx43^{Cre-ER(T)/fl} mice after Tamoxifen-induction are in agreement with previous studies^{15, 28}. Here we showed that VT+ mice have decreased Cx43 protein levels compared to VT- mice, suggesting that the actual reduction in Cx43 expression is an important arrhythmogenic factor. With regard to conduction reserve, which is defined as ‘the ability of the heart to maintain near normal impulse conduction velocity in the background of moderate changes in tissue characteristics’, this might have important implications²⁹. Several studies have shown that when this conduction reserve is exceeded, the heart becomes susceptible for arrhythmias^{24, 30, 31}. Although conduction was considerably slowed in VT- mice compared to mice with normal Cx43 expression (Cx43^{fl/fl} mice, for data see³²), arrhythmias were absent. Noteworthy, we found that the further reduction in Cx43 expression in VT+ mice was accompanied by an increased heterogeneity of Cx43. From our data we cannot determine whether the extremely low total Cx43 expression levels, or the global heterogeneity, with regions of total depletion of Cx43, is the main arrhythmogenic factor. Concerning this vulnerability to arrhythmias, it is likely that also the decreased expression of the cardiac sodium channel Nav1.5 plays a role. Interestingly, we previously showed that a combined 50% decrease in Cx43 and Nav1.5 did not increase arrhythmia susceptibility³³. Apparently, a moderate reduction in both proteins did not exceed conduction reserve. However, a reduced Nav1.5 expression combined with extremely low levels of Cx43 as found in VT+ mice in this study, presumably makes the heart highly vulnerable to arrhythmias.

In remodeled hearts, reduced Cx43 levels are generally accompanied by an increased heterogeneity of Cx43 expression¹⁻³. Besides that, we and others have shown that arrhythmogeneity is highly associated with a heterogeneous distribution of Cx43, both in mice and in patients¹¹⁻¹⁴. Therefore, we thoroughly analyzed Cx43 heterogeneity in this study by distinguishing local from global inhomogeneity. We calculated micro heterogeneity, which quantified differences in Cx43 intensity within a small region (420 x 300 μm , divided in squares of $\pm 1000 \mu\text{m}^2$) of the heart. Interestingly, we found no differences in this micro heterogeneity between VT- and VT+ mice. In contrast, macro heterogeneity, indicating variations in Cx43 intensities among different regions (size of 1 region is 420 x 300 μm) of the heart, was significantly increased in VT+ compared to VT- mice. This indicates that in our study, global, rather than local, heterogeneity is associated

with arrhythmia vulnerability. This implies that the large areas in which Cx43 is totally depleted (lowest pictures Figure 3A) significantly contribute to the formation of an arrhythmogenic substrate. This arrhythmogenic mechanism is supported by a study of Gutstein and coworkers in which global Cx43 heterogeneity was induced by chimeric Cx43 expression in mice, which also showed high arrhythmia susceptibility in the absence of fibrosis¹¹.

Nav1.5 expression and fibrosis

Besides gap junctional coupling between cardiomyocytes, impulse conduction in the heart is also dependent on the expression and function of the cardiac sodium channel Nav1.5, and the tissue architecture, mainly determined by the amount of collagen. Therefore, we stained for Nav1.5 and found a reduced expression in VT+ compared to VT- mice. This raises the question whether this reduction in Nav1.5 is a direct consequence of the very low Cx43 protein levels. Recent studies have shown that Cx43 and Nav1.5 are both present in the intercalated disc, and that destabilization of the desmosome by a loss of Plakophilin-2 resulted in Cx43 remodeling as well as a decreased functioning of Nav1.5^{16, 18, 19}. We have previously shown that stressing mice with reduced or mutated Nav1.5 by aging or pressure overload resulted in a decreased expression of Cx43^{34, 35}. These studies show a close relation between both channel proteins, which suggests that the depletion of Cx43, as found in large areas throughout the hearts of VT+ mice, may directly affect Nav1.5 expression. On the other hand, Johnson et al showed that in isolated neonatal cardiomyocytes from Cx43 null mice, Nav1.5 expression and function was unaffected³⁶. However, the consequences of Cx43 depletion in isolated cells may differ from the effects in an intact heart i.e. by stretch on the cardiomyocytes and/or the lack of coupling to surrounding cells. Additional research is required to prove a direct link between the decreased Cx43 and Nav1.5 levels in VT+ mice.

Recently (in chapter 3), we have shown that both aging and pressure overload in mice with reduced cellular coupling (non-induced Cx43^{Cre-ER(T)/fl} mice) results in more excessive collagen deposition, due to enhanced fibroblast activity, compared to mice with normal Cx43 expression (Cx43^{fl/fl} mice)²⁴. In the current study, we checked whether extremely low levels of Cx43 would also increase fibroblast activity, leading to increased collagen deposition. However, we found only low levels of interstitial fibrosis, which was similar in VT- and VT+ mice. A possible explanation for these results is that the stress on the different hearts is not comparable, mainly because the hearts in this study are not hypertrophic (Table 1), in contrast to aged and pressure overloaded hearts. Nevertheless, fibrosis did not play a role in determining arrhythmia vulnerability in this study.

Impulse conduction

ECG analysis and epicardial activation mapping was performed on VT+ and VT- hearts to determine the electrical effects of the heterogeneous reduction in Cx43 and decreased Nav1.5 expression. We found a significant increased QRS-duration in VT+ compared to VT- mice, although epicardial conduction during Langendorff-perfusion was not significantly slowed during S1S1 pacing. This discrepancy could be explained by (1) small differences in longitudinal and transversal conduction resulted in a significantly prolonged ventricular activation at the ECG, (2) transmural conduction contributes to the QRS-complex, whereas it cannot be determined by epicardial activation mapping. Previous data have shown that QRS-duration and transmural conduction velocity are inversely related³⁷. However, we showed that conduction was more dispersed (only significant for RV) in VT+ compared to VT- mice. It is likely that the global heterogeneity of Cx43 expression is mainly responsible for this dispersed conduction: conduction is slowed in the regions of Cx43-depletion, whereas it is relatively normal in parts that express Cx43. Challenging the hearts by premature stimulation resulted in a more severe conduction slowing in VT+ than in VT- hearts (only significant for RV). The decreased Nav1.5 availability in VT+ mice could play a fundamental role, since the upstroke velocity of the action potential is restricted by the number of active Nav1.5 channels, which is particularly crucial during premature stimulation. The slow impulse conduction during premature stimulation in VT+ mice enables the induction of ventricular tachycardias. Interestingly, we found no differences in ERP between VT- and VT+ mice, indicating that arrhythmia vulnerability was not caused by alterations in refractoriness. Previous studies have shown that a reduction in Cx43 expression was associated with decreased ERP, whereas decreased Nav1.5 levels prolonged the ERP^{24, 34}. Apparently, the opposing effects of Cx43 and Nav1.5 on the ERP neutralize in VT+ mice, as was also found in murine hearts with a genetically 50% decreased expression of both Cx43 and Nav1.5³³.

Study limitations

In this study we used different methods to quantify Cx43 and Nav1.5 expression. Because of the relatively high background staining in Nav1.5 labeled sections, we could not apply a standardized method by Image J. Therefore, pictures were ranked by 3 blinded observers and statistically analyzed by a Wilcoxon Ranked Sum Test. However, the variance among the observers was very low, and all 3 individual tests showed a significant difference between VT+ and VT- mice, indicating a very high reliability of this quantification.

In conclusion we have shown that in the background of low Cx43 levels, arrhythmogenic mice have a more severe reduction in Cx43, which together with global, but not local, heterogeneity of Cx43 expression, account for slowed and dispersed conduction. In combination with a decreased Nav1.5 expression, this allows for the occurrence of ventricular arrhythmias.

References

1. Peters NS. New insights into myocardial arrhythmogenesis: Distribution of gap-junctional coupling in normal, ischaemic and hypertrophied human hearts. *Clin Sci (Lond)*. 1996;90:447-452
2. Kaprielian RR, Gunning M, Dupont E, Sheppard MN, Rothery SM, Underwood R, Pennell DJ, Fox K, Pepper J, Poole-Wilson PA, Severs NJ. Downregulation of immunodetectable connexin43 and decreased gap junction size in the pathogenesis of chronic hibernation in the human left ventricle. *Circulation*. 1998;97:651-660
3. Kostin S, Rieger M, Dammer S, Hein S, Richter M, Klovekorn WP, Bauer EP, Schaper J. Gap junction remodeling and altered connexin43 expression in the failing human heart. *Mol Cell Biochem*. 2003;242:135-144
4. La Vecchia L, Ometto R, Bedogni F, Finocchi G, Mosele GM, Bozzola L, Bevilacqua P, Vincenzi M. Ventricular late potentials, interstitial fibrosis, and right ventricular function in patients with ventricular tachycardia and normal left ventricular function. *Am J Cardiol*. 1998;81:790-792
5. Swynghedauw B. Molecular mechanisms of myocardial remodeling. *Physiol Rev*. 1999;79:215-262
6. Kawara T, Derksen R, de Groot JR, Coronel R, Tasseron S, Linnenbank AC, Hauer RN, Kirkels H, Janse MJ, de Bakker JM. Activation delay after premature stimulation in chronically diseased human myocardium relates to the architecture of interstitial fibrosis. *Circulation*. 2001;104:3069-3075
7. Borlak J, Thum T. Hallmarks of ion channel gene expression in end-stage heart failure. *Faseb J*. 2003;17:1592-1608
8. Winterton SJ, Turner MA, O'Gorman DJ, Flores NA, Sheridan DJ. Hypertrophy causes delayed conduction in human and guinea pig myocardium: Accentuation during ischaemic perfusion. *Cardiovasc Res*. 1994;28:47-54
9. McIntyre H, Fry CH. Abnormal action potential conduction in isolated human hypertrophied left ventricular myocardium. *J Cardiovasc Electrophysiol*. 1997;8:887-894
10. Levy D, Anderson KM, Savage DD, Balkus SA, Kannel WB, Castelli WP. Risk of ventricular arrhythmias in left ventricular hypertrophy: The framingham heart study. *Am J Cardiol*. 1987;60:560-565
11. Gutstein DE, Morley GE, Vaidya D, Liu F, Chen FL, Stuhlmann H, Fishman GI. Heterogeneous expression of gap junction channels in the heart leads to conduction defects and ventricular dysfunction. *Circulation*. 2001;104:1194-1199
12. Kitamura H, Ohnishi Y, Yoshida A, Okajima K, Azumi H, Ishida A, Galeano EJ, Kubo S, Hayashi Y, Itoh H, Yokoyama M. Heterogeneous loss of connexin43 protein in nonischemic dilated cardiomyopathy with ventricular tachycardia. *J Cardiovasc Electrophysiol*. 2002;13:865-870
13. Cabo C, Yao J, Boyden PA, Chen S, Hussain W, Duffy HS, Ciaccio EJ, Peters NS, Wit AL. Heterogeneous gap junction remodeling in reentrant circuits in the epicardial border zone of the healing canine infarct. *Cardiovasc Res*. 2006;72:241-249
14. Boulaksil M, Winckels SK, Engelen MA, Stein M, van Veen TA, Jansen JA, Linnenbank AC, Bierhuizen MF, Groenewegen WA, van Oosterhout MF, Kirkels JH, de Jonge N, Varro A, Vos MA, de Bakker JM, van Rijen HV. Heterogeneous connexin43 distribution in heart failure is associated with dispersed conduction and enhanced susceptibility to ventricular arrhythmias. *Eur J Heart Fail*. 2010;12:913-921
15. van Rijen HV, Eckardt D, Degen J, Theis M, Ott T, Willecke K, Jongsma HJ, Opthof T, de Bakker JM. Slow conduction and enhanced anisotropy increase the propensity for ventricular tachyarrhythmias in adult mice with induced deletion of connexin43. *Circulation*. 2004;109:1048-1055
16. Petitprez S, Zmoos AF, Ogrodnik J, Balse E, Raad N, El-Haou S, Albesa M, Bittihn P, Luther S, Lehnart SE, Hatem SN, Coulombe A, Abriel H. Sap97 and dystrophin macromolecular complexes determine two pools of cardiac sodium channels nav1.5 in cardiomyocytes. *Circ Res*. 108:294-304
17. Malhotra JD, Thyagarajan V, Chen C, Isom LL. Tyrosine-phosphorylated and nonphosphorylated sodium channel beta1 subunits are differentially localized in cardiac myocytes. *J Biol Chem*. 2004;279:40748-40754

18. Oxford EM, Musa H, Maass K, Coombs W, Taffet SM, Delmar M. Connexin43 remodeling caused by inhibition of plakophilin-2 expression in cardiac cells. *Circ Res.* 2007;101:703-711
19. de Boer TP, Houtman MJ, Compier M, van der Heyden MA. The mammalian k(ir)2.X inward rectifier ion channel family: Expression pattern and pathophysiology. *Acta Physiol (Oxf).* 2010;199:243-256
20. Royer A, van Veen TA, Le Bouter S, Marionneau C, Griol-Charhbil V, Leoni AL, Steenman M, van Rijen HV, Demolombe S, Goddard CA, Richer C, Escoubet B, Jarry-Guichard T, Colledge WH, Gros D, de Bakker JM, Grace AA, Escande D, Charpentier F. Mouse model of scn5a-linked hereditary lenegre's disease: Age-related conduction slowing and myocardial fibrosis. *Circulation.* 2005;111:1738-1746
21. van Rijen HV, van Veen TA, van Kempen MJ, Wilms-Schopman FJ, Potse M, Krueger O, Willecke K, Opthof T, Jongsma HJ, de Bakker JM. Impaired conduction in the bundle branches of mouse hearts lacking the gap junction protein connexin40. *Circulation.* 2001;103:1591-1598
22. van Veen TA, van Rijen HV, Wiegerinck RF, Opthof T, Colbert MC, Clement S, de Bakker JM, Jongsma HJ. Remodeling of gap junctions in mouse hearts hypertrophied by forced retinoic acid signaling. *J Mol Cell Cardiol.* 2002;34:1411-1423
23. Alcolea S, Jarry-Guichard T, de Bakker J, Gonzalez D, Lamers W, Coppen S, Barrio L, Jongsma H, Gros D, van Rijen H. Replacement of connexin40 by connexin45 in the mouse: Impact on cardiac electrical conduction. *Circ Res.* 2004;94:100-109
24. Jansen J, van Veen T, de Jong S, van der Nagel R, Driessen H, Labzowski R, Vos M, de Bakker J, van Rijen H. Reduced cx43 expression leads to increased fibrosis and arrhythmias due to enhanced fibroblast activity in aged and pressure overloaded mice. *Circulation Arrhythmia and Electrophysiology.* 2011;Submitted
25. Walker MJ, Curtis MJ, Hearse DJ, Campbell RW, Janse MJ, Yellon DM, Cobbe SM, Coker SJ, Harness JB, Harron DW, et al. The lambeth conventions: Guidelines for the study of arrhythmias in ischaemia infarction, and reperfusion. *Cardiovasc Res.* 1988;22:447-455
26. Potse M, Linnenbank AC, Grimbergen CA. Software design for analysis of multichannel intracardial and body surface electrocardiograms. *Comput Methods Programs Biomed.* 2002;69:225-236
27. Lammers WJ, Schaliq MJ, Kirchhof CJ, Allesie MA. Quantification of spatial inhomogeneity in conduction and initiation of reentrant atrial arrhythmias. *Am J Physiol.* 1990;259:H1254-1263
28. Eckardt D, Theis M, Degen J, Ott T, van Rijen HV, Kirchhoff S, Kim JS, de Bakker JM, Willecke K. Functional role of connexin43 gap junction channels in adult mouse heart assessed by inducible gene deletion. *J Mol Cell Cardiol.* 2004;36:101-110
29. de Bakker JM, van Rijen HM. Continuous and discontinuous propagation in heart muscle. *J Cardiovasc Electrophysiol.* 2006;17:567-573
30. Stein M, Noorman M, van Veen TA, Herold E, Engelen MA, Boulaksil M, Antoons G, Jansen JA, van Oosterhout MF, Hauer RN, de Bakker JM, van Rijen HV. Dominant arrhythmia vulnerability of the right ventricle in senescent mice. *Heart Rhythm.* 2008;5:438-448
31. Noorman M, van Rijen HV, van Veen TA, de Bakker JM, Stein M. Differences in distribution of fibrosis in the ventricles underlie dominant arrhythmia vulnerability of the right ventricle in senescent mice. *Neth Heart J.* 2008;16:356-358
32. van Rijen HVM, Eckardt D, Degen J, Theis M, Ott T, Willecke K, Jongsma HJ, Opthof T, De Bakker JMT. Slow conduction and enhanced anisotropy increase the propensity for ventricular tachyarrhythmias in adult mice with induced deletion of connexin43. *Circulation.* 2004;109:1048-1055
33. Stein M, van Veen TA, Remme CA, Boulaksil M, Noorman M, van Stuijvenberg L, van der Nagel R, Bezzina CR, Hauer RN, de Bakker JM, van Rijen HV. Combined reduction of intercellular coupling and membrane excitability differentially affects transverse and longitudinal cardiac conduction. *Cardiovasc Res.* 2009;83:52-60
34. van Veen TA, Stein M, Royer A, Le Quang K, Charpentier F, Colledge WH, Huang CL, Wilders R, Grace AA, Escande D, de Bakker JM, van Rijen HV. Impaired impulse propagation in scn5a-knockout mice: Combined contribution of excitability, connexin expression, and tissue architecture in relation to aging. *Circulation.* 2005;112:1927-1935

35. Jansen JA, de Jong S, Remme CA, Van Veen TA, van der Nagel R, Labzowski R, Vos MA, Bezzina C, de Bakker JM, Van Rijen HV. Progressive av-block in a mouse-model of lev / lenègre disease. *In preparation*
36. Johnson CM, Green KG, Kanter EM, Bou-Abboud E, Saffitz JE, Yamada KA. Voltage-gated na⁺ channel activity and connexin expression in cx43-deficient cardiac myocytes. *J Cardiovasc Electrophysiol.* 1999;10:1390-1401
37. Boulaksil M. Arrhythmogenesis in the remodeled heart; The role of spatially dispersed Cx43 expression (general discussion). 2010

Chapter 6 – General discussion

John Jansen

Proper impulse propagation in the heart is a prerequisite for successful activation, and subsequent contraction of the heart. The velocity with which the impulse is conducted from cell to cell is dependent on three different factors: excitability, cell-to-cell coupling and tissue characteristics. The first factor as mentioned is mainly determined by Nav1.5 channels, responsible for the upstroke of the action potential, although Kir2.1 channels also play an important role. The second determinant, cell-to-cell coupling, is dependent on the expression of gap junctional channels by forming a bridge for low-resistance communication between adjacent cells. An extensive overview of the regional expression of different gap junctional proteins throughout the mammalian heart is given in chapter 1. The last factor is the tissue architecture, mainly determined by the amount of collagen. Whereas thin fibers of collagen provide strength during contraction and relaxation of the heart, excessive deposition of collagen, which is called fibrosis, can hamper intracellular communication^{1,2}.

In several cardiac disorders, one or more conduction-determinants are affected. Decreased expression of Nav1.5 and Cx43, possibly accompanied by a more heterogeneous expression of those proteins, and increased fibrosis can result in a slowed and / or dispersed conduction, making the heart more vulnerable for life-threatening arrhythmias³⁻⁷. In hearts of patients with arrhythmogenic right ventricular cardiomyopathy (ARVC), decreased levels of Cx43 are found, together with an increased deposition of collagen in a later stage^{8,9}. Lev / Lenègre disease, recently related to Scn5a-mutations, was originally diagnosed by fibrosis and degeneration of the conduction system^{10,11}. Hypertrophic and ischemic cardiomyopathy is hallmarked by lower expression levels of Nav1.5 and Cx43, combined with an increased deposition of collagen¹²⁻¹⁵. Further remodeling can progressively impair impulse conduction in the pathological process towards heart failure, increasing the risk for sudden cardiac death due to triggered activity and reentry-based ventricular tachycardias^{16,17}.

Previous animal studies have shown that the heart has ‘conduction reserve’, a resistance to moderate changes in a single conduction parameter¹⁸. However, combined reductions in Nav1.5 and Cx43, or a decrease in Nav1.5 together with increased fibrosis, did affect impulse conduction, although arrhythmias were still absent^{19,20}. Severely disturbed conduction and high arrhythmia vulnerability were found in mice with extremely reduced Cx43 levels to ~5% and in senescent mice, in which all conduction parameters were affected (Cx43 and Nav1.5 expression reduced by ~50%, collagen content increased by 160%)^{21,22}.

A central role for fibrosis in the susceptibility to arrhythmias can be appreciated from studies with aged and TAC-operated mice and cardiomyopathic hamsters in which the renin-angiotensin-aldosterone system (RAAS) was inhibited: fibrosis was reduced, as well as the vulnerability for arrhythmias. Besides, Cx43 remodeling was prevented, indicating that increased fibrosis generally goes hand in hand with reduced Cx43 expression²³⁻²⁵. Data of aged mice with a 50% reduction in Nav1.5 expression are in favor of this last point, since

both a decrease in Cx43 and an increase in fibrosis was found¹⁹. From these studies we came to the following general hypothesis of this thesis:

'Abnormal Nav1.5 expression leads to abnormal Cx43 expression, which in turn enhances the formation of fibrosis. This ultimately forms the arrhythmogenic substrate.'

Reduced Cx43 expression and enhanced fibrosis

To verify this hypothesis, we first focused on the relation between Cx43 expression and the amount of fibrosis. For this purpose, mice with 50% Cx43 expression (Cx43^{Cre-ER(T)/fl} mice) were compared to control mice with normal Cx43 expression (Cx43^{fl/fl} mice) in chapter 3^{26, 27}. We investigated the potential role of reduced Cx43 expression levels in triggering collagen deposition during physiological (aging to 18-21 months) and pathophysiological (pressure overload by TAC-surgery) stress. Previous studies have shown that aged mice have highly increased levels of interstitial fibrosis²². Likewise, 16 weeks of pressure overload by TAC-operation is known to result in higher amounts of collagen^{6, 28}. We found that stress induced a more pronounced increase of fibrosis in Cx43^{Cre-ER(T)/fl} compared to Cx43^{fl/fl} mice, independent of the nature of stress. In conclusion, these data show that abnormal Cx43 expression indeed enhances the formation of fibrosis.

To investigate the relationship between an abnormal Nav1.5 expression and Cx43 levels and / or collagen deposition, we used Scn5a^{1798insD/+} mice, which have both decreased peak and increased persistent sodium current²⁹. In chapter 4, these animals were stressed by pressure overload, and showed a Lev / Lenègre phenotype within 2 weeks after surgery. We measured a decreased expression of Cx43 in TAC-operated Scn5a^{1798insD/+} mice, but not in TAC-operated WT mice. Furthermore, collagen deposition was increased in TAC-operated Scn5a^{1798insD/+} mice, whereas 2 weeks of pressure overload did not result in a fibrotic response in WT mice. These data fit in our hypothesis that an abnormal sodium channel expression leads to Cx43 remodeling and fibrosis.

A few remarks regarding these two important observations should be made. First of all, the observed relations among the three conduction parameters were found in the background of stress. Sham-operated Cx43^{Cre-ER(T)/fl} and Cx43^{fl/fl} mice both show very low amounts of collagen. Comparably, Sham-operated Scn5a^{1798insD/+} and WT mice had similar low levels of fibrosis. Furthermore, no significant decrease in Cx43 expression was found in Sham-operated Scn5a^{1798insD/+} compared to WT mice. This suggests that under physiological conditions, abnormal Nav1.5 or Cx43 expression has no detectable effect on the other conduction parameters. However, some data imply that stress is not a prerequisite for this link, but more likely a stimulating factor, accelerating the process. First of all, aging is a physiological process, in which no artificial stress was applied, whereas TAC-operation instantly increased afterload³⁰. Nevertheless, a severely enhanced collagen deposition in Cx43^{Cre-ER(T)/fl} compared to Cx43^{fl/fl} mice was found in both aged and TAC-operated mice.

Besides, a small decrease in Cx43 expression levels was found in Sham-operated Scn5a^{1798insD/+} compared to WT mice, although not significantly. A previous study showed that hearts of aged Scn5a heterozygous mice had markedly altered Cx43 expression and severe fibrosis¹⁹. All these data are in favor of a gradual, chronological process of remodeling that can be accelerated by stress: abnormal Nav1.5 expression initiates Cx43 remodeling that in time leads to enhanced fibrosis.

It is important to notice that the duration and nature of stress differs in the studies of chapter 3 and 4. As mentioned previously, stress due to aging is physiologic, whereas pressure overload is a pathophysiological process. Different types of stress may result in different types of remodeling. Moreover, TAC-operated Scn5a^{1798insD/+} mice were analyzed 2 weeks after operation, whereas TAC-operated Cx43^{Cre-ER(T)/fl} mice were sacrificed after 16 weeks of pressure overload. It has been shown that myocardial hypertrophy and systolic dysfunction after TAC-operation is a time-dependent process³¹. Furthermore, the response to pressure overload depends on the genetic background, which is different in both studies (C57BL/6 in chapter 3, FVB/N in chapter 4)³². Considering data of control mice, we found that the actual effect of the applied stress was indeed not equal in both studies: aged and 16 weeks TAC-operated Cx43^{fl/fl} mice had significantly increased levels of fibrosis compared to Sham-operated Cx43^{fl/fl} mice (chapter 3), whereas 2 weeks TAC- and Sham-operated WT mice showed comparable amounts of collagen (chapter 4). In contrast, a fibrotic response with decreased Cx43 expression was found as early as 2 weeks after TAC-operation in C57BL/6 mice²⁵. Although the hearts were challenged differently, which hampers comparison, both models support our central hypothesis. In fact, the severe downregulation of Cx43 and increase in fibrosis after only 2 weeks of pressure overload in Scn5a^{1798insD/+} mice implies a tight relationship between Nav1.5 expression, Cx43 expression and collagen deposition.

A third remark concerns the causal connection between abnormal Nav1.5 expression, Cx43 remodeling and fibrosis. In chapter 3 we showed that reduced Cx43 levels trigger the formation of fibrosis. Chapter 4 revealed that abnormal Nav1.5 expression leads to both reduced Cx43 expression and increased fibrosis. Although these data fit exactly to our hypothesis that '*abnormal Nav1.5 expression leads to abnormal Cx43 expression, which in turn enhances the formation of fibrosis*', we cannot exclude the possibility that abnormal Nav1.5 expression directly influences collagen deposition. Both Lev / Lenègre disease and Brugada syndrome have been associated with mutations in the Scn5a gene, which eventually lead to extensive fibrosis^{10, 11, 33-35}. However, we are not aware of any study that has analyzed Cx43 expression in these patients. To unravel the exact mechanism for the increased collagen deposition in mice with abnormal sodium channel expression, future experiments should focus on the consecutive alterations in an aging model. Since old heterozygous Scn5a mice show both Cx43 remodeling and fibrosis, analysis at earlier time-points could clarify this 'chicken or egg dilemma'¹⁹.

Interaction at the intercalated disc

Recent studies have shown that the intercalated disc is a highly dynamic structure, at which not only Cx43 is localized, but also a regulatory mechanism for Nav1.5³⁶. Furthermore, Nav1.5 and Cx43 could be coprecipitated, and loss of Plakophilin-2 has been shown to result in both Cx43 remodeling and decreased sodium currents in cultured cardiomyocytes³⁷⁻³⁹. These studies show a close connection between those proteins, which suggests that expression and functioning of one protein affects expression and functioning of the other protein. In the first place, this implies that a decreased sodium channel expression would result in reduced Cx43 levels, which is in favor of our hypothesis that abnormal Nav1.5 enhances fibrosis via Cx43 remodeling. Secondly, it suggests that a reduction in Cx43 directly affects Nav1.5 expression. In chapter 5, we analyzed this relationship by injecting Cx43^{Cre-ER(T)/fl} mice with Tamoxifen to further reduce Cx43 protein levels to ~5%. We found that the arrhythmogenic (VT+) mice had more severe Cx43 remodeling compared to non-arrhythmogenic (VT-) mice, and that this was accompanied by a lower expression of Nav1.5. This suggests that the reduction in Nav1.5 is a direct consequence of the very low Cx43 expression. However, a previous study using isolated neonatal cardiomyocytes from Cx43 null mice showed no effect on Nav1.5 expression or functioning⁴⁰. Although the effect of Cx43 depletion *in vivo* may differ from isolated cultured cells i.e. by stretch on cardiomyocytes or the lack of coupling to surrounding cells, an additional study is required to prove a direct link between the very low Cx43 levels and reduced Nav1.5 channel availability in VT+ mice. Furthermore, additional experiments should be performed on aged and TAC-operated Cx43^{Cre-ER(T)/fl} mice (chapter 3): lower Nav1.5 protein levels after long-term stress in the background of reduced Cx43 expression would be in favor of a direct connection between Cx43 and Nav1.5.

Our main conclusion in chapter 5 was that in Tamoxifen-induced Cx43^{Cre-ER(T)/fl} mice, arrhythmia vulnerability in VT+ mice was associated with lower Cx43 expression and higher macroscopic Cx43 heterogeneity, combined with lower Nav1.5 expression compared to VT- mice. Interestingly, we found only low levels of interstitial fibrosis, which were comparable between VT+ and VT- mice. Apparently, although both Cx43 and Nav1.5 expression is abnormal, collagen deposition is not increased within the 2 weeks after Tamoxifen-induction. Importantly, hearts in this study were not hypertrophic, in contrast to aged and pressure overloaded hearts in chapter 3 and 4, pointing to a different type of stress. This might explain why fibrosis is absent in Tamoxifen-induced Cx43^{Cre-ER(T)/fl} mice after 2 weeks, but abundantly present in Scn5a^{1798insD/+} mice after 2 weeks of pressure overload. However, we believe that collagen deposition would increase at a later time-point after Tamoxifen-induction in Cx43^{Cre-ER(T)/fl} mice. Unfortunately, this cannot be tested since these mice die due to ventricular tachycardias within 3 weeks after Tamoxifen-induction²⁶.

Low Cx43, enhanced fibrosis and fibroblast activity

An important issue is how abnormal Cx43 expression enhances the formation of fibrosis, which was investigated by thorough analysis of Sham- and TAC-operated Cx43^{Cre-ER(T)/fl} and Cx43^{fl/fl} mice (chapter 3). In general, 2 different types of fibrosis can be defined: replacement fibrosis, which is due to cell necrosis, resulting in large areas or patches of collagen, and reactive fibrosis, produced by fibroblasts, leading to thickening of the interstitial strands of collagen without cell-dead⁴¹. Since we mainly found interstitial fibrosis, we focused on the proliferation and activity of fibroblasts. Gap junctional connections between cardiomyocytes and fibroblasts and between fibroblasts have been identified previously, suggesting that reduced Cx43 levels may alter communication between fibroblasts or of fibroblasts with surrounding cells, leading to increased fibroblast proliferation and / or activity^{42, 43}. We showed that the propeptides of procollagen I and III (P1NP and P3NP) were significantly increased after TAC-operation, which was more pronounced in Cx43^{Cre-ER(T)/fl} than in Cx43^{fl/fl} hearts, whereas discoidin domain receptor 2 (DDR2) expression was unchanged. Together with increased mRNA levels of COL1A2, encoding for the pro- α 2 chain of procollagen type I, in TAC-operated Cx43^{Cre-ER(T)/fl} hearts, these data indicate that an increased fibroblast activity, but not proliferation, is the underlying mechanism for enhanced fibrosis in pressure overloaded Cx43^{Cre-ER(T)/fl} hearts.

These results directly raise 2 interesting questions. First of all, what is the underlying mechanism for the increased fibroblast activity in stressed hearts with reduced Cx43 availability? Recent *in vitro* studies have shown that communication via Cx43 between cardiomyocytes and fibroblasts significantly influences cytokine secretion: inhibition of these interactions resulted in increased tumor necrosis factor- α (TNF- α) levels, whereas it reduces interleukin-6 (IL-6) secretion⁴⁴. Both cytokines have been reported to be upregulated in several cardiac disorders, and both are associated with increased collagen synthesis⁴⁵. However, whereas TNF- α induces apoptosis of cardiomyocytes, IL-6 is currently thought to have a cardioprotective role⁴⁶⁻⁴⁸. We tried to measure mRNA levels of TNF- α and IL-6, but found no significant changes, possibly due to large variations among the samples (data not shown). This discrepancy with the data of Bowers et al⁴⁴ can be explained by the Langendorff experiments, during which cytokines could (partly) be washed out. Future investigation is required to determine the role of these cytokines in our model. Besides, other possible pathways that can lead to increased fibroblast activity and enhanced fibrosis require further attention, for instance: (1) activation of the renin-angiotensin-aldosterone system (RAAS) could result in an angiotensin II induced secretion of transforming growth factor β (TGF- β), which is known to induce collagen gene transcription⁴⁵, (2) transition of fibroblasts into myofibroblasts increases collagen synthesis, a process that is also promoted by TGF- β ⁴⁹. Independent of fibroblast activity, a decreased breakdown of collagen could also contribute to the observed increase in fibrosis. Extensive additional research is required to unravel the exact mechanism of the enhanced formation of fibrosis in challenged Cx43^{Cre-ER(T)/fl} hearts.

The second point of discussion is whether these data in TAC-operated Cx43^{Cre-ER(T)/fl} hearts can be translated to other models, and thus whether increased fibroblast activity can be considered as the general mechanism for increased collagen deposition in this thesis. With regard to the enhanced formation of fibrosis in aged Cx43^{Cre-ER(T)/fl} mice, we assumed a similar mechanism very likely, since both the models (stress in the background of reduced Cx43 levels) and the outcomes (enhanced fibrosis) are comparable. Nevertheless, this should be validated empirically. However, comparison with TAC-operated Scn5a^{1798insD/+} mice is more complicated, due to larger differences between the models. As mentioned previously, we have not proven that the increased formation of fibrosis is caused by the reduced Cx43 expression in pressure overloaded Scn5a^{1798insD/+} hearts. Therefore, we cannot exclude that abnormal Nav1.5 expression by itself affects collagen deposition and / or breakdown. Besides, Scn5a^{1798insD/+} mice are known to have not only a reduced peak sodium current, but also an increased persistent sodium current, which can result in Na-overload, and consequently Ca-overload^{29, 50}. This in turn results in calcium / calmodulin induced calcineurin activation, which can dephosphorylate nuclear factor of activated T-cells (NFAT)⁵¹. This enables NFAT to enter the nucleus and activate the fetal gene program, resulting in an upregulation of hypertrophic markers and deposition of collagen^{52, 53}. Future studies should elucidate whether this pathway is involved in the formation of fibrosis in TAC-operated Scn5a^{1798insD/+} mice, for instance by treatment with calcineurin-inhibitors such as cyclosporin A and FK506⁵⁴⁻⁵⁶.

The arrhythmogenic substrate

The final part of the general hypothesis describes that abnormal Nav1.5 or Cx43 expression, combined with the resulting formation of fibrosis, ultimately forms the arrhythmogenic substrate. Chapter 3 shows that this is entirely valid for aged mice with reduced Cx43 expression: no arrhythmias could be induced in aged Cx43^{fl/fl} mice, which only have a moderate amount of collagen with normal Cx43 expression. Likewise, 5 months old Cx43^{Cre-ER(T)/fl} mice, showing decreased Cx43 levels in the absence of fibrosis, were not susceptible for arrhythmias (data not shown). In contrast, in the majority of aged Cx43^{Cre-ER(T)/fl} hearts, ventricular tachycardias could be induced, caused by heterogeneously reduced Cx43 expression in concert with enhanced fibrosis. Previous studies are in favor of the idea that in the background of moderate changes in expression levels of Nav1.5 and / or Cx43, fibrosis is required to make the heart vulnerable. Mice that were haplo-insufficient for both Cx43 and Nav1.5 showed only minor conduction disturbances, but no arrhythmias²⁰. However, in senescent mice the arrhythmia vulnerability was high (55%), and tissue analysis revealed both a reduction in Nav1.5 and Cx43 expression, and an increase in fibrosis²². The important role for fibrosis with regard to arrhythmia susceptibility in aged Cx43^{Cre-ER(T)/fl} mice was underlined by the observation that collagen deposition in VT+ mice was more pronounced than in VT- mice. In line with these data, a positive correlation

between the severity of fibrosis and arrhythmia vulnerability has been demonstrated previously²³.

Differences in arrhythmia vulnerability between TAC-operated Cx43^{fl/fl} and Cx43^{Cre-ER(T)/fl} mice were less explicit. A possible explanation may be that these polymorphic arrhythmias were probably based on triggered activity, considering the increased effective refractory period (ERP) which indicates prolonged action potential durations⁶. Whereas a slowed and dispersed conduction, due to fibrosis and / or a heterogeneous reduction of Cx43, considerably increases the susceptibility for monomorphic ventricular tachycardias, based on anisotropic reentry, it hardly affects the vulnerability to triggered activity⁵⁷.

TAC-operated Scn5a^{1798insD/+} hearts showed both a decrease in Nav1.5 and Cx43 expression and an increased collagen content, suggesting that these animals would be very prone to arrhythmias (chapter 4). However, no ventricular arrhythmias could be induced in these mice. Several data may explain these differences, i.e. (1) increased ERP, (2) low amounts of collagen compared to aged and TAC-operated Cx43^{Cre-ER(T)/fl} mice, probably because of differences in the duration of pressure overload, and consequently (3) no transverse conduction slowing. Previous data of aged Scn5a heterozygous mice showed remarkable similarities: Nav1.5 reduction, Cx43 remodeling and increased fibrosis, but no arrhythmias due to an increased ERP¹⁹.

In general, these data show that increased fibrosis in the background of an abnormal Nav1.5 and / or Cx43 expression is indeed a key factor in determining arrhythmia susceptibility, but that other factors, such as refractoriness, can play an important role as well. Furthermore, in chapter 5 we showed that Tamoxifen-induced Cx43^{Cre-ER(T)/fl} mice were highly prone for arrhythmias in the absence of fibrosis, an observation that has been published previously²¹. So apparently, other molecular changes in the cardiac tissue also have an effect on arrhythmia vulnerability in our models. A possible alteration could be that the Cx43 expression became more heterogeneous, which has been related to increased arrhythmia inducibility in both animals and patients⁴⁻⁷. Therefore, we thoroughly studied heterogeneity in Cx43 expression in this thesis, for which we have used several methods. In chapter 3 we used a previously published procedure in which the averaged standard deviation of the shortest distances of a Cx43 positive spot to another spot was determined⁶. An important drawback of this method is that it is not completely insensitive to the amount of Cx43, particularly if expression is extremely low as found in Tamoxifen-induced Cx43^{Cre-ER(T)/fl} mice (chapter 5). Therefore, we developed another system, which measured normalized differences in Cx43 intensities in defined squares of a photograph. This method is not only independent of absolute protein levels, but also enables quantification of intensity-variations between different regions of the heart, as a measure for global heterogeneity.

In chapter 3, we found higher values for local Cx43 heterogeneity in aged and TAC-operated Cx43^{Cre-ER(T)/fl} compared to Cx43^{fl/fl} hearts. However, we could not detect

differences in Cx43 distribution between VT- and VT+ mice, which was in contrast with a previous study on TAC-operated WT mice, showing a strong positive correlation between arrhythmia inducibility and Cx43 heterogeneity⁶. The reason for this discrepancy is unclear, but possibly the influence of the enormous increase in fibrosis is dominant over other factors. However, chapter 5 shows that local heterogeneity was also comparable between Tamoxifen-induced Cx43^{Cre-ER(T)/fl} VT- and VT+ mice, in which fibrosis did not play a role. Interestingly, values for global heterogeneity were higher in VT+ mice, implying that large areas, totally depleted of Cx43, rather than local variations in Cx43 expression, contribute to the formation of an arrhythmogenic substrate. To strengthen this point, it would be interesting to check whether global heterogeneity in Cx43 expression is also increased in aged Cx43^{Cre-ER(T)/fl} VT+ compared to VT- mice.

Epicardial activation mapping was performed to determine impulse conduction velocities. We found in all models that the alterations in conduction parameters resulted in a disturbed impulse propagation: in aged, TAC-operated and Tamoxifen-induced Cx43^{Cre-ER(T)/fl} hearts, this conduction slowing was found in the ventricles, whereas TAC-operated Scn5a^{1798insD/+} hearts mainly show slowing through the atrioventricular conduction system. In general, during physiologically normal pacing frequencies (BCL-pacing), the effects on ventricular impulse conduction velocity were relatively small. Comparable results were found at the ECG: only minor prolongations in QRS duration were found, with the exception of Tamoxifen-induced Cx43^{Cre-ER(T)/fl} VT+ mice, in which the QRS-duration > 15ms. However, comparing epicardial activation maps of VT+ and VT- mice in all studies of this thesis reveals one consistent finding: areas of local slow conduction, resulting in a high dispersion of conduction index, were found specifically in VT+ mice. This suggests that local disturbances, rather than global ventricular conduction, are related to arrhythmia vulnerability. These data match exactly with histological data: heterogeneous reduced Cx43 expression and non-uniform deposition of collagen will hamper impulse conduction locally, and not equally in the total ventricle. Those areas of slow conduction are more prone to conduction block with decreasing coupling intervals, generating a substrate for reentry based arrhythmias^{7, 58, 59}. Analysis of epicardial conduction during premature stimulation in Tamoxifen-induced Cx43^{Cre-ER(T)/fl} hearts validated this statement, showing more prominent conduction slowing in VT+ compared to VT- animals.

Next to these overall findings, one important difference among the studies requires further attention: the direction of conduction slowing was not the same in all models. Aged Cx43^{Cre-ER(T)/fl} hearts only showed transversal conduction slowing in VT+ animals, which could be explained by the increased amount of interstitial fibrosis, that mainly affects transversal conduction⁶⁰. In contrast, TAC-operated mice mainly presented conduction slowing in the longitudinal direction, which is in agreement with a previous report⁶. Likewise, mice carrying the 1798insD mutation in the Scn5a gene specifically showed slower longitudinal impulse conduction. Finally, a heterogeneous reduction in Cx43, combined with decreased Nav1.5 expression in Tamoxifen-induced Cx43^{Cre-ER(T)/fl} VT+ hearts resulted in both longitudinal and transverse conduction slowing. The decreased CV_L

in mice with less peak sodium current is in agreement with previous data²⁰. However, this study showed that the combination of reduced Nav1.5 and Cx43 resulted in slower CV_T , but also in attenuation of CV_L , in contrast to our data. A plausible explanation is the actual protein level of Cx43, which is so drastically decreased in Tamoxifen-induced Cx43^{Cre-ER(T)/fl} hearts that it presumably overrules additional changes. The original published data on Tamoxifen-induced Cx43^{Cre-ER(T)/fl} mice also showed severe conduction slowing in both the longitudinal and transverse direction²¹.

Finally, our data significantly contribute to the concept of ‘conduction reserve’. Several studies have shown that a moderate change in a single parameter of impulse conduction hardly impairs conduction, without increasing arrhythmia vulnerability^{18, 19, 21, 61}. Furthermore, arrhythmias were absent in mice with a combined reduction in Nav1.5 and Cx43, and in mice with both decreased Nav1.5 expression and increased fibrosis^{19, 20}. Chapter 3 shows that the combination of reduced Cx43 protein levels, together with enhanced collagen deposition, not only disturbed impulse conduction, but also resulted in high arrhythmia susceptibility, indicating that conduction reserve is exceeded in these mice. Furthermore, in chapter 5 we confirmed previous data that very low expression levels of Cx43 by itself can form a highly arrhythmogenic substrate, although the decreased Nav1.5 expression in VT+ mice might also play a role²¹.

Many studies have shown that RV is more vulnerable for conduction slowing and arrhythmias than LV¹⁹⁻²³. Although the exact mechanism for this difference between the ventricles is unclear, it is general thought that the thickness of the ventricular free wall is a major factor. In senescent mice, the higher arrhythmia vulnerability in RV was attributed to patchy fibrosis²². The studies in this thesis have not focused on left-right differences, but also showed more severe conduction slowing and higher arrhythmia vulnerability in RV, supporting the idea of a lower conduction reserve of RV.

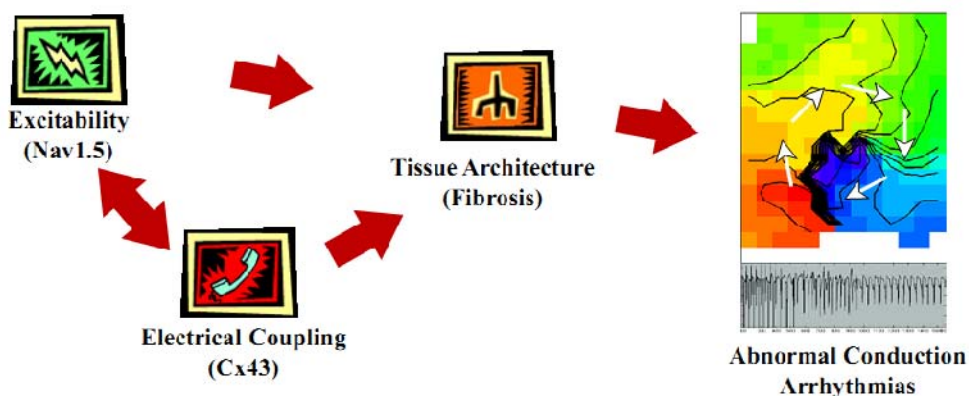


Figure 1 – Model of interrelations among conduction determinants and arrhythmia vulnerability

In summary, we have shown that our proposed hypothesis ‘*Abnormal Nav1.5 expression leads to abnormal Cx43 expression, which in turn enhances the formation of fibrosis. This ultimately forms the arrhythmogenic substrate*’ is largely supported by our data, but somewhat oversimplified. Other factors like heterogeneity of Cx43 expression, ERP and type of arrhythmia also determined arrhythmia vulnerability, and arrhythmias can even occur in the absence of fibrosis. Besides, we have proven that abnormal Nav1.5 expression enhances the formation of fibrosis, but not that this process goes via reduced Cx43 expression. A final model, including the effect of reduced Cx43 expression on Nav1.5, is shown in Figure 1.

Synthesis

So what is the clinical relevance of the findings in this thesis? Or what is the scientific contribution of this thesis in the understanding of cardiac pathologies? Here we have listed the most important implications of our results:

- 1) A combined decrease in Cx43 and increase in collagen deposition is found in various pathophysiological conditions, such as hypertrophic and ischemic cardiomyopathy, making the heart highly prone for arrhythmias^{1, 2, 12-16, 62, 63}. In patients with arrhythmogenic right ventricular cardiomyopathy (ARVC), both reduced Cx43 expression and enhanced deposition of collagen are found. The current thought is that mutations in desmosomal proteins cause the decrease in Cx43. Recent insight revealed that this reduction in Cx43 precedes the formation of fibrosis^{8, 9}. We have shown that reduced Cx43 levels in stressed hearts can promote fibroblasts to produce collagen. This could explain the temporal evolution of ARVC and the commonly found combination of Cx43 remodeling and fibrosis in cardiac pathologies. Furthermore, it implies that normalization of Cx43 expression in the concealed phase of ARVC may prevent the formation of fibrosis, thereby reducing the risk for lethal ventricular tachycardias.
- 2) Recently, several studies have suggested that Cx43 and Nav1.5 are co-localized in the intercalated disc, and that expression and functioning of one protein effects functioning of the other protein³⁶⁻³⁹. In this thesis, we have actually shown that an abnormal Cx43 expression results in a reduction of Nav1.5, and *vice versa*. This may explain why both Cx43 and Nav1.5 are downregulated in many cardiac pathologies^{13, 15, 17, 62}.
- 3) Lev / Lenègre disease is characterized by a senile degeneration of the conduction system. Although it was originally diagnosed by fibrosis in the atrioventricular conduction system, it has more recently been related to mutations in Scn5a^{10, 11, 33, 64, 65}. However, animal models of Lev / Lenègre disease are currently unknown, complicating the search for mechanisms and possible treatments. We have described a mouse-model with a typical Lev / Lenègre phenotype by applying

aortic stenosis to mice carrying an *Scn5a*-mutation: high mortality due to progressive AV-conduction slowing, eventually resulting in AV-block. This accelerated mouse-model of Lev / Lenègre disease could be very useful for future intervention studies.

- 4) Reduced expression of Kir2.1-channels, largely responsible for the I_{K1} current, is found in patients suffering from heart failure⁶⁶. Although we mainly focused on Nav1.5 in this thesis, a downregulation of Kir2.1 can also decrease excitability, thereby impairing impulse conduction^{67, 68}. Besides, loss-of-function mutations lead to Andersen-Tawil syndrome, which is characterized by a high mortality due to ventricular arrhythmias. Inhibiting degradation of Kir2.1 proteins could be a possible intervention to increase expression levels^{69, 70}. However, the exact degradation pathway for Kir2.1, as for many other ion channels, is currently unknown. We have shown that the lysosomal degradation pathway is involved in the breakdown of Kir2.1, creating a therapeutic target to increase Kir2.1 expression. Furthermore, inhibiting this degradation pathway may also increase expression of other cardiac ion channels.

In conclusion, we have shown that abnormal Nav1.5 or Cx43 expression enhances the formation of fibrosis in stressed hearts, making the heart more vulnerable for arrhythmias. Fibroblast activity, but not proliferation, was increased in mice with reduced expression of Cx43, accounting for the enhanced fibrosis. Furthermore, Nav1.5 protein levels are dependent on Cx43 expression, and *vice versa*, raising an important interrelation between both proteins.

References

1. La Vecchia L, Ometto R, Bedogni F, Finocchi G, Mosele GM, Bozzola L, Bevilacqua P, Vincenzi M. Ventricular late potentials, interstitial fibrosis, and right ventricular function in patients with ventricular tachycardia and normal left ventricular function. *Am J Cardiol.* 1998;81:790-792
2. Swynghedauw B. Molecular mechanisms of myocardial remodeling. *Physiol Rev.* 1999;79:215-262
3. Dhein S. Cardiac ischemia and uncoupling: Gap junctions in ischemia and infarction. *Adv Cardiol.* 2006;42:198-212
4. Polontchouk L, Haefliger JA, Ebelt B, Schaefer T, Stuhlmann D, Mehlhorn U, Kuhn-Regnier F, De Vivie ER, Dhein S. Effects of chronic atrial fibrillation on gap junction distribution in human and rat atria. *J Am Coll Cardiol.* 2001;38:883-891
5. Wiegerinck RF, van Veen TA, Belterman CN, Schumacher CA, Noorman M, de Bakker JM, Coronel R. Transmural dispersion of refractoriness and conduction velocity is associated with heterogeneously reduced connexin43 in a rabbit model of heart failure. *Heart Rhythm.* 2008;5:1178-1185
6. Boulaksil M, Winkels SK, Engelen MA, Stein M, van Veen TA, Jansen JA, Linnenbank AC, Bierhuizen MF, Groenewegen WA, van Oosterhout MF, Kirkels JH, de Jonge N, Varro A, Vos MA, de Bakker JM, van Rijen HV. Heterogeneous connexin43 distribution in heart failure is associated with dispersed conduction and enhanced susceptibility to ventricular arrhythmias. *Eur J Heart Fail.* 2010;12:913-921
7. Kitamura H, Ohnishi Y, Yoshida A, Okajima K, Azumi H, Ishida A, Galeano EJ, Kubo S, Hayashi Y, Itoh H, Yokoyama M. Heterogeneous loss of connexin43 protein in nonischemic dilated cardiomyopathy with ventricular tachycardia. *J Cardiovasc Electrophysiol.* 2002;13:865-870
8. Saffitz JE. Arrhythmogenic cardiomyopathy and abnormalities of cell-to-cell coupling. *Heart Rhythm.* 2009;6:S62-65
9. Oxford EM, Everitt M, Coombs W, Fox PR, Kraus M, Gelzer AR, Saffitz J, Taffet SM, Moise NS, Delmar M. Molecular composition of the intercalated disc in a spontaneous canine animal model of arrhythmogenic right ventricular dysplasia/cardiomyopathy. *Heart Rhythm.* 2007;4:1196-1205
10. Lev M. Anatomic basis for atrioventricular block. *Am J Med.* 1964;37:742-748
11. Lenegre J, Moreau P, Iris L. 2 cases of complete auriculo-ventricular block due to primary sarcoma of the heart. *Arch Mal Coeur Vaiss.* 1964;56:361-387
12. Winterton SJ, Turner MA, O'Gorman DJ, Flores NA, Sheridan DJ. Hypertrophy causes delayed conduction in human and guinea pig myocardium: Accentuation during ischaemic perfusion. *Cardiovasc Res.* 1994;28:47-54
13. Peters NS. New insights into myocardial arrhythmogenesis: Distribution of gap-junctional coupling in normal, ischaemic and hypertrophied human hearts. *Clin Sci (Lond).* 1996;90:447-452
14. McIntyre H, Fry CH. Abnormal action potential conduction in isolated human hypertrophied left ventricular myocardium. *J Cardiovasc Electrophysiol.* 1997;8:887-894
15. Kostin S, Rieger M, Dammer S, Hein S, Richter M, Klovekorn WP, Bauer EP, Schaper J. Gap junction remodeling and altered connexin43 expression in the failing human heart. *Mol Cell Biochem.* 2003;242:135-144
16. Levy D, Anderson KM, Savage DD, Balkus SA, Kannel WB, Castelli WP. Risk of ventricular arrhythmias in left ventricular hypertrophy: The framingham heart study. *Am J Cardiol.* 1987;60:560-565
17. Borlak J, Thum T. Hallmarks of ion channel gene expression in end-stage heart failure. *Faseb J.* 2003;17:1592-1608
18. van Rijen HV, de Bakker JM, van Veen TA. Hypoxia, electrical uncoupling, and conduction slowing: Role of conduction reserve. *Cardiovasc Res.* 2005;66:9-11
19. van Veen TA, Stein M, Royer A, Le Quang K, Charpentier F, Colledge WH, Huang CL, Wilders R, Grace AA, Escande D, de Bakker JM, van Rijen HV. Impaired impulse propagation in scn5a-knockout mice: Combined contribution of excitability, connexin expression, and tissue architecture in relation to aging. *Circulation.* 2005;112:1927-1935

20. Stein M, van Veen TA, Remme CA, Boulaksil M, Noorman M, van Stuijvenberg L, van der Nagel R, Bezzina CR, Hauer RN, de Bakker JM, van Rijen HV. Combined reduction of intercellular coupling and membrane excitability differentially affects transverse and longitudinal cardiac conduction. *Cardiovasc Res.* 2009;83:52-60
21. van Rijen HV, Eckardt D, Degen J, Theis M, Ott T, Willecke K, Jongasma HJ, Opthof T, de Bakker JM. Slow conduction and enhanced anisotropy increase the propensity for ventricular tachyarrhythmias in adult mice with induced deletion of connexin43. *Circulation.* 2004;109:1048-1055
22. Stein M, Noorman M, van Veen TA, Herold E, Engelen MA, Boulaksil M, Antoons G, Jansen JA, van Oosterhout MF, Hauer RN, de Bakker JM, van Rijen HV. Dominant arrhythmia vulnerability of the right ventricle in senescent mice. *Heart Rhythm.* 2008;5:438-448
23. Stein M, Boulaksil M, Jansen JA, Herold E, Noorman M, Joles JA, van Veen TA, Houtman MJ, Engelen MA, Hauer RN, de Bakker JM, van Rijen HV. Reduction of fibrosis-related arrhythmias by chronic renin-angiotensin-aldosterone system inhibitors in an aged mouse model. *Am J Physiol Heart Circ Physiol.* 2010;299:H310-321
24. De Mello WC, Specht P. Chronic blockade of angiotensin ii at1-receptors increased cell-to-cell communication, reduced fibrosis and improved impulse propagation in the failing heart. *J Renin Angiotensin Aldosterone Syst.* 2006;7:201-205
25. Qu J, Volpicelli FM, Garcia LI, Sandeep N, Zhang J, Marquez-Rosado L, Lampe PD, Fishman GI. Gap junction remodeling and spironolactone-dependent reverse remodeling in the hypertrophied heart. *Circ Res.* 2009;104:365-371
26. Eckardt D, Theis M, Degen J, Ott T, van Rijen HV, Kirchhoff S, Kim JS, de Bakker JM, Willecke K. Functional role of connexin43 gap junction channels in adult mouse heart assessed by inducible gene deletion. *J Mol Cell Cardiol.* 2004;36:101-110
27. Feil R, Brocard J, Mascrez B, LeMeur M, Metzger D, Chambon P. Ligand-activated site-specific recombination in mice. *Proc Natl Acad Sci U S A.* 1996;93:10887-10890
28. Xia Y, Lee K, Li N, Corbett D, Mendoza L, Frangogiannis NG. Characterization of the inflammatory and fibrotic response in a mouse model of cardiac pressure overload. *Histochem Cell Biol.* 2009;131:471-481
29. Remme CA, Verkerk AO, Nuyens D, van Ginneken AC, van Brunschot S, Belterman CN, Wilders R, van Roon MA, Tan HL, Wilde AA, Carmeliet P, de Bakker JM, Veldkamp MW, Bezzina CR. Overlap syndrome of cardiac sodium channel disease in mice carrying the equivalent mutation of human scn5a-1795insd. *Circulation.* 2006;114:2584-2594
30. Toischer K, Rokita AG, Unsold B, Zhu W, Kararigas G, Sossalla S, Reuter SP, Becker A, Teucher N, Seidler T, Grebe C, Preuss L, Gupta SN, Schmidt K, Lehnart SE, Kruger M, Linke WA, Backs J, Regitz-Zagrosek V, Schafer K, Field LJ, Maier LS, Hasenfuss G. Differential cardiac remodeling in preload versus afterload. *Circulation.* 122:993-1003
31. Liao Y, Ishikura F, Beppu S, Asakura M, Takashima S, Asanuma H, Sanada S, Kim J, Ogita H, Kuzuya T, Node K, Kitakaze M, Hori M. Echocardiographic assessment of lv hypertrophy and function in aortic-banded mice: Necropsy validation. *Am J Physiol Heart Circ Physiol.* 2002;282:H1703-1708
32. Barrick CJ, Rojas M, Schoonhoven R, Smyth SS, Threadgill DW. Cardiac response to pressure overload in 129s1/svimj and c57bl/6j mice: Temporal- and background-dependent development of concentric left ventricular hypertrophy. *Am J Physiol Heart Circ Physiol.* 2007;292:H2119-2130
33. Schott JJ, Alshinawi K, Kyndt F, Probst V, Hoorntje TM, Hulsbeek M, Wilde AA, Escande D, Mannens MM, Le Marec H. Cardiac conduction defects associate with mutations in scn5a. *Nat Genet.* 1999;23:20-21
34. Coronel R, Casini S, Koopmann TT, Wilms-Schopman FJ, Verkerk AO, de Groot JR, Bhuiyan Z, Bezzina CR, Veldkamp MW, Linnenbank AC, van der Wal AC, Tan HL, Brugada P, Wilde AA, de Bakker JM. Right ventricular fibrosis and conduction delay in a patient with clinical signs of brugada syndrome: A combined electrophysiological, genetic, histopathologic, and computational study. *Circulation.* 2005;112:2769-2777
35. Ohkubo K, Watanabe I, Okumura Y, Takagi Y, Ashino S, Kofune M, Sugimura H, Nakai T, Kasamaki Y, Hirayama A, Morimoto S. Right ventricular histological substrate and conduction delay in patients with brugada syndrome. *Int Heart J.* 51:17-23

36. Petitprez S, Zmoos AF, Ogrodnik J, Balse E, Raad N, El-Haou S, Albesa M, Bittihn P, Luther S, Lehnart SE, Hatem SN, Coulombe A, Abriel H. Sap97 and dystrophin macromolecular complexes determine two pools of cardiac sodium channels nav1.5 in cardiomyocytes. *Circ Res.* 2011;108:294-304
37. Malhotra JD, Thyagarajan V, Chen C, Isom LL. Tyrosine-phosphorylated and nonphosphorylated sodium channel beta1 subunits are differentially localized in cardiac myocytes. *J Biol Chem.* 2004;279:40748-40754
38. Oxford EM, Musa H, Maass K, Coombs W, Taffet SM, Delmar M. Connexin43 remodeling caused by inhibition of plakophilin-2 expression in cardiac cells. *Circ Res.* 2007;101:703-711
39. de Boer TP, Houtman MJ, Compier M, van der Heyden MA. The mammalian k(ir)2.X inward rectifier ion channel family: Expression pattern and pathophysiology. *Acta Physiol (Oxf).* 2010;199:243-256
40. Johnson CM, Green KG, Kanter EM, Bou-Abboud E, Saffitz JE, Yamada KA. Voltage-gated na⁺ channel activity and connexin expression in cx43-deficient cardiac myocytes. *J Cardiovasc Electrophysiol.* 1999;10:1390-1401
41. Weber KT, Pick R, Jalil JE, Janicki JS, Carroll EP. Patterns of myocardial fibrosis. *J Mol Cell Cardiol.* 1989;21 Suppl 5:121-131
42. Camelliti P, Green CR, Kohl P. Structural and functional coupling of cardiac myocytes and fibroblasts. *Adv Cardiol.* 2006;42:132-149
43. Baudino TA, McFadden A, Fix C, Hastings J, Price R, Borg TK. Cell patterning: Interaction of cardiac myocytes and fibroblasts in three-dimensional culture. *Microsc Microanal.* 2008;14:117-125
44. Bowers SL, Borg TK, Baudino TA. The dynamics of fibroblast-myocyte-capillary interactions in the heart. *Ann N Y Acad Sci.* 2010;1188:143-152
45. Sarkar S, Vellaichamy E, Young D, Sen S. Influence of cytokines and growth factors in ang ii-mediated collagen upregulation by fibroblasts in rats: Role of myocytes. *Am J Physiol Heart Circ Physiol.* 2004;287:H107-117
46. Baumgarten G, Knuefermann P, Kalra D, Gao F, Taffet GE, Michael L, Blackshear PJ, Carballo E, Sivasubramanian N, Mann DL. Load-dependent and -independent regulation of proinflammatory cytokine and cytokine receptor gene expression in the adult mammalian heart. *Circulation.* 2002;105:2192-2197
47. Matsushita K, Iwanaga S, Oda T, Kimura K, Shimada M, Sano M, Umezawa A, Hata J, Ogawa S. Interleukin-6/soluble interleukin-6 receptor complex reduces infarct size via inhibiting myocardial apoptosis. *Lab Invest.* 2005;85:1210-1223
48. Banerjee I, Fuseler JW, Intwala AR, Baudino TA. Il-6 loss causes ventricular dysfunction, fibrosis, reduced capillary density, and dramatically alters the cell populations of the developing and adult heart. *Am J Physiol Heart Circ Physiol.* 2009;296:H1694-1704
49. Santiago JJ, Dangerfield AL, Rattan SG, Bathe KL, Cunnington RH, Raizman JE, Bedosky KM, Freed DH, Kardami E, Dixon IM. Cardiac fibroblast to myofibroblast differentiation in vivo and in vitro: Expression of focal adhesion components in neonatal and adult rat ventricular myofibroblasts. *Dev Dyn.* 2010;239:1573-1584
50. Hoyer K, Song Y, Wang D, Phan D, Balschi J, Ingwall JS, Belardinelli L, Shryock JC. Reducing the late sodium current improves cardiac function during sodium pump inhibition by ouabain. *J Pharmacol Exp Ther.* 2011;337:513-523
51. Luoma JI, Zirpel L. Deafferentation-induced activation of nfat (nuclear factor of activated t-cells) in cochlear nucleus neurons during a developmental critical period: A role for nfatc4-dependent apoptosis in the CNS. *J Neurosci.* 2008;28:3159-3169
52. Wilkins BJ, Molkentin JD. Calcium-calcineurin signaling in the regulation of cardiac hypertrophy. *Biochem Biophys Res Commun.* 2004;322:1178-1191
53. Bourajaj M, Armand AS, da Costa Martins PA, Weijts B, van der Nagel R, Heeneman S, Wehrens XH, De Windt LJ. Nfatc2 is a necessary mediator of calcineurin-dependent cardiac hypertrophy and heart failure. *J Biol Chem.* 2008;283:22295-22303
54. Rao A, Luo C, Hogan PG. Transcription factors of the nfat family: Regulation and function. *Annu Rev Immunol.* 1997;15:707-747

55. Crabtree GR. Generic signals and specific outcomes: Signaling through ca^{2+} , calcineurin, and nf-at. *Cell*. 1999;96:611-614
56. Lim HW, De Windt LJ, Mante J, Kimball TR, Witt SA, Sussman MA, Molkentin JD. Reversal of cardiac hypertrophy in transgenic disease models by calcineurin inhibition. *J Mol Cell Cardiol*. 2000;32:697-709
57. Wit AL, Dillon SM. Anisotropic reentry. *Cardiac Mapping, Chapter 8*. 1993
58. Peters NS, Coromilas J, Severs NJ, Wit AL. Disturbed connexin43 gap junction distribution correlates with the location of reentrant circuits in the epicardial border zone of healing canine infarcts that cause ventricular tachycardia. *Circulation*. 1997;95:988-996
59. Cabo C, Yao J, Boyden PA, Chen S, Hussain W, Duffy HS, Ciaccio EJ, Peters NS, Wit AL. Heterogeneous gap junction remodeling in reentrant circuits in the epicardial border zone of the healing canine infarct. *Cardiovasc Res*. 2006;72:241-249
60. Spach MS, Boineau JP. Microfibrosis produces electrical load variations due to loss of side-to-side cell connections: A major mechanism of structural heart disease arrhythmias. *Pacing Clin Electrophysiol*. 1997;20:397-413
61. Morley GE, Vaidya D, Samie FH, Lo C, Delmar M, Jalife J. Characterization of conduction in the ventricles of normal and heterozygous cx43 knockout mice using optical mapping. *J Cardiovasc Electrophysiol*. 1999;10:1361-1375
62. Kaprielian RR, Gunning M, Dupont E, Sheppard MN, Rothery SM, Underwood R, Pennell DJ, Fox K, Pepper J, Poole-Wilson PA, Severs NJ. Downregulation of immunodetectable connexin43 and decreased gap junction size in the pathogenesis of chronic hibernation in the human left ventricle. *Circulation*. 1998;97:651-660
63. Kawara T, Derksen R, de Groot JR, Coronel R, Tasseron S, Linnenbank AC, Hauer RN, Kirkels H, Janse MJ, de Bakker JM. Activation delay after premature stimulation in chronically diseased human myocardium relates to the architecture of interstitial fibrosis. *Circulation*. 2001;104:3069-3075
64. Bezzina C, Veldkamp MW, van Den Berg MP, Postma AV, Rook MB, Viersma JW, van Langen IM, Tan-Sindhunata G, Bink-Boelkens MT, van Der Hout AH, Mannens MM, Wilde AA. A single na(+) channel mutation causing both long-qt and brugada syndromes. *Circ Res*. 1999;85:1206-1213
65. Kyndt F, Probst V, Potet F, Demolombe S, Chevallier JC, Baro I, Moisan JP, Boisseau P, Schott JJ, Escande D, Le Marec H. Novel scn5a mutation leading either to isolated cardiac conduction defect or brugada syndrome in a large french family. *Circulation*. 2001;104:3081-3086
66. Nattel S, Maguy A, Le Bouter S, Yeh YH. Arrhythmogenic ion-channel remodeling in the heart: Heart failure, myocardial infarction, and atrial fibrillation. *Physiol Rev*. 2007;87:425-456
67. Dharmoon AS, Jalife J. The inward rectifier current (ik1) controls cardiac excitability and is involved in arrhythmogenesis. *Heart Rhythm*. 2005;2:316-324
68. Sekar RB, Kizana E, Cho HC, Molitoris JM, Hesketh GG, Eaton BP, Marban E, Tung L. Ik1 heterogeneity affects genesis and stability of spiral waves in cardiac myocyte monolayers. *Circ Res*. 2009;104:355-364
69. Hodgkin AL, Huxley AF. A quantitative description of membrane current and its application to conduction and excitation in nerve. *J Physiol*. 1952;117:500-544
70. Einthoven W. Ueber die form des menschlichen electrocardiogramms. *Arch Ges Physiol*. 1895;60:101-123

Chapter 7 - Summary

John Jansen

Fast cardiac impulse conduction is required for electrical activation, and subsequent contraction of the heart. This cardiac activation follows a strictly coordinated path: starting at the sinoatrial (SA) node, the impulse goes via the atria to the atrioventricular (AV) node, where it is delayed, after which it travels through the His-bundle and bundle branches to the Purkinje fibers, which activate the ventricular myocardium. The velocity with which the impulse is conducted is dependent on three different factors: excitability, cell-to-cell coupling and tissue characteristics. Excitability is mainly determined by Nav1.5 channels, determining the upstroke-velocity of the action potential, but also by Kir2.1 channels. Gap junctions, in the ventricles of the heart mainly Cx43, enable low resistance communication between adjacent cells, thereby increasing cell-to-cell coupling. The last determinant of impulse conduction, the tissue architecture, is largely dependent on the amount of collagen. Thin fibers of collagen between cardiomyocytes provide essential strength, but an excessive deposition of collagen, called fibrosis, can hamper impulse conduction.

A decreased expression of Kir2.1, Nav1.5, Cx43 and / or an increase in collagen is found in many cardiac disorders, such as Arrhythmogenic Right Ventricular Cardiomyopathy (ARVC), Lev / Lenègre disease and hypertrophic and ischemic cardiomyopathy, which can deteriorate into heart failure. These alterations in conduction-determinants can severely disturb impulse propagation, making the heart vulnerable for sudden cardiac death due to triggered activity and reentry-based ventricular tachycardias. Interestingly, although cardiac excitability, cell-to-cell coupling and tissue architecture are considered as individual parameters, their remodeling generally occurs in concert in the diseased hearts.

Previous animal studies have shown that the heart has ‘conduction reserve’, indicating that a moderate change in a single conduction parameter does not disturb impulse conduction or increase arrhythmia susceptibility. Consequently, a combination of changes in conduction determinants is required to exceed this conduction reserve, resulting in disturbed conduction and increased arrhythmia vulnerability. These studies also pointed towards fibrosis as key factor in determining the vulnerability for arrhythmias.

In this thesis we focused on the interrelations among the different conduction determinants, and their effects on the vulnerability for arrhythmias. We hypothesized that abnormal sodium channel function results in abnormal Cx43 expression which in turn leads to enhanced collagen deposition. By using different types of stress in mice with a genetically abnormal expression of Nav1.5 or Cx43, we analyzed their interaction and effects on collagen deposition and subsequent effects on impulse propagation and arrhythmia inducibility.

This thesis started with an extensive overview of the regional expression pattern of the 3 major cardiac connexin isoforms, Cx40, Cx43 and Cx45, in the mammalian heart (chapter 1). This review describes studies using genetically modified mice to unravel the importance

of each connexin protein in specific parts of the heart. Moreover, changes in connexin expression in several cardiac disorders are discussed.

In Chapter 2, we focused on one of the mechanisms, i.e. modified degradation via the lysosomal or proteasomal pathway, that could be responsible for a decreased expression of ion channels, as found in many cardiac diseases. For many ion channels like Kir2.1, the exact degradation pathway is unknown. By incubating Kir2.1-overexpressing cells with different inhibitors of the lysosomal degradation pathway, the contribution of lysosomal breakdown of Kir2.1 could be examined. After treatment for 24 hours, both an increased Kir2.1 protein expression and an increased I_{K1} current was measured, demonstrating involvement of the lysosomal protease pathway in the breakdown of Kir2.1.

Both aging and pressure overload after transverse aortic constriction (TAC) are known to increase collagen content in the heart. In chapter 3, the effect of aging and TAC-operation on mice with a genetically 50% reduction in Cx43 expression was investigated and compared to mice with normal Cx43 expression. Reduced expression of Cx43 resulted in more excessive fibrosis in both aged and TAC-operated mice, due to an increased activity of fibroblasts. Besides, this enhanced fibrosis, combined with a heterogeneously reduced expression of Cx43, made the heart highly arrhythmogenic due to dispersed conduction.

Mutations in Scn5a, the gene encoding for the cardiac sodium channel Nav1.5, are associated with several cardiac disorders, such as Lev / Lenègre disease, which is characterized by a senile degeneration of the conduction system. Post-mortem analysis of Lev / Lenègre patients showed a high prevalence of secondary cardiac defects, such as aortic stenosis, suggesting that these pathologies are required for, or at least accelerate, the process towards clinical manifestation. In chapter 4, TAC-operation was applied to mice with a mutated Scn5a gene, to mimic aortic stenosis, and 24h telemetry was performed. Within 2 weeks, 42% of the animals showed a typical Lev / Lenègre phenotype: progressively slowed impulse conduction through the specific conduction system, eventually evolving into AV-block. Surviving mice showed no abnormalities *in vivo*, but AV-conduction was delayed *ex vivo*, and tissue analysis showed increased collagen deposition.

If Cx43 expression is reduced to extremely low levels (~5%) in mice, conduction is disturbed, increasing the susceptibility for arrhythmias. However, arrhythmias could not be induced in all animals, suggesting important differences between arrhythmogenic (VT+) and non-arrhythmogenic (VT-) mice. In chapter 5, Cx43 expression was reduced to very low levels, and VT+ mice were compared to VT- mice. In VT+ mice, arrhythmia vulnerability was associated with lower Cx43 expression and higher macroscopic Cx43 heterogeneity. Besides, Nav1.5 expression was reduced in VT+ compared to VT- mice.

Finally, chapter 6 discussed all data of preceding chapters. The general hypothesis, as proposed in the preface, is verified and adjusted to our results.

In conclusion, the studies in this thesis have shown that Nav1.5 and Cx43 expression are strongly interrelated, and that abnormal expression of one of those proteins enhances the formation of fibrosis. The resultant is an electrically unstable heart, prone to arrhythmias.

Chapter 8 – Nederlandse samenvatting

John Jansen

Snelle voortgeleiding van de cardiale impuls is essentieel voor elektrische activatie, en de erop volgende contractie van het hart. Deze cardiale activatie volgt een stringent gecoördineerde weg: beginnend bij de sinusknoop gaat de impuls via de atria naar de atrioventriculaire knoop, waar deze wordt vertraagd, waarna de impuls zijn reis vervolgt door de His-bundel en bundeltakken naar de Purkinje vezels, welke het ventriculaire myocard activeren. De snelheid waarmee de impuls wordt geleid is afhankelijk van drie verschillende factoren: exciteerbaarheid, de koppeling tussen cellen en de eigenschappen van het weefsel. De exciteerbaarheid is grotendeels afhankelijk van Nav1.5 kanalen, die de snelheid van de opgaande fase van de actie potentiaal bepalen, al spelen Kir2.1 kanalen ook een belangrijke rol. Gap junction kanalen, in het ventrikel van het hart met name Cx43, maken communicatie met een lage weerstand mogelijk tussen aangrenzende cellen, waardoor de koppeling tussen cellen toeneemt. De laatste bepalende factor voor impulsgeleiding, de eigenschappen van het weefsel, is merendeels afhankelijk van de hoeveelheid collageen. Dunne vezels bindweefsel tussen cardiomyocyten leveren essentiële stevigheid, maar een buitensporige afzetting van bindweefsel, wat fibrose wordt genoemd, kan de impulsgeleiding verstoren.

Een verlaagde expressie van Kir2.1, Nav1.5, Cx43 en / of een toename in collageen wordt aangetroffen in vele cardiale aandoeningen, zoals aritmogene rechter ventrikel cardiomyopathie (ARVC), de ziekte van Lev / Lenègre en hypertrofe en ischemische cardiomyopathie, wat op den duur kan leiden tot hartfalen. Deze veranderingen in de factoren die conductie bepalen kunnen de impulsgeleiding ernstig verstoren, waardoor het hart gevoelig wordt voor plotse hartdood als gevolg van getriggerde activiteit of een ventriculaire tachycardie, gebaseerd op reentry. Alhoewel cardiale exciteerbaarheid, de koppeling tussen cellen en de eigenschappen van het weefsel als individuele parameters worden beschouwd, vindt de remodulering van deze factoren over het algemeen gezamenlijk plaats in zieke harten.

Eerdere dierstudies hebben aangetoond dat het hart een 'conductie reserve' heeft, wat wil zeggen dat matige veranderingen in een enkele conductie-determinant niet resulteert in een verstoorde geleiding of een toegenomen gevoeligheid voor ritmestoornissen. Als gevolg hiervan is een combinatie van veranderingen in deze factoren noodzakelijk om de conductie reserve te overschrijden, en zo de conductie te belemmeren en de vatbaarheid voor aritmieën te vergroten. Deze studies indiceerden tevens dat fibrose een sleutelrol speelt in het bepalen van de gevoeligheid voor ritmestoornissen.

In dit proefschrift hebben we de focus gelegd op de interrelaties tussen de verschillende geleidingsfactoren, en hun effect op de kwetsbaarheid van het hart voor ritmestoornissen. Onze hypothese was dat een abnormale natriumkanal functie resulteert in een abnormale Cx43 expressie, wat op zijn beurt zal leiden tot een toegenomen depositie van collageen. Door verschillende soorten stress toe te dienen aan muizen met een genetisch abnormale expressie van Nav1.5 of Cx43, waren we in staat de interactie tussen Cx43 en Nav1.5 en

het effect op fibrose te analyseren, alsmede de consequenties voor impulsgeleiding en de induceerbaarheid van ritmestoornissen.

Dit proefschrift begint met een uitgebreid overzicht van het regionale expressiepatroon van de drie belangrijkste cardiale connexine isovormen in het hart van zoogdieren, Cx40, Cx43 en Cx45 (hoofdstuk 1). Dit review beschrijft studies waarin genetisch gemodificeerde muizen worden gebruikt, om zo het belang van ieder connexine eiwit in specifieke delen van het hart te bestuderen. Bovendien worden de veranderingen in connexine expressie in verschillende cardiale aandoeningen behandeld.

In hoofdstuk 2 hebben we ons gericht op één van de mogelijke mechanismen, namelijk een veranderde afbraak via de lysosomale of proteasomale route, die de verlaagde expressie van ionkanalen zouden kunnen verklaren, zoals veelal gevonden wordt in cardiale aandoeningen. Voor veel ionkanalen is de exacte afbraakroute onbekend, zoals ook voor Kir2.1. Door cellen die Kir2.1 tot overexpressie brengen te incuberen met verschillende remmers van de lysosomale degradatie route, kon de bijdrage van lysosomale afbraak van Kir2.1 onderzocht worden. Na 24 uur behandeling waren zowel de Kir2.1 eiwit expressie als de I_{K1} stroomdichtheid toegenomen, wat aantoont dat lysosomale afbraak route betrokken is bij de degradatie van Kir2.1.

Het is bekend dat zowel veroudering als drukoverbelasting als gevolg van een transversale aorta constrictie (TAC) resulteert in een toegenomen hoeveelheid bindweefsel in het hart. In hoofdstuk 3 is het effect van veroudering en TAC-operatie onderzocht in muizen met een genetische 50% afname in de expressie van Cx43, en vergeleken met muizen met een normale Cx43 expressie. In oude en TAC-geopereerde dieren die een verminderde expressie van Cx43 hadden, was de vorming van fibrose excessiever, vanwege een toegenomen activiteit van fibroblasten. Tevens zorgde dit bindweefsel, samen met een heterogeen gereduceerde expressie van Cx43, ervoor dat het hart hoogst gevoelig werd voor ritmestoornissen, als gevolg van een hoge mate van dispersie in conductie.

Mutaties in *Scn5a*, het gen dat codeert voor het natriumkanal Nav1.5 in het hart, zijn geassocieerd met verschillende cardiale aandoeningen, zoals de ziekte van Lev / Lenègre, wat wordt gekarakteriseerd door een ouderdoms-gerelateerde degeneratie van het conductiesysteem. Post-mortem analyse van patiënten met de ziekte van Lev / Lenègre toonde een hoge prevalentie van secundaire cardiale defecten, zoals aorta stenose, wat suggereert dat deze pathologieën noodzakelijk zijn voor het proces richting klinische manifestatie, of dit proces in ieder geval versnellen. In hoofdstuk 4 hebben muizen met een gemuteerd *Scn5a* gen een TAC-operatie ondergaan om aorta stenose te imiteren, waarna ze gevolgd zijn door middel van 24h telemetrie. Binnen 2 weken vertoonde 42% van de dieren een typisch Lev / Lenègre fenotype: de impulsgeleiding door het specifieke conductiesysteem vertraagde progressief, wat zich uiteindelijk ontwikkelde tot AV-blok. Overlevende muizen lieten geen abnormaliteiten zien *in vivo*, maar *ex vivo* was de AV-

conductie wel vertraagd, en analyse van het weefsel toonde een toegenomen afzetting van bindweefsel.

Wanneer de expressie van Cx43 in muizen wordt verlaagd tot extreem lage niveaus (~5%), leidt dit tot een verstoorde impulsgeleiding, wat de vatbaarheid voor aritmieën vergroot. Echter, ritmestoornissen kunnen niet in alle dieren worden opgewekt, wat suggereert dat er belangrijke verschillen zijn tussen aritmogene (VT+) en niet-aritmogene (VT-) muizen. In hoofdstuk 5 is de expressie van Cx43 verlaagd tot zeer lage levels, en zijn VT+ muizen vergeleken met VT- muizen. In VT+ dieren was de gevoeligheid voor ritmestoornissen geassocieerd met een lagere expressie van Cx43 en een hogere mate van macroscopische heterogeniteit in de expressie van Cx43. Daarnaast was de expressie van Nav1.5 gereduceerd in VT+, vergeleken met VT- muizen.

Tenslotte werden alle data van de voorafgaande hoofdstukken besproken in hoofdstuk 6. De algemene hypothese, die werd geopperd in het voorwoord, is geverifieerd en aangepast aan onze resultaten.

In conclusie hebben de studies in dit proefschrift aangetoond dat de expressie van Nav1.5 en Cx43 sterk aan elkaar gerelateerd zijn, en dat een abnormale expressie van één van deze eiwitten leidt tot een toename in de vorming van fibrose. Het resultaat is een elektrisch instabiel hart, dat vatbaar is voor ritmestoornissen.

Chapter 9 - Dankwoord

John Jansen

Het dankwoord....tjah....het meest favoriete hoofdstuk om te schrijven van vrijwel iedere AIO. Inderdaad,vrijwel iedere AIO. Ikzelf heb met veel plezier dit proefschrift geschreven, maar ik had echt moeite om me ertoe te zetten dit dankwoord te gaan schrijven. Dit resulteerde in een situatie die het best te vergelijken is met het invullen van de belastingpapieren, of in mijn geval, het kopen van nieuwe kleren: zo lang mogelijk uitstellen totdat er echt geen ontkomen meer aan is. En vandaar dat ik nu op 17 september, 3 dagen voordat het geheel naar de drukker moet, mijn vrije zaterdagavond achter mijn laptop door moet brengen om toch nog met een (enigszins) leuk verhaal op de proppen te komen, want oh wee, wat zouden jullie (mijn collega's) anders teleurgesteld zijn!

Laat me wel even uitleggen waarom ik een dankwoord eigenlijk nutteloos vind, voordat jullie het beeld krijgen dat ik ervan overtuigd ben dat ik het allemaal wel alleen had gekund, want dat is zeker niet zo! Maar ik denk dat het heel ernstig is wanneer een dankwoord noodzakelijk is om duidelijk te maken dat je mensen dankbaar bent voor hun bijdrage aan je onderzoek of aan het creëren van een prettige werkomgeving. Ik hoop dan ook oprecht dat ik iedereen, die mij op welke manier dan ook gesteund heeft gedurende mijn promotieproject, eigenlijk al voldoende blijk van waardering heb gegeven. Zo niet, sorry, en lees dan verder!

Want ja, ondanks dat het niet verplicht is, heb ik toch een, in ieder geval qua volume, behoorlijk dankwoord geschreven. Ik weet natuurlijk ook dat, alle inspanning van de laatste jaren ten spijt die hebben geleid tot dit proefschrift, ironisch genoeg dit op een zaterdagavond in elkaar geflanst stukje tekst het enige deel van dit proefschrift is dat wel door meer dan 10 mensen wordt gelezen. Dus doe mij een plezier: als je dit leest, doe dan ook de moeite om minstens 1 ander hoofdstuk te lezen, al is het maar de samenvatting. Dit is tevens om te voorkomen dat je het idee krijgt dat ik het collectegeld van de Nederlandse Hartstichting enkel heb gebruikt voor het schrijven van klinisch irrelevante onzin.

Maar goed, nu genoeg van mijn laagdrempelig filosofisch geneuzel, tijd voor het daadwerkelijke dankwoord. Om het geheel in een juiste chronologische volgorde te zetten, ga ik terug naar de stagemarkt van Biomedische Wetenschappen in 2003. Nadat **Marcel** met al zijn ziel en zaligheid mij probeerde te overtuigen stage te komen lopen op de afdeling Medische Fysiologie, besloot ik ergens anders heen te gaan en een jaar lang niks meer van me te laten horen. Ik wilde mijn eerste stage 'gewoon' biomedisch onderzoek doen, zonder nerd-achtige stroompjes in het hart. Ja, ik was nog jong hè! Maar toch gaf ik hem een jaar later een nieuwe kans, en dit keer hapte het visje wel. En laat ik vast voor 1 keer heel duidelijk zijn tegen al mijn oud-collega's: daar heb ik nooit spijt van gehad! Gedurende deze stage ben ik uitstekend begeleid door Marcel (voor de moleculaire experimenten) en **Teun** (toen nog AIO, voor de cellulaire elektrofysiologie), die beide nooit te beroerd waren me te helpen. Ook wil ik hier **Martin** bedanken, die evenals Teun uitzonderlijk bekwaam is in patch clamping, en die ook altijd ruimschoots de tijd nam me bij te staan. Mede door deze goede begeleiding heeft het werk tijdens deze stage geleid tot een publicatie (hoofdstuk 2 van dit proefschrift).

Alhoewel studenten toentertijd schaars waren op onze afdeling, was er wel 1 die later eveneens werd aangenomen, namelijk **Marien**. Ik heb eigenlijk geen idee waarom we het (in ieder geval vanuit mijn perspectief) altijd goed konden vinden samen, want erg veel overeenkomsten hebben we niet. Ik kan me de lol om ergens in weiland te gaan liggen om foto's te maken van vliegtuigen al moeilijk voorstellen, maar goed, als het lekker weer is.....maar neem dan wel een krat bier mee! Hoe dan ook, als ik weer eens geen zin had om te koken en in het UMC een uiterst gevarieerde maaltijd verorberde, heb ik me altijd goed vermaakt tijdens onze veelal politieke gesprekken.

Laat ik op dit punt nog even verder in de geschiedenis duiken, even een mooie flashback, dan gaat het nog echt op literatuur lijken! Want voordat ik aan mijn stages begon, had ik er natuurlijk al 3 jaar studie opzitten. En daarom wil ik ook kort die mensen bedanken, waarmee ik het meeste plezier heb gehad in die periode, en waarmee ik ook veelal het beste heb samengewerkt in vele projecten. **Willem-Jan, Antoine, Nienke, Gineke, Liza**, zonder jullie was ik misschien wel wiskunde gaan studeren.....

Maar goed, ik liep dus stage, en om onverklaarbare redenen ben ik halverwege deze stage gevraagd om AIO te worden op deze afdeling. Volgens mij heb ik er voor de vorm nog even over nagedacht, maar uiteraard heb ik ja gezegd. Waar kun je nog meer zulk leuk werk doen, in zo'n gezellige omgeving?

Dus ben ik eind 2005 begonnen op de afdeling medische fysiologie. Het zal menigeen verbazen, maar als startende AIO, vol met ambitie, moest ik 's ochtends enkel **Stephan** goedemorgen wensen op de grote AIO-kamer. Wellicht nog verbazingwekkender is dat ik me onze dialogen (voor 8 uur 's ochtends!!!) enkel kan herinneren als zeer informatief en relevant. Ik kreeg echter snel door dat ambitie niet tijdsgebonden was, dus dan kun je net zo goed om half 10 beginnen, toch? Dat was ook veel meer in lijn met de begintijden van de andere toenmalige conductie-AIO's, **Mohamed** en **Mèra** (ja kijk, streepje op de e!). De diversiteit in begintijden van de conductie-groep was sowieso opvallend: waar de AIO's graag 's avonds (en 's nachts, ik heb Mèra toen voor gek verklaard, maar mijn proefschrift is ook grotendeels 's nachts geschreven) werkten, was Harold (nog niet dikgedrukt, je komt nog uitgebreid aan bod) altijd voor dag en dauw om half 6 aanwezig. Mohamed, ik denk niet dat er iemand anders op deze wereld zo geduldig is als jij. Daarnaast denk ik dat je zelf nauwelijks in de gaten hebt hoe uitzonderlijk intelligent je bent! En ik ben echt jaloers op de uiterst rustige manier waarop jij enorm grappig kunt zijn. Mèra, de overgave waarmee jij je op je werk stort is enorm bewonderenswaardig, en daarmee ben je echt een voorbeeld geweest! We hebben niet veel samengewerkt, maar desalniettemin (intermezzo: dit is echt het mooiste woord van de Nederlandse taal) heb je een belangrijk aandeel gehad in hoofdstuk 5 van dit proefschrift. Mohamed en Mèra, ik denk dat jullie onbewust erg belangrijk zijn geweest voor mijn ontwikkeling als AIO, nog naast het feit dat ik jullie erg prettige collega's vond.

Uiteraard zijn er in de 5 en een half jaar dat ik werkzaam was op de afdeling nog veel meer collega's omgedoopt tot oud-collega's. Allereerst de oud-analisten **Nancy** en **Anita** (waarom moest jij nou ook Jansen heten?), **Rianne**, bedankt voor een jaar lang samenwerking, en die daarna in feite ook helemaal niet gestopt was, omdat je nu in Amsterdam werkt aan een gezamenlijk project, en spelletjes-goeroe vega-**Joost**, de altijd vrolijke collega, zolang we het maar niet over politiek hadden. Daarnaast nog andere oud-AIO's, zoals **Peter**, die wel eng handig was met software, en het op de een of andere manier altijd voor elkaar kreeg om zijn laptop eruit te laten zien alsof er een vrachtwagen overheen gereden was, maar ja, hij deed het nog wel. Over sommige mensen kun je verder niet heel veel zeggen, behalve dat je ze ontzettend vriendelijk vindt.....dat geldt dus voor Peter. Dan **Lukas**, die niet veel eerder vertrokken is dan ik, I would specially thank you for the organization of the trip to Tsjech Republiek. Although most people would be ashamed to go on holiday with their colleagues, I think it was a very nice time! **Wendy**, onze vrolijke AIO die steeds minder vrolijk vanwege haar werk. Ik vind het erg jammer dat je zo snel bent vertrokken, maar ik bewonder je dappere keuze. **Avram**, kun jij je ook nog een heerlijke discussie over wiskunde herinneren? En tenslotte natuurlijk Stephan, die ik al eerder genoemd had, maar aangezien hij heeft samengewerkt met de eveneens vertrokken **Antoinette**, is op die manier de cirkel rond. Maar niet voordat ik onze ex-Tielenaar, Vlaamse bootbewoner **Gudrun** heb genoemd, want ondanks dat ik nooit met je samengewerkt hebt, vind ik je, zoals zovelen, echt een fantastisch mens. Vaak heel rustig en geconcentreerd aan het werk, maar allee, tijdens de borrels kwam je helemaal los.

Het is tijdens een promotieproject gebruikelijk om studenten te begeleiden, met als ultieme doel een vorm van synergisme te bereiken: de studenten doen experimenten voor de AIO, en de AIO brengt kennis over aan de student. Bij mij is dit proces echter zover doorgevoerd, dat ik me alle samenwerkingsverbanden niet meer kan herinneren. Het domste wat je dan kunt doen is een poging wagen de namen van alle studenten te noteren, omdat je uiteraard veel mensen gaat vergeten. Toch wil ik de volgende studenten wel even kort persoonlijk bedanken: **Helen**, de echt doorzetter, die ondanks de pech met dat verschrikkelijke Cx40 project toch hele bruikbare experimenten heeft gedaan voor andere studies, **Ronald**, mijn telemetrie-uitlees-student, en **Astrid** en **Carolin**, die belangrijke immuno's hebben gedaan voor hoofdstuk 3. Daarnaast waren jullie ook allemaal erg vriendelijke studenten, die zeker niet te lui waren om de handen uit de mouwen te steken. Terecht staan jullie dan ook vermeld in de auteurslijsten van de verschillende hoofdstukken. Dan wil ik nog 1 naam noemen, die van **Justin**, met afstand de raarste student die ik ooit gehad heb. Ik ken echt niemand die na een hele fles tequila nog gewoon rechtop staat....ik heb in ieder geval erg met je kunnen lachen!!

Dan zijn we nu aangekomen bij het heden, en is het tijd voor een rondje langs de huidige werknemers. En laten we maar eens beginnen met de analisten: kleine, maar dappere **Bart**, ondanks zijn lengte toch beschouwd als hoofdanalist van het moleculaire lab. Jammer dat je geen verstand van muziek had, maar je was altijd behulpzaam als ik je vroeg een experiment te doen. Dit laatste geldt ook voor **Leonie**. We hebben niet heel veel

samengewerkt, maar je punctualiteit tijdens het uitvoeren van de experimenten was opvallend. Daar zou ik inderdaad wat van kunnen leren! Op de analistenkamer zat soms ook **Tamara**, ‘de nieuwe studente van Marien’ (ik heb je tenminste niet te oud geschat!), die absoluut wel verstand had van muziek, en **Shirley**, van wie ik het isoleren van neonatale cardiomyocyten heb geleerd. En tenslotte **Jet**, die ik samen met **Linda** toch nog 1 keer wil bewonderen om de kunst zich af te sluiten voor de onzin die door de andere kamergenoten (Roel en ik uiteraard) uitgekraamd werd. Ik heb het echt enorm gezellig gehad op deze kamer, die ook strategisch gunstig gelegen was (dicht bij het koffie-apparaat, en bij de plaats waar je dan 10 minuten later heen moet). Linda, veel succes met het afronden van je boekje!

Dan zijn er nog een heel aantal andere AIO’s, waar ik eigenlijk niet mee heb samengewerkt, maar die ik natuurlijk wel even wil noemen. Ten eerste **Malin**, die nog studente was toen ik al als AIO bezig was, en toch maar een maand later gaat promoveren. Jou kunnen we echt geen dom blondje noemen. **Siddarth**, we actually we never collaborated, but I really had a great time during several congresses. And if I will ever find a job in the Mora-factory, I gonna make a non-beef croquette for you! **Vincent**, die eigenlijk wel een beetje op Mohamed lijkt: ook jij hebt een heel speciaal soort intelligente humor, die ik goed kan waarderen. **Thom**, waar ik wel altijd een beetje om moest lachen tijdens presentaties, maar je zult geen spataderen krijgen van te lang stilstaan. **Christian**, de zonder twijfel enorm vriendelijke kindercardioloog, **Rosanne**, die het liefst een ‘non-horse croquette’ zou willen, en die als enige ’s ochtends concurreert met Harold om de ideale parkeerplaats, en dan nog **Rianne**, die ik eigenlijk nog niet zo goed ken, maar die in ieder geval een vrolijke indruk maakt, welk verhaal eigenlijk ook geldt voor **Sofieke**:

Wat is beter dan een maandagochtendgoed beginnen met iemand een brede (enigszins gemene) glimlach te wensen. En dat kon het laatste seizoen erg vaak gebeuren, toch **Marti**, onze Feyenoorder in hart en nieren. Gelukkig kon je er altijd goed tegen, en hebben we Beverwijk-praktijken buiten de deur kunnen houden. Verder wil ik **Tobias** bedanken voor zijn fantastische anekdotes, en **Maria** voor haar agressie t.o.v. (computer-)muizen, zeker op vrijdagmiddagen. We durfden dan echt niet je kamer in te lopen! En **Rob van Someren**, bedankt kerel, voor mij om 4 uur geen cup-a-soup, maar 5 minuten wetenschapsloze humor.

Tonny, natuurlijk ook een stukje over Tonny! Waar velen je zien als mama van de afdeling, vertrouwenspersoon en degene waarbij je je stukje fruit opeet om 3 uur ’s middags (of waar je een iets minder gezonde snack gaat halen), wil ik daaraan toevoegen dat je ook gewoon een ontzettend goede ~~secretaresse~~ office manager bent. Wanneer iemand een vraag heeft over een declaratie, inbinden van een verslag of het opmaken van een proefschrift, maak jij altijd tijd vrij om te helpen! En daarnaast kun je er dan ook nog vanuit gaan dat het goed gaat! Tonny, bedankt voor alle administratieve hulp (en natuurlijk ook de sociale kant)!

Als we het nu toch over de opmaak van mijn proefschrift hebben, dan wil ik ook **Bolle** bedanken voor het ontwerpen van de cover (ja hij heeft ook een andere naam, maar dat weet bijna niemand).

En dan blijven nog alleen mijn (co-)promotoren en andere leden van de conductie-bende over. Natuurlijk ga ik over iedereen individueel een korte analyse geven, maar er was niets leuker dan een conductie-lunch. Ook al waren er altijd goede bedoelingen om binnen een half uur klaar te zijn, uiteindelijk duurde het vaak een uur of 2 (maar het was wel erg nuttig natuurlijk!).

Allereerst de 3 AIO's: **Sanne**, ik denk niet dat er iemand ooit wat verkeerd over jou in een dankwoord gaat schrijven. Je had eigenlijk al genoemd moeten worden bij de studenten, want je hebt zeker een belangrijke bijdrage geleverd (met name aan hoofdstuk 4). Ik ben gelukkig niet vaak sacherijig (toch?), maar dat bleef ik zeker niet met jou in de buurt, daarvoor ben je eenvoudigweg te opgewekt. En dat is natuurlijk erg positief voor de werksfeer! **Maartje**, nu de senior-conduction-AIO, ja, dat is een hele last, nu verwacht iedereen dat jij de volgende bent die gaat promoveren. Maar mocht het allemaal echt niet lukken, dan heb jij altijd nog een mogelijke carrièremove met je viool, want dat concert was echt super! Maar eerst veel plezier in de U.S.A. en daarna zie ik je boekje graag verschijnen. Je was in ieder geval een fijne collega. Finally **Magda**, working on the project of cardiac tissue slices, which has great potential in my opinion. Please don't blame me for my indefinite hatred against the Portuguese soccer team! Anyhow, I wish you all the best during your project!

Roel, tjah, die kan ik natuurlijk niet overslaan! Niet alleen heb je een essentiële rol gespeeld in alle dierstudies van dit proefschrift, het zal ook niemand ontgaan zijn dat we het ontzettend goed konden vinden samen. Maar eigenlijk kon ik naast de enorme voorliefde voor chocola (in allerlei vormen en maten, zolang het maar veel was) en broodjes Döner eigenlijk niks bedenken waarin we overeenkomsten vertoonden. En daarnaast is je muzieksmaak gewoon lachwekkend! Vele studenten hebben we op een geheel eigen wijze laten wennen aan het uitvoeren van dierproeven: iedereen was hoogst verbaasd om de enorm gezellige sfeer die er hing op het muizenlab, maar moest uiteindelijk wel concluderen dat er toch erg hard gewerkt werd. En dat is exact zoals ik me de samenwerking met jou herinner: gezellig maar effectief. Het was dan ook voor weinig collega's een verrassing dat ik jou als paranimf heb gevraagd.

In dit muizenlab kwamen we ook mensen tegen van andere afdelingen. Hiervan wil ik er ook nog 2 noemen vanwege een aantal gezellige conversaties. **Marcel**, de altijd vrolijke analist die altijd een praatje kwam maken (en met een opmerkelijke resistentie tegen M&M's; wie kan er nou 1 M&M pakken?), en **Lennart**, we moeten nog steeds een keer de muizenlab-borrel organiseren!

Dan wordt het nu echt tijd voor de serieuze verhalen! Allereerst mijn promotor **Jacques**, voor wie ik oneindig veel respect hebt. Waar veel mensen erg veel praten, maar eigenlijk

niks zeggen (zoals ik inderdaad), heeft Jacques de eigenschap om heel goed te luisteren, en dan met weinig woorden heel veel te zeggen. Je enorme bescheidenheid, die eigenlijk in schril contrast staat met je enorme bijdrage aan de huidige cardio-elektrofysiologische kennis, maakt je een nog bewonderenswaardiger persoon. De uitzonderlijke intelligentie van Jacques werd pas echt duidelijk als opponent tijdens een verdediging van een thesis. Ik meen oprecht dat ik nooit iemand betere vragen heb horen stellen! Ik bedank je voor je bijdrage, en wens je een fijne, verdiende, rustigere tijd toe.

Marc, mijn andere promotor, en tevens hoofd van de afdeling. Ik weet weinig van management, maar ik zag wel dat jij een fantastische manager van onze afdeling was. Daarnaast is een goede sfeer, zoals op onze afdeling, enkel mogelijk als het ‘opperhoofd’ daaraan meewerkt, of het minstens toelaat. Ik heb eigenlijk niet erg veel samengewerkt met je, maar de gesprekken die we gehad hebben, waren wel altijd nuttig. Daarnaast zou ik het niet in mijn hoofd halen ooit nog bier en pils te verwarren. Marc, bedankt voor de fijne tijd die ik gehad heb op je afdeling.

Dan is het tijd voor de co-promotoren, allereerst **Toon**. Je meest bekende eigenschap is je directheid, wat enorm prettig is. Net als bij Mohamed, werd jij pas aan het eind van mijn promotieproject toegevoegd als co-promotor, en ik denk dat dat ook wat over je persoonlijkheid zegt: je houdt je op de achtergrond, maar stiekem ben je wel zo slim en handig dat je uiteindelijk een grote bijdrage heb geleverd aan mijn proefschrift. In het begin kwam ik met name naar je toe als ik hulp nodig had met immuno's, maar in de laatste maanden ben je je steeds nadrukkelijker gaan bemoeien met mijn proefschrift. Jouw kennis is essentieel geweest voor het tot stand komen van dit proefschrift!

Harold, ondanks de vele handen die mij geholpen hebben, wil ik toch eindigen met jou te bedanken, omdat jij van begin tot eind mijn eerste aanspreekpunt bent geweest. Helaas moet ik je mijn co-promotor noemen, want ik had het je graag gegund om promotor te zijn. Ik heb vele dingen van je geleerd, zoals de Langendorff-experimenten, het analyseren van de data met maplab, en natuurlijk was je ook nauw betrokken bij het schrijven van dit proefschrift. Maar ik wil er toch nog 1 gave uitlichten, waarvan ik enorm veel geleerd heb, en waar je echt als voorbeeld heb gediend: het geven van presentaties. Ik denk dat jouw manier van presenteren, met al je enthousiasme en oog voor detail en opbouw bij het maken van de powerpoint een vaardigheid is die nuttig zou zijn voor iedere wetenschapper. Verder was je een collega waar ik met veel plezier mee heb samengewerkt, en het was altijd een gezellig uitje om even naar jullie (Toon en Harold's) kamer te gaan (als er nog plek was). Harold, bedankt en hopelijk mogen Sanne, Maartje en Magda jou wel promotor noemen!

Daarmee wil ik de lijst van mensen die mij inhoudelijk bijgestaan hebben graag afsluiten. Maar natuurlijk wil ik bij deze ook mijn ouders, **Herman** en **Siny**, bedanken voor de steun gedurende mijn gehele promotie (en natuurlijk ook al daarvoor!). Eindelijk kunnen jullie rustig lezen wat ik de laatste jaren uitgevoerd heb, en ik wil daar natuurlijk ook graag iets bij uitleggen.

Om nog even terug te komen op de vergelijking met belastingpapieren, of het kopen van kleren...wanneer het eenmaal af is, ben je ook blij dat je het gedaan hebt. Zo ben ik nu ook blij dat ik hiermee mijn dank voor iedereen, die mij op welke manier dan ook gesteund heeft tijdens mijn promotie, vereeuwigd heb. Ik zal jullie niet vergeten!

ps. Roel, Sanne, Maartje en de rest die dan een racefiets heeft, zet in je agenda: vrijdag 1 juni 2012 om 15.00 uur, eindelijk dat rondje fietsen!

John Jansen

Tiel, 2011

Chapter 10 – Curriculum Vitae

John Jansen

Johannes Arnoldus (John) Jansen was born in Tiel, on January 11th, 1982. From 1986 to 1988, he attended the primary school *Princes Julianaschool* in Tiel, after which he continued primary education at *De Adamshof* in Tiel, from 1988 to 1994. From 1994, he attended the Gymnasium at the *RSG Lingecollege* in Tiel. After graduation in 2000, he started the academic study *Biomedical Sciences* at the *University of Utrecht*. During his master, joining the masterprogram *Biology of Disease*, he performed his internships at the department of Vascular Medicine and the department of Medical Physiology, both at the *University of Utrecht*. After he obtained his master-degree in 2005, he did his PhD traineeship at the department of Medical Physiology at the *University of Utrecht* under the supervision of prof.dr.ir. Jacques de Bakker, prof.dr. Marc Vos, dr. Harold van Rijen and dr. Toon van Veen. At November 1st, 2011, he will defend this thesis on mouse models with cardiac conduction disturbances.